

# **Do Multi-year Droughts Increase Floods?**

Yang Zhao



# Do Multi-year Droughts Increase Floods?

by

Y. Zhao

to obtain the degree of Master of Science  
at the Delft University of Technology,  
to be defended publicly on Thursday 4 November, 2021 at 16:00 PM.

Student number: 4347404  
Project duration: March 2021 – November 2021  
Thesis committee: Dr. M. Hrachowitz TU Delft, supervisor  
Dr. ir. M. Coenders, TU Delft  
Dr. R. Taormina, TU Delft

An electronic version of this thesis is available at <http://repository.tudelft.nl/>.



# Preface

This thesis marks the final chapter of the master program Water Management, at the department of Civil Engineering, Delft University of Technology. I have learnt a lot during this thesis, as it has allowed me to dive deeper into the different concepts I have learnt in the courses, as well as how to do independent research.

Studying during COVID-19 had been more difficult than I have anticipated and it took some time to get used to working from home. I would like to thank my supervisor Mr. Hrachowitz, and my committee Ms. Coenders and Mr. Taormina, for their guidance throughout this project. I would also like to thank my boyfriend, friends and family for their unconditional support throughout my master.

*Y. Zhao*  
*Delft, October 2021*



# Summary

Due to climate change, drought-flood alternations have become more frequent and more severe in many countries in the world. However, little research has been done on the relationship between flood and drought. Thus, this research aims to investigate whether a relationship exists between multi-year droughts and the floods that follow in the post-drought period. The hypothesis is that vegetation decreases as a result of long-term drought, which decreases evaporation and increases the proportion of precipitation that becomes runoff, and thus, increases flood.

To test this hypothesis, the United States is chosen as a case study area. Hydrological data and remote sensing data are collected for 671 basins in the case study area, from around 1980 till 2014. A list of criteria is established to detect the occurrence of long-term droughts, verify the water balance, and to ensure data availability. 83 basins fulfill all criteria and for these basins, a 5-year pre-drought period, a drought period, and a 5-year post-drought period are identified.

These 83 basins are plotted inside the Budyko space and Fu's equation is fitted to find the free parameter that indicates the runoff ratio,  $\omega$ . The Wilcoxon rank-sum test has shown that in general, no increase in runoff ratio is detected after drought. Drought duration, intensity, and severity also do not seem to have impacts on the rainfall-runoff relationship. However, looking at the basins individually, changes in the runoff ratio do exist. Thus, these basins are investigated further to see what causes these changes.

This is done by first looking at the effects of drought on the partitioning of hydrological fluxes. The movement of the basins inside the Budyko space is investigated, followed by a separation of the basins' movements into climate effects and residual effects. The results show that for basins that display a decrease in runoff ratio, an increase in evaporation is observed as well as larger landscape-related residual effects. These basins are mostly located in humid regions, with an aridity index smaller than 0.5. However, basins that show an increase in runoff ratio seem to be more related to changes in the climate rather than landscape.

Vegetation is one of the indicators for landscape changes. This research tries to detect vegetation changes using the maximum storage deficit and the vegetation index NDVI, where storage deficit measures the volume of water vegetation needs for optimal growth, and NDVI measures the density of healthy vegetation. The maximum storage deficit in the post-drought period and the change in NDVI between the pre-drought period and the post-drought period are plotted against the residual effects. If the residual effects are mostly caused by vegetation changes, a strong correlation should be found between the residual effects  $\Delta\Psi_r$ , the maximum storage deficit, and the change in NDVI. However, a weak correlation is found between the residual effects and the maximum storage deficit, and no relationship is found between the residual effects and changes in the vegetation index NDVI.

Lastly, certain basins that display more significant changes in the runoff ratio or vegetation are revisited and investigated further. It is found that the more humid basins display a decrease in runoff ratio, have more dominant residual effects, and show an increase in vegetation density. However, vegetation does not seem to be the main cause for this change in runoff ratio. It can also be argued how significant these results are since only a small portion of the basins belong to the group of more humid basins with an aridity index of less than 0.5

It can be concluded that using the method in this research, no significant relationship is found between the multi-year droughts and floods that occur after drought.



# Contents

Summary	v
List of Figures	ix
List of Tables	xiii
Nomenclature	xv
1 Introduction	1
1.1 Research question	2
1.2 Report Structure	2
2 Literature Study	3
2.1 Meteorological Drought Indices	3
2.2 Drought Identification	3
2.3 Drought Recovery	4
2.4 Budyko Framework	4
2.4.1 Runoff Ratio	5
2.4.2 Changes in Hydrological Fluxes	5
2.5 Post-drought Vegetation Changes	5
3 Study Area and Data	7
3.1 Case Study Area	7
3.1.1 Basin Locations	7
3.2 Hydrological Data	7
3.2.1 Long-term Water Balance	8
3.2.2 Aridity Level Classification	9
3.3 Remote Sensing Data	10
4 Methodology	11
4.1 Drought Index	11
4.1.1 Accumulation Period	12
4.2 Basin Selection	12
4.2.1 Drought Period	13
4.2.2 Pre-drought and Post-drought Period	13
4.2.3 Criteria Overview	14
4.3 Changes in Runoff Ratio	15
4.3.1 Fitting Fu's Equation	15
4.3.2 The Wilcoxon Rank-Sum Test	16
4.3.3 Effects of Drought Duration, Intensity and Severity	16
4.3.4 Regional Differences	17
4.4 Effects of Drought on the Partitioning of Fluxes	17
4.4.1 Movement Inside the Budyko Space	17
4.4.2 Dominance of Residual Effects	19
4.5 Detecting Vegetation Changes	19
4.5.1 Storage Deficit	19
4.5.2 NDVI	20
5 Results	21
5.1 Basin Selection	21
5.1.1 Aridity Indices of the Selected Basins	22

5.2	Changes in Runoff Ratio . . . . .	23
5.2.1	Rank-Sum Test and $\Delta\omega$ . . . . .	23
5.2.2	Effects of Drought Duration, Intensity and Severity . . . . .	25
5.2.3	Regional Differences . . . . .	25
5.3	Effects of Drought on the Partitioning of Fluxes . . . . .	27
5.3.1	Drought Effects on Basin Movement . . . . .	27
5.3.2	Separating Climate and Residual Effects . . . . .	28
5.3.3	Dominance of Residual Effects . . . . .	30
5.4	Vegetation Changes . . . . .	31
5.4.1	Storage Deficit . . . . .	31
5.4.2	NDVI. . . . .	32
5.4.3	Correlation Between the Maximum Storage Deficit and NDVI . . . . .	34
5.5	Overview . . . . .	34
5.6	Basins Revisited. . . . .	35
5.6.1	Basins with Dominant Residual Effects . . . . .	35
5.6.2	Residual Effects in Different Regions . . . . .	36
5.6.3	Regional Differences in $S_{R,5yr}$ and NDVI. . . . .	37
6	Discussion . . . . .	39
6.1	Basin Selection . . . . .	39
6.1.1	Drought Index . . . . .	40
6.2	Change in Runoff Ratio . . . . .	41
6.3	Changes Inside the Budyko Space. . . . .	43
6.3.1	Residual Effects . . . . .	44
6.4	Vegetation Changes . . . . .	44
6.4.1	Storage Deficit . . . . .	45
6.4.2	NDVI. . . . .	45
6.5	Regional Differences . . . . .	45
7	Conclusion . . . . .	47
	Bibliography . . . . .	49
A	Examples of the Drought Periods of the Selected Basins . . . . .	51
B	Examples of the Basins' Movements from Pre- to Post-drought Period . . . . .	53
B.1	Basins that experience an increase in runoff ratio: $\Delta\omega < 0$ . . . . .	53
B.2	Basins that experience a decrease in runoff ratio: $\Delta\omega > 0$ . . . . .	55
C	The Basins' Yearly Changes in Residual Effects Post-drought . . . . .	57
C.1	Basins that experience an increase in runoff ratio: $\Delta\omega < 0$ . . . . .	57
C.2	Basins that experience a decrease in runoff ratio: $\Delta\omega > 0$ . . . . .	59
D	Yearly Changes in NDVI Post Drought . . . . .	61
E	Results of Clustering the Basins Using Changes in NDVI . . . . .	63
F	Results of Clustering the Vegetation-related Variables Using Aridity Index . . . . .	65

# List of Figures

2.1	An illustration of the Budyko framework showing the energy limit, water limit, and the Budyko curve . . . . .	4
3.1	Map showing the locations of catchments in the CAMELS dataset in the United States . . . . .	8
3.2	Basins in the CAMELS dataset plotted inside the Budyko space, after removing the basins that do not meet the long-term water balance . . . . .	9
3.3	Basins in the CAMELS dataset grouped by aridity index . . . . .	9
3.4	Map generated using the NDVI data for basin 12358500 . . . . .	10
4.1	Change in the drought indices SPI, SPEI and SRI over time, for basin number 01047000, using a 24-month accumulation period . . . . .	12
4.2	Differences between SPEI accumulation of 12 months and 24 months, for basin number 01047000 . . . . .	13
4.3	The drought periods selected for basin 01539000, using an accumulation period of 24 months, threshold level of 0 and a minimum drought period of 18 months . . . . .	14
4.4	Fu's equation plotted inside the Budyko space using different values of $\omega$ . . . . .	15
4.5	Illustration of the drought characteristics: duration, intensity and severity . . . . .	17
4.6	Schematic representation of the upward and downward movement of the basin inside the Budyko space . . . . .	18
4.7	Bucket model showing the vegetation related fluxes . . . . .	19
4.8	Illustration of the largest storage deficit . . . . .	20
5.1	Number of basins that meet all selection criteria for different combinations of threshold level, minimum drought period length, and SPEI accumulation period . . . . .	21
5.2	Map showing the locations of the basins selected using threshold level = 1, minimum drought period = 12 months, and SPEI accumulation period = 12 months . . . . .	22
5.3	Long-term averages of the post-drought period and pre-drought period for the selected basins and their fitted $\omega$ values . . . . .	23
5.4	Histogram showing the distribution of the runoff ratio in the pre-drought period, $\omega_0$ . . . . .	24
5.5	Histogram showing the distribution of the runoff ratio in the post-drought period, $\omega_1$ . . . . .	24
5.6	Histogram showing the distribution in the changes in runoff ratio from the pre-drought period to the post-drought period, $\Delta\omega$ . . . . .	24
5.7	Correlation between the change in evaporative index $\Delta E_A/P$ and the change in runoff ratio $\Delta\omega$ . . . . .	24
5.8	Correlation between the change in runoff ratio $\Delta\omega$ and drought duration . . . . .	25
5.9	Correlation between the change in runoff ratio $\Delta\omega$ and drought intensity . . . . .	25
5.10	Correlation between the change in runoff ratio $\Delta\omega$ and drought severity . . . . .	25
5.11	Box plots showing the changes in runoff ratio $\Delta\omega$ for every aridity index . . . . .	26
5.12	Examples of the movements of the basins inside the Budyko space for different aridity indices . . . . .	26
5.13	Movement of the basins inside the Budyko space: basins with an increase in runoff ratio $\Delta\omega < 0$ . . . . .	27
5.14	Radial plot of the magnitude and the direction of movement of the basins inside the Budyko space: basins with an increase in runoff ratio $\Delta\omega < 0$ . . . . .	27
5.15	Movement of the basins inside the Budyko space: basins with a decrease in runoff ratio $\Delta\omega > 0$ . . . . .	28
5.16	Radial plot of the magnitude and the direction of movement of the basins inside the Budyko space: basins with a decrease in runoff ratio $\Delta\omega > 0$ . . . . .	28
5.17	Correlation between the residual effects $\Delta\Psi_r$ and the change in evaporative index $\Delta E_A/P$ . . . . .	28
5.18	Correlation between the residual effects $\Delta\Psi_r$ and the change in runoff ratio $\Delta\omega$ . . . . .	28
5.19	Histogram showing the distribution of the residual effects $\Delta\Psi_r$ , for basins with an increase in runoff ratio $\Delta\omega < 0$ . . . . .	29
5.20	Histogram showing the distribution of the residual effects $\Delta\Psi_r$ , for basins with a decrease in runoff ratio $\Delta\omega > 0$ . . . . .	29

5.21	Box plots showing the residual effects $\Delta\Psi_r$ for every aridity index . . . . .	29
5.22	Box plots showing the absolute ratio between the residual effects and the climate effects $ \frac{\Delta\Psi_r}{\Delta\Psi_c} $ for every aridity index . . . . .	30
5.23	Histogram showing the distribution of the maximum storage deficit $S_{R,5yr}$ . . . . .	31
5.24	Correlation between the maximum storage deficit $S_{R,5yr}$ and residual effects $\Delta\Psi_r$ . . . . .	31
5.25	Correlation between the maximum storage deficit $S_{R,5yr}$ and the change in runoff ratio $\Delta\omega$ . . . . .	31
5.26	Box plots showing the maximum storage deficit $S_{R,5yr}$ for every aridity index . . . . .	32
5.27	Boxplot of NDVI in the before and after drought . . . . .	32
5.28	Histogram showing the distribution of the change in NDVI from the pre-drought period to the post-drought period . . . . .	32
5.29	Correlation between $\Delta\text{NDVI}$ and the residual effects $\Delta\Psi_r$ . . . . .	33
5.30	Correlation between $\Delta\text{NDVI}$ and the change in runoff ratio $\Delta\omega$ . . . . .	33
5.31	Box plots showing the change in vegetation index NDVI for every aridity index . . . . .	33
5.32	Correlation between the maximum storage deficit $S_{R,5yr}$ and the change in NDVI . . . . .	34
5.33	Matrix showing Pearson's correlation coefficient between all variables . . . . .	34
5.34	Correlation between the change in runoff ratio $\Delta\omega$ and drought duration, for basins that experience a decrease in runoff ratio . . . . .	35
5.35	Correlation between the change in runoff ratio $\Delta\omega$ and drought intensity, for basins that experience a decrease in runoff ratio . . . . .	35
5.36	Correlation between the runoff ratio $\Delta\omega$ and drought severity, for basins that experience a decrease in runoff ratio . . . . .	35
5.37	Movement of the basins inside the Budyko space: basins with aridity index $< 0.5$ . . . . .	36
5.38	Radial plot of the magnitude and the direction of movement of the basins inside the Budyko space: basins with aridity index $< 0.5$ . . . . .	36
5.39	Movement of the basins inside the Budyko space: basins with aridity index $> 0.5$ . . . . .	36
5.40	Radial plot of the magnitude and the direction of movement of the basins inside the Budyko space: basins with aridity index $> 0.5$ . . . . .	36
6.1	Selected drought periods for basin 2011460 . . . . .	40
6.2	Selected drought periods for basin 3010655 . . . . .	40
6.3	The change in SPEI and the 3-months average value of $E_A/P$ over the years, for basin 1013500 . . . . .	41
6.4	The correlation between $\Delta\omega$ and $\Delta E_A/P$ , clustered by aridity index . . . . .	42
6.5	The correlation between $\Delta\omega$ and $\Delta E_A/P$ , clustered by aridity index and with outliers removed . . . . .	43
6.6	Movement of basin 1057000 from the pre-drought period to the post-drought period . . . . .	44
6.7	Elevation map showing the altitudes of the selected basins . . . . .	46
A.1	The drought periods selected for basin 1047000 . . . . .	51
A.2	The drought periods selected for basin 1013500 . . . . .	51
A.3	The drought periods selected for basin 1139800 . . . . .	52
A.4	The drought periods selected for basin 1532000 . . . . .	52
A.5	The drought periods selected for basin 3049800 . . . . .	52
B.1	Movement of basin 1022500 . . . . .	53
B.2	Movement of basin 1434025 . . . . .	53
B.3	Movement of basin 1510000 . . . . .	54
B.4	Movement of basin 12358500 . . . . .	54
B.5	Movement of basin 1055000 . . . . .	54
B.6	Movement of basin 1030500 . . . . .	55
B.7	Movement of basin 1139000 . . . . .	55
B.8	Movement of basin 3500000 . . . . .	55
B.9	Movement of basin 12010000 . . . . .	56
B.10	Movement of basin 14187000 . . . . .	56
C.1	Change in average $\Delta\Psi_r$ for every year in the post-drought period: basins with $\Delta\omega < 0$ . . . . .	57
C.2	Yearly movement of basin 211180 . . . . .	58
C.3	Yearly movement of basin 3161000 . . . . .	58
C.4	Yearly movement of basin 3464400 . . . . .	58

---

C.5	Change in average $\Delta\Psi_r$ for every year in the post-drought period: basins with $\Delta\omega > 0$ . . . . .	59
C.6	Yearly movement of basin 1030500 . . . . .	59
C.7	Yearly movement of basin 2015700 . . . . .	60
C.8	Yearly movement of basin 4213075 . . . . .	60
D.1	Average NDVI for every year in the post-drought period . . . . .	61
E.1	The correlation between $\Delta\omega$ and $\Delta E_A/P$ , clustered using $\Delta\text{NDVI}$ . . . . .	63
E1	The correlation between $S_{R,5yr}$ and $\Delta\omega$ , clustered using the aridity index . . . . .	65
E2	The correlation between $S_{R,5yr}$ and $\Delta\text{NDVI}$ , clustered using the aridity index . . . . .	66



# List of Tables

4.1	Index values per category . . . . .	11
4.2	Table showing the range of Pearson's correlation coefficient $r$ . . . . .	17
5.1	Table showing the number of basins per aridity index, for the basins selected using threshold level = 1, minimum drought period = 12 months, and SPEI accumulation period = 12 months . .	22
5.2	Correlation coefficient $r$ between $S_{R,5yr}$ and $\Delta\Psi_r$ . . . . .	37
5.3	Correlation coefficient $r$ between $S_{R,5yr}$ and $\Delta\omega$ . . . . .	37
5.4	Correlation coefficient $r$ between $\Delta\text{NDVI}$ and $\Delta\Psi_r$ . . . . .	37
5.5	Correlation coefficient $r$ between $\Delta\text{NDVI}$ and $\Delta\omega$ . . . . .	37
5.6	Correlation coefficient $r$ between $S_{R,5yr}$ and $\Delta\text{NDVI}$ . . . . .	37



# Nomenclature

$\overline{P}$	Mean annual precipitation	[mm/d]
$\overline{E_A}$	Mean annual actual precipitation	[mm/d]
$\overline{Q}$	Mean annual runoff	[mm/d]
$Q$	Runoff	[mm]
$\overline{E_P}$	Mean annual potential evaporation	[mm/d]
$P$	Precipitation	[mm]
$P_e$	Effective precipitation	[mm]
$E_A$	Actual evaporation	[mm]
$E_P$	Potential evaporation	[mm]
$E_i$	Evaporation due to interception	[mm]
$E_t$	Evaporation due to transpiration	[mm]
$\overline{E_t}$	Long-term average evaporation due to transpiration	[mm]
$\frac{dS}{dt}$	Change in storage over time	[mm/s]
$S_D$	Daily storage deficit	[mm]
$S_{R,5yr}$	5-year maximum storage deficit	[mm]
$\Delta S$	Change in water storage	[mm]
SPI	Standard Precipitation Index	[-]
SPEI	Standard Precipitation Evaporation Index	[-]
SRI	Standard Runoff Index	[-]
$E_A/P$	Evaporative index of Budyko's Framework	[-]
$\Delta E_A/P$	Difference in $E_A/P$ between pre-drought and post-drought	[-]
$E_P/P$	Aridity index of Budyko's framework	[-]
$\omega$	Free parameter of Fu's equation	[-]
$\omega_0$	Free parameter of Fu's equation in the pre-drought period	[-]
$\omega_1$	Free parameter of Fu's equation in the post-drought period	[-]
$\Delta\omega$	Difference between $\omega_1$ and $\omega_0$	[-]
$\Delta\Psi$	Change in evaporative index from the pre-drought period to the post-drought period	[-]
$\Delta\Psi_r$	Residual effects	[-]
$\Delta\Psi_c$	Climate effects	[-]
$r$	Magnitude of the movement inside the Budyko space	[-]
$\theta$	Direction of the movement inside the Budyko space	[-]
NDVI	Normalized Difference Vegetation Index	[-]
$\Delta\text{NDVI}$	Difference in NDVI between pre-drought and post-drought	[-]



# 1

## Introduction

Drought is one of the most commonly occurring natural disasters that have become more extreme, more frequent, and less predictable due to climate change (Strzepek et al., 2010). According to predictions of the United Nations, by 2030, 700 million people worldwide are at risk of leaving their homes as a consequence of droughts<sup>1</sup>. This can lead to significant short and long-term economic and social losses. The United States is one of the many countries that has suffered greatly from the consequences of drought. Economically, a drought event costs the country 9.6 billion dollars on average<sup>2</sup>. This sum is of course much higher during the historic dry spell in 2012 which affected two-thirds of the country, and from 2012 to 2016 where California has undergone the worst drought in 1200 years<sup>2</sup>.

Another natural disaster that is aggravated by climate change are floods, which occur as a result of the increase in the frequency and intensity of precipitation extremes (Davenport et al., 2021). In the United States, evidence has shown an increased flooding frequency that results from changes in temperature and seasonal precipitation (Mallakpour and Villarini, 2015). Floods add to the economic and social costs that droughts have already created, making matters even worse.

Interestingly, it is observed that there is an increasing trend in the occurrence of abrupt drought-flood alternations in the 21st century (Zhao et al., 2020b). Flood and drought events are both the results of climate change, but little research has been done on whether they are independent of each other. It is not clear whether long-term droughts also affect floods. The question thus arises: Do multi-year droughts increase floods?

It may be possible to answer this question by studying the role of vegetation in the hydrological partitioning of catchments. Driven by higher temperatures, higher evaporation and lower precipitation that are characteristic for droughts (Dai, 2013), the photosynthetic activity of plants can be influenced, which in turn has an effect on the plant productivity (Zhang et al., 2016). After a prolonged period of severe drought, a shift in vegetation can occur (Mueller et al., 2005). This vegetation shift can have an impact on the hydrological response of the catchment to precipitation in the post-drought period, potentially increasing the chance of flooding.

To be able to start this research, the word 'drought' first needs to be defined. In 2012, Sheffield and Wood has defined drought as 'A deficit of water compared with normal conditions'. However, due to its complexity, there is no universally accepted definition for drought (Esfahanian et al., 2016). Based on the characteristics of droughts, they can be classified into several categories, which include meteorological droughts, hydrological droughts, and agricultural droughts. Meteorological droughts take place when dry weather patterns are observed. Over time, this leads to a decrease in water supply, also known as hydrological drought. Agricultural droughts happen when the soil moisture becomes insufficient for the growth of crops. Droughts can further be classified into short-term and long-term droughts based on their timescales. Short-term droughts last from several weeks to several months, whereas long-term droughts last for more than six months.

---

<sup>1</sup>URL <https://www.unccd.int/actions/drought-initiative> [cited 17/02/2021]

<sup>2</sup>URL <https://www.nrdc.org/stories/drought-everything-you-need-know> [cited 17/02/2021]

This research focuses on meteorological droughts, which are characterized by a period of below-normal precipitation and above normal temperatures (Lyon et al., 2012). Furthermore, this research focuses on multi-year droughts that are at the extreme end of long-term droughts, which more specifically, are prolonged periods of meteorological droughts that last for longer than 12 consecutive months. On the other hand, flood is represented by the runoff ratio, which is the proportion of precipitation that is not used for evaporation and ended up as runoff. The higher the runoff ratio, the higher the chance of flood.

### **1.1. Research question**

The goal of this research is to investigate whether a link can be established between multi-year droughts and the floods that occur in the post-drought period. To do so, the United States is chosen as a case study area. Using the data collected for this area, the change in runoff ratio between and after drought is investigated, followed by a study on the effects of drought on the partitioning of the hydrological fluxes and vegetation. The hypothesis is that drought decreases vegetation and decreases evaporation, which increases the runoff ratio and causes floods.

The main research question is, therefore: Is there a relationship between multi-year droughts and the floods that occur in the post-drought period in the United States?

To answer this main question, the following sub-research questions can be established:

- Do long-term droughts lead to an increase in the runoff ratio in the post-drought period as compared to the pre-drought period?
- Is vegetation the main driver for the change in the precipitation partitioning in the post-drought period?
- Can a correlation be found between vegetation changes and runoff ratio?
- What are the regional differences in the results?

### **1.2. Report Structure**

This report starts with a short literature study, where the relevant concepts and past researches are explored and described. The literature study is the foundation of this research, as it is used as guidance in formulating the research methodology.

Next, data is collected for the case study area. This includes hydrological data as well as remote sensing data. Data pre-processing is done to preliminarily sort and structure the data. This data is then used in the various calculations described in the 'Methodology' section, to systematically find answers to the research questions.

The outcome of the methodology is presented in the section 'Results', followed by a discussion. Finally, conclusions are drawn based on the results, and the research questions are answered.

# 2

## Literature Study

In this chapter, the literature that is relevant to this research is described. The goal of this literature study is to obtain the background knowledge that can be used as guidance in formulating the research methodology.

### 2.1. Meteorological Drought Indices

To identify the drought period and to quantify the severity of drought, different drought indices can be used. These drought indices indicate how much a flux, such as precipitation or runoff, departs from its normal conditions. Similar to the definition of drought, there is no single perfect universal drought index.

One of the most commonly used meteorological drought indices is the Standard Precipitation Index (SPI). SPI is calculated using only monthly precipitation data as an input. To achieve optimal performance, data for at least a continuous period of 30 years is needed. The advantage of SPI is that it is spatially invariant, which allows for comparisons between different climate zones. (McKee et al., 1993)

The Standard Precipitation Evaporation Index (SPEI) is another drought index that is built on top of SPI. These indices are very similar, with the exception that SPEI also takes the potential evaporation into account. This way, SPEI can capture the impacts of temperature on water demand.

Another drought index that is computed similarly is the Standard Runoff Index (SRI), with the difference being that runoff is used as the variable. The advantage of SRI is that the seasonal influences on streamflow are incorporated into the index. (Shukla and Wood, 2008)

### 2.2. Drought Identification

Using drought indices, the intensity, severity, and duration of drought events can be identified. A negative index value indicates drier conditions relative to the average long-term states. According to Schwalm et al. (2017), a drought event starts when the drought index value is lower than -1 for at least 3 consecutive months and ends the moment it becomes higher than -1 again. However, amongst different researches with different objectives, the threshold index value for which drought starts and ends varies from 0 to -2.

The duration of the drought period is the cumulative amount of time when the index is continuously below a threshold level, which can range from several months to several years (Mishra and Singh, 2010). The intensity of the drought is described by the average value of the drought index below the threshold level over the drought period. The lower the average, the more intense the drought.

Other characteristic parameters of drought include drought magnitude and drought severity. Drought magnitude is calculated as the sum of the drought index values, of the months within the drought event (Morid et al., 2006), whereas drought severity is the strength of the drought, measured by the total area below the threshold level within the drought period (Hayes et al., 2011).

### 2.3. Drought Recovery

When a large amount of precipitation has fallen that alleviates the water deficit, it means that drought has ended and that drought recovery has started. Drought recovery is the amount of time a basin needs to revert to its pre-drought state, and it is dependent on the rate at which the water deficit from the initial conditions are minimized (Schwalm et al., 2017). Therefore, a direct relationship exists between drought recovery time and drought intensity: the more intense the drought, the longer the recovery time (DeChant and Moradkhani, 2015).

In the current literature, contradictions exist in drought recovery time estimations. Liu et al. (2019) have found that the contradictions are mainly caused by the differences in the method of drought identification and the definition of drought recovery level. In a recent research done by Peterson et al. (2021), they have found that some catchments that undergo severe, long-term droughts, may never recover.

Furthermore, vegetation can be affected by droughts, and its ability to respond to drought events play a role in drought recovery. Anderegg et al. (2015) have found that after severe droughts, forests display a 'legacy effect', where a reduced growth is observed for 1 to 4 years following the drought event. This has an impact on the recovery time as well as the speed of recovery.

### 2.4. Budyko Framework

The Budyko framework (Budyko et al., 1974) is used to represent the long-term water balance of catchments, by partitioning the mean annual precipitation into evaporation and runoff. For every catchment, the ratio between the actual evaporation and precipitation (evaporative index) can be written as a function of the ratio between potential evaporation and precipitation (aridity index).

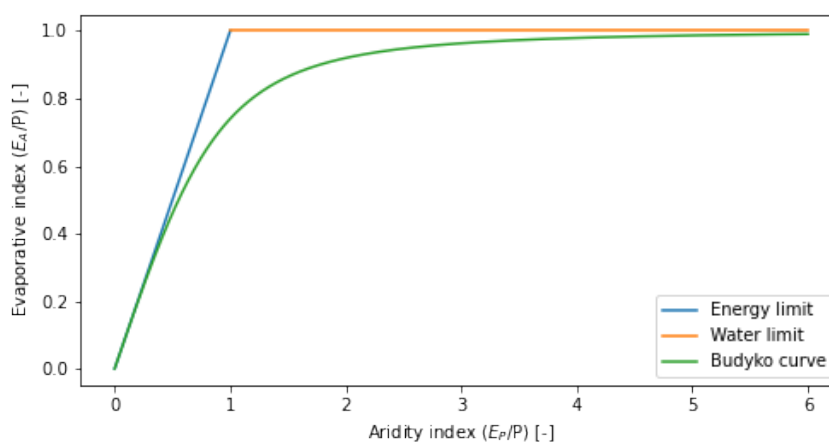


Figure 2.1: An illustration of the Budyko framework showing the energy limit, water limit, and the Budyko curve

A visual representation of the Budyko framework is shown in figure 2.1. According to Budyko, all catchments are bounded by the energy limit and the water limit, which respectively represents the amount of energy and water available for evaporation. Under dry conditions, evaporation is limited by water availability, which is precipitation. Under wet conditions, evaporation is limited by the available energy, which is the potential evaporation.

When the aridity index is below 1, potential evaporation is smaller than precipitation, meaning that the evaporative index has to be smaller than the aridity index since actual evaporation can never be larger than potential evaporation. When the potential evaporation is larger than precipitation at an aridity index of larger than 1, the evaporative index is bounded by the water limit, as the evaporation can never be larger than precipitation.

The Budyko framework can be used to detect and predict changes. Based on this framework, different models are made to estimate the mean annual evaporation of the basins by describing the relationship between the evaporative index and the aridity index. To do so, in 1974, Budyko et al. came up with the Budyko equation used to plot the Budyko curve:

$$\frac{E_A}{P} = \left[ \frac{E_P}{P} * \tanh \left( \frac{1}{\frac{E_P}{P}} \right) \left[ 1 - \exp \left( -\frac{E_P}{P} \right) \right] \right]^{1/2} \quad (2.1)$$

In the following years, several other equations are developed that show a similar trend as the Budyko equation, whilst also taking the catchment characteristics into consideration. These include the equations developed by Fu (1981), Zhang et al. (2001), and Pike (1964).

### 2.4.1. Runoff Ratio

One of the formulas that aims to describe the relationship between the evaporative index and the aridity index is the equation of Fu (Fu, 1981), as can be seen in equation 2.2. For small values of  $E_A/P$ ,  $E_P/P$  is expected to increase linearly with  $E_A/P$ . However, as  $E_A/P$  gradually becomes larger, the rate of increase of  $E_P/P$  decreases, until it reaches the water limit where it becomes constant. Thus, Fu's equation can be used to detect changes in the runoff ratio.

$$\frac{E_A}{P} = 1 + \frac{E_P}{P} - \left[ 1 + \left( \frac{E_P}{P} \right)^\omega \right]^{\frac{1}{\omega}} \quad (2.2)$$

Fu's equation expresses the partitioning of rainfall into runoff and evaporation. This equation contains a free parameter,  $\omega$ , which has no physical meaning. However, it can be used as an indicator for the characteristics of catchments. A large value of  $\omega$  indicates that for a given aridity index, a small fraction of the precipitation in the basin becomes runoff, which leads to large actual evaporation. The opposite is true for a small value of  $\omega$ , as it is associated with low water storage capacity and low plant availability. (Zhang et al., 2004). Thus, Fu's equation can be used to detect changes in the runoff ratio.

### 2.4.2. Changes in Hydrological Fluxes

Apart from detecting changes in the rainfall-runoff relationship, Budyko's framework can also be used to detect changes in other hydrological fluxes. Worldwide, it has been used in many different countries to study the effects of forest controls on the partitioning of water. By studying the changes in the evaporative ratio, it is possible to detect the effects of forest changes on evaporation. (Jaramillo et al., 2014)

Inside the Budyko space, the changes in evaporative ratio can be separated into climate effects and residual effects. The climate effects on evaporation are related to changes in aridity index, which is mainly affected by changes in precipitation and surface air temperature (Kundzewicz et al., 2008). The residual effects on the other hand, are related to other drivers of change related to the landscape, such as increased water usage by humans and vegetation changes (Jaramillo et al., 2018).

To separate the change inside the Budyko space into climate and residual effects, 2 periods need to be defined. For the first period, an equation describing the Budyko curve (such as Fu's equation) is fitted to the aridity index and evaporative index. For the second period, a point is plotted in the Budyko space and the movement of this point relative to the curve of the first period is calculated. (Jaramillo et al., 2018)

## 2.5. Post-drought Vegetation Changes

Vegetation plays an important role in the partitioning of hydrological fluxes, such as transpiration, evaporation, canopy interception, and runoff. Due to drought, changes in vegetation productivity can influence these fluxes and therefore, change the proportion of precipitation that turns into evaporation and runoff.

In the current literature, contradictions exist in the response of vegetation to drought. Depending on the can the dynamics of the forest, vegetation can either aggravate or mitigate the response of catchments to drought, which may either increases or decreases the runoff ratio (Vose et al., 2016). Certain tree species may exhibit higher tolerance to drought than others, showing little changes in the hydrological fluxes post-drought. Drought can also cause a shift in the density of the biomass as well as the type of vegetation growing in the catchment, which can lead to differences in the drought response per catchment.

An attempt to find the relationship between vegetation cover and runoff is made by Bosch and Hewlett (1982). They have investigated the response of vegetation for 94 catchments for 5 years, and have found that a decrease in forest cover leads to an increase in water yield and vice versa. Different plant species also lead to different magnitudes of effects. For a 10% change in the forest cover, it is found that:

- Coniferous and eucalypt plants cause around 40mm change in the annual runoff
- Deciduous hardwood trees cause around 25mm change in the annual runoff
- Bushes and grasslands cause around 10mm change in the annual runoff

This is supported by Bruijnzeel (1989). They have found that different types of vegetation lead to different balances between surface infiltration and evaporation. Thus, vegetation type plays a key role in the runoff response after changes in forest biomass. Furthermore, runoff also depends on the water storage capacity of the soil and the natural climate variabilities (Bruijnzeel, 1989; Vertessy, 1999).

However, in 2013, Vicente-Serrano et al. found that after drought, a different type of plant spices that is more resistant to drought can become more dominant. This has lead to a decrease in the runoff. Moreover, the increase in carbon dioxide due to climate change can also increase plant biomass, as well as the plant's water use efficiency (IF et al., 2010).

The post-drought runoff changes also vary depending on the region and the time scale. Differences exist in the way arid and humid basins respond to drought, and the amount of time the catchment needs to adjust its flow behavior. (Vertessy, 1999; Vicente-Serrano et al., 2013)

In arid areas and humid areas, fast response to short-term drought is detected. The vegetation reacts immediately as soon as the water availability falls below normal conditions. Plants in semi-arid and semi-humid regions are responsive to long-term droughts. These plants can withstand long-term water shortage, but they also respond slowly to the changing hydrological conditions (Vicente-Serrano et al., 2013). However, in 2015, Saft et al. have found that long-term droughts are more likely to affect the rainfall-runoff relationship in drier, less forested regions.

# 3

## Study Area and Data

This chapter gives an overview of the data collected for this research. First, a case study area is selected, followed by a description of the hydrological time-series and the remote sensing data. To make the data easier to use, preliminary data processing is carried out and the methods to do so are described.

### 3.1. Case Study Area

The case study area of this research is the United States, as it is a country that is severely affected by droughts as well as floods. Furthermore, the United States is a large country with different climates and diverse vegetation. The unique characteristics of each climate zone will most likely respond differently to drought and flood, which allows for regional comparison.

#### 3.1.1. Basin Locations

In this research, 671 basins across the United States are used for preliminary research. The basins are small to medium-sized, with an average area of  $336 \text{ km}^2$ . From the large number of basins in the US, these basins are selected by Newman et al. (2015) for the CAMELS (Catchment Attributes and Meteorology for Large-sample Studies) database, as an attempt to develop a large sample hydro-meteorological dataset for the United States. The CAMELS dataset is gridded, with a spatial resolution of  $1 \times 1 \text{ km}^2$ . The data is also calibrated and peer-reviewed.

This dataset is chosen because it contains at least 30 years of data. The basins represent natural flow conditions and are minimally influenced by human activities. The locations of these basins are shown in figure 3.1.

### 3.2. Hydrological Data

For the basins selected in this study, different hydrological data are collected. The hydrological time-series collected for this research include:

- Precipitation
- Potential evaporation
- Runoff

The data is sampled every day, starting from around the year 1980 until 2014. However, the exact length of the data varies per catchment.

The precipitation and runoff amounts are measured. The potential evaporation is estimated using the Priestly-Taylor method, as described by Newman et al. (2015), and are therefore the model output of their study.

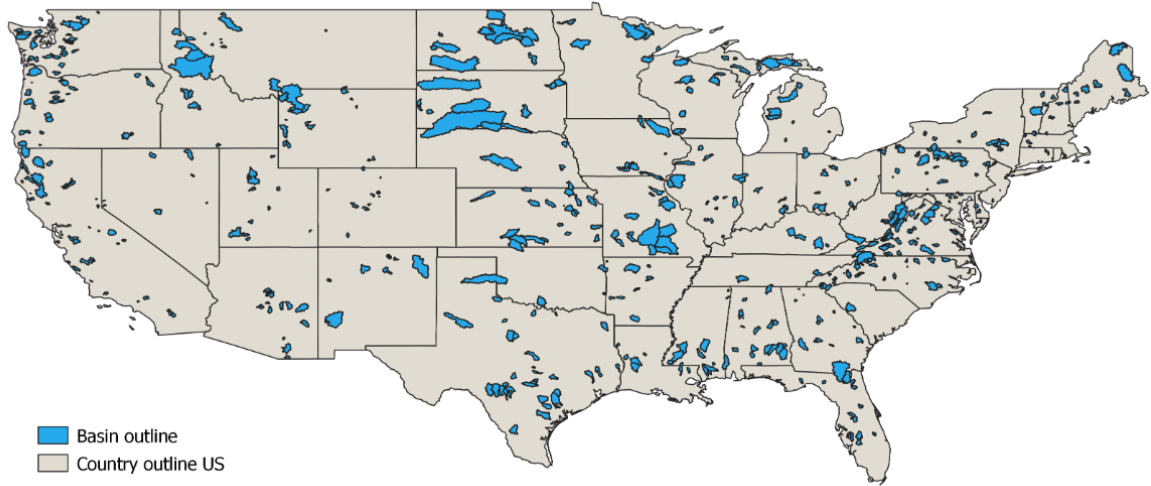


Figure 3.1: Map showing the locations of catchments in the CAMELS dataset in the United States

### 3.2.1. Long-term Water Balance

The basins selected in the previous section should satisfy the condition of long-term water balance. If the water balance is not closed, it means that errors exist in the data, or that some water is not taken into consideration. Therefore, these basins should be excluded from the dataset.

To check the water balance, the parameters needed are precipitation, potential evaporation, and runoff. The equation of the long-term water balance is given in equation 3.1 and the entire duration of the time series is used to test this balance.

$$\overline{P} - (\overline{E}_A + \overline{Q}) + \Delta S = 0 \quad (3.1)$$

Where:

$\overline{P}$  = mean annual precipitation [mm/d]

$\overline{E}_A$  = mean annual actual evaporation [mm/d]

$\overline{Q}$  = mean annual runoff [mm/d]

$\Delta S$  = change in water storage [mm]

Since water balance is calculated for a long time period, the change in water storage within the basin,  $\Delta S$ , is assumed to be small and therefore can be neglected.

Furthermore, data on actual evaporation is not available. This means that potential evaporation can be used instead as it is always bigger or equal to the actual evaporation. The sum of discharge and actual evaporation should also be smaller than precipitation. The long-term water balance thus becomes:

$$\overline{P} - \overline{E}_p - \overline{Q} < 0 \quad (3.2)$$

Where  $\overline{E}_p$  is the mean annual potential evaporation [mm/d].

To illustrate this, the basins are plotted inside the Budyko space. In the long run, all catchments should stay within the water limit and the energy limit. Basins that do not meet this requirement are taken out of this research.

To plot the basins in the Budyko space, actual mean annual evaporation  $\overline{E}_A$  is needed. This is estimated with equation 3.3. The conditions for the evaporative index are given in equation 3.4.

Of the 671 basins, 659 satisfy the requirements of the long-term water balance. These basins are plotted in figure 3.2 in the Budyko space.

$$\overline{E_A} = \overline{P} - \overline{Q} \quad (3.3)$$

$$0 \leq \frac{E_A}{P} \leq \begin{cases} \frac{E_P}{P}, & \text{if } \frac{E_P}{P} \leq 1 \\ 1, & \text{if } \frac{E_P}{P} > 1 \end{cases} \quad (3.4)$$

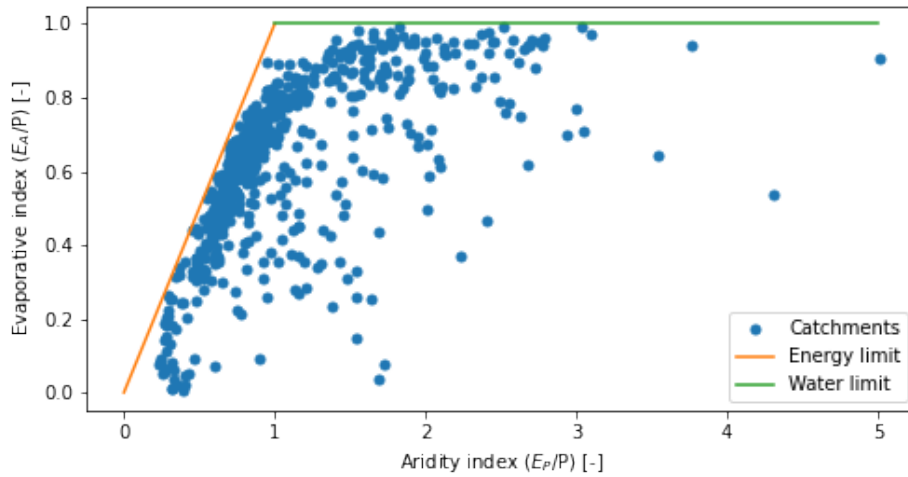


Figure 3.2: Basins in the CAMELS dataset plotted inside the Budyko space, after removing the basins that do not meet the long-term water balance

### 3.2.2. Aridity Level Classification

Based on the aridity index, different groups can be made where each group represents a specific aridity level. In this research, the aridity index is grouped using intervals of 0.1. For example, all basins that have an aridity index of 0 - 0.1 belong to the first group, where they are located in the most humid regions. All basins with an aridity index of 0.1 - 0.2 belong to the second group, in a slightly less humid area. This is done for all basins in the catchment.

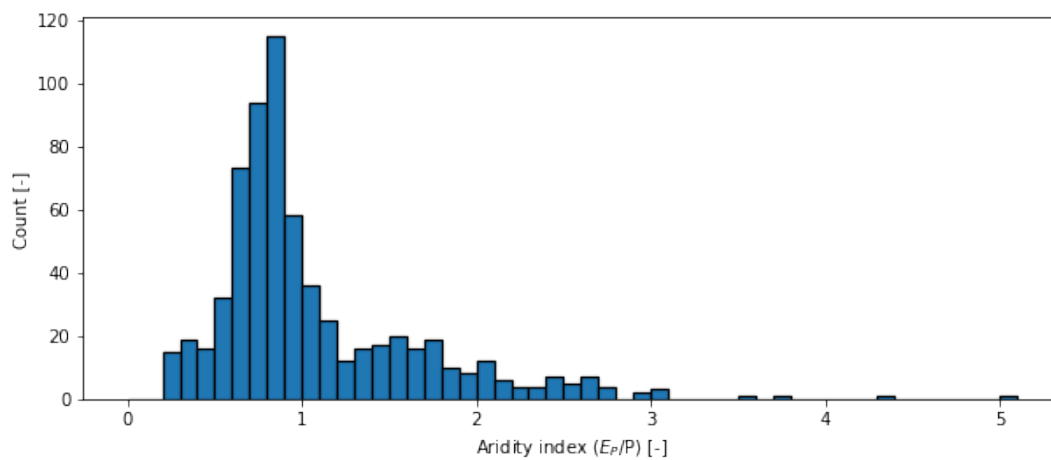


Figure 3.3: Basins in the CAMELS dataset grouped by aridity index

As can be seen in figure 3.3, most basins in the dataset are located in relatively humid climates, with an aridity index below 1.5.

### 3.3. Remote Sensing Data

To measure the density of the vegetation, the Normalized Difference Vegetation Index (NDVI) is used. The NDVI is an indicator that analyzes remote sensing measurements from satellites and it detects whether the targeted surface contains healthy live green vegetation. The value of NDVI ranges from -1 to 1, where values approaching -1 correspond to water. Values close to 0 (around -0.1 to 0.1) correspond to barren surfaces such as sand, snow, or rock, and higher values of around 0.6 - 0.8 indicate dense vegetation found in tropical forests.

To obtain the NDVI for the basins, the shapefile of the basins is first downloaded from the CAMELS dataset to obtain the geometry and the coordinates of the basins. Next, data from the satellite AVHRR (Advanced Very High Resolution Radiometer) is extracted using Google Earth Engine. The AVHRR contains long-term NDVI data, from June 1981 to 2019, which matches the length of the CAMELS dataset. The NDVI data has a temporal resolution of 1 day and a spatial resolution of  $5.5 \times 5.5 \text{ km}^2$ .

For a given time period, the average values of every pixel inside the basins are calculated, which yields a NDVI map. An example of this is shown in figure 3.4.

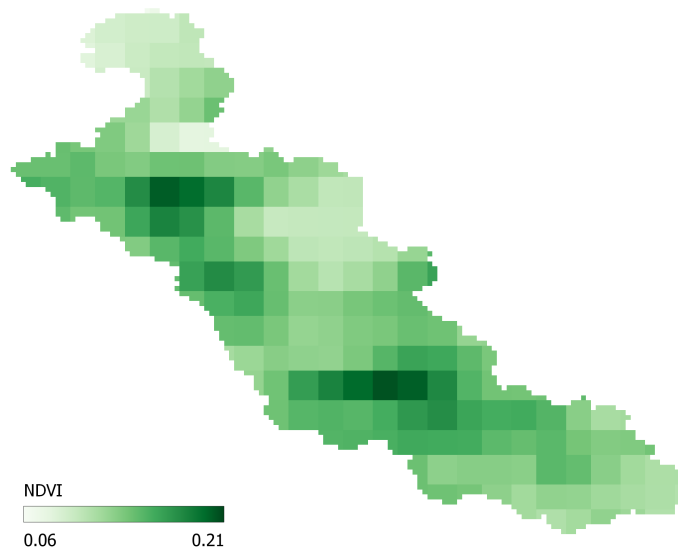


Figure 3.4: Map generated using the NDVI data for basin 12358500

# 4

## Methodology

In this chapter, the methodology used to answer the research questions is described and explained. First, drought is defined using a drought index and set of criteria. This yields three time periods: the pre-drought period, the drought period, and the post-drought period. Next, the changes in runoff ratio before and after the drought are investigated, followed by the changes in vegetation. For the basins that display relatively big changes, a more detailed analysis is carried out to find the potential reasons for these changes.

### 4.1. Drought Index

To determine the drought period and to define drought, three different drought indices are calculated using the time-series of the basins. Their results are compared and the index that shows the best performance is chosen. The indices are:

- Standard Precipitation Index (SPI)
- Standard Precipitation Evaporation Index (SPEI)
- Standard Runoff Index (SRI)

SPI, SPEI, and SRI indicate how wet or dry a specific month is relative to the entire duration of the dataset. The different categories are shown in table 4.1. These indices can be used to determine the duration and the magnitude of the drought conditions relative to the basins' normal conditions.

Categories	Index Value
Extremely wet	more than 2.00
Very wet	1.50 to 1.99
Moderately wet	1.00 to 1.49
Near normal	-0.99 to 0.99
Moderately dry	-1.00 to -1.49
Severely dry	-1.50 to -1.99
Extremely dry	less than -2.00

Table 4.1: Index values per category

The computation of these indices is similar. The method is based on the concept of SPI calculation, illustrated by McKee et al. (1993). The following steps are taken to calculate the drought indices:

1. For the entire time-series, the daily precipitation, potential evaporation, and runoff data are resampled into mean monthly values.
2. For the calculation of SPI, take the rolling sum of the monthly precipitation, for  $i$  months (where  $i$  is 12 or 24 months). This is known as the accumulation period. The accumulation period represents the time scales for which the precipitation deficit would have an effect on other water fluxes. The rolling

sum means that for each month, a new value is determined from the previous  $i$  months. For SRI, take the rolling sum of runoff. For SPEI, take the rolling sum of the difference between  $P$  and  $E_P$ .

3. Fit an extreme value distribution through the rolling sums using its parameters (the maximum likelihood estimate of shape and scale) to estimate the cumulative probabilities of the values. The gamma distribution is used here. The extreme value distribution yields the probability of  $P$  (SPI),  $P - E_P$  (SPEI), or  $Q$  (SRI).
4. Transform the cumulative probabilities into a standard normal deviate with a mean of 0 and a standard deviation of 1 using a percentage point function. This will give the monthly values of the index of choice, which is the probability of the variable ( $P$ ,  $P - E_P$  or  $Q$ ) being less or equal to its normal value.

Plotting SPI, SPEI and SRI for different catchments shows that SPI and SPEI yield very similar results. SRI follows the same general pattern as SPI and SPEI, but does not display an exact match. An example of this is shown in figure 4.1. As mentioned in section 2.1, SPEI is able to capture the effects of temperature on water demand, which makes it more sophisticated than the other two indices. Thus, SPEI is the drought index used in this research.

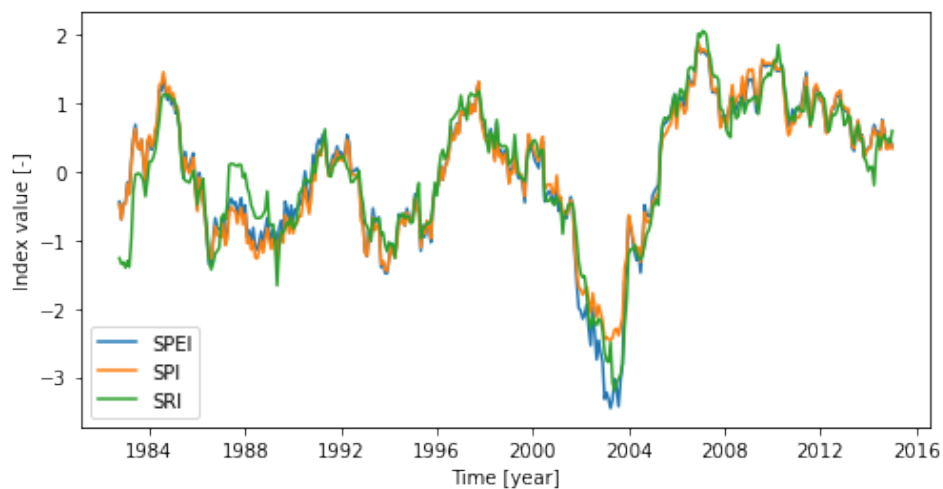


Figure 4.1: Change in the drought indices SPI, SPEI and SRI over time, for basin number 01047000, using a 24-month accumulation period

#### 4.1.1. Accumulation Period

Comparing the different accumulation periods for the basins, it can be observed that a shorter accumulation period displays more fluctuations in the index, as it reacts more quickly to the changes in water fluxes. The duration of the drought period is thus shorter, as a short, relatively wet period can lead to a big increase in the value of SPEI, which ends the drought. On the contrary, a longer accumulation period has a slower reaction time but can have a bigger time lag between when drought happens and when drought is detected. Figure 4.2 shows the differences between two accumulation periods: 12 months and 24 months.

Since each accumulation period has its advantages and disadvantages, both will be used in determining the drought period. This is elaborated further in section 4.2.

## 4.2. Basin Selection

In this research, there are 3 time periods that are taken into consideration:

- Pre-drought period
- Drought period
- Post-drought period

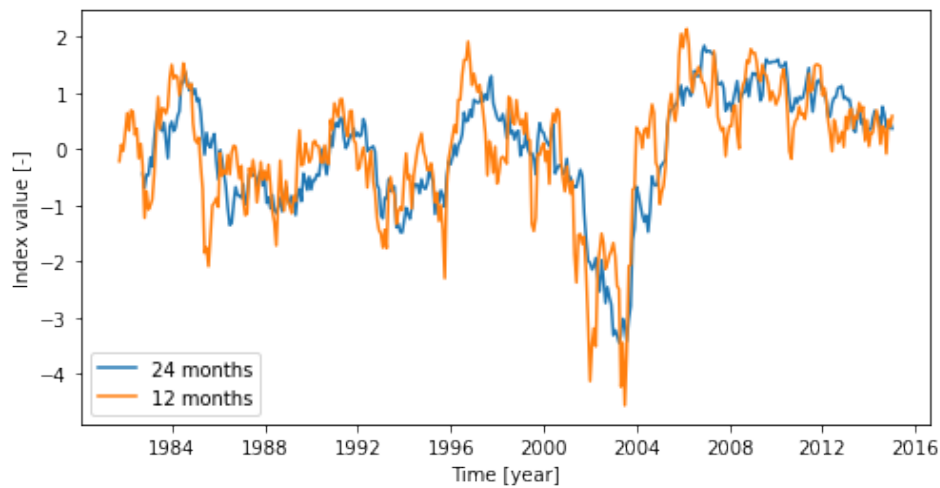


Figure 4.2: Differences between SPEI accumulation of 12 months and 24 months, for basin number 01047000

To find these periods, different criteria are established. This, for example, includes conditions related to duration, the value of SPEI, and data availability. The basins are filtered based on these criteria and ones that do not meet the requirements are taken out of this research.

When filtering the basins, there are 3 variables that can greatly influence the results: the accumulation period, threshold level, and the minimum drought period duration. Different values of these variables will lead to a different total number of basins that meet the selection criterion. However, it is unclear what the optimal combination of parameters is. Thus, different values are given to these variables and the results are compared. The one combination of parameters that leads to the highest number of basins is used.

#### 4.2.1. Drought Period

As shown in table 4.1, drought happens when SPEI is negative. Therefore, the starting point of the drought period is set to when SPEI reaches below a certain threshold level. In this case, the threshold level is a fixed value for the entire time-series of the basin, and it is set to 0, -0.5 or -1.

According to literature, drought ends when SPEI goes above the threshold again. However, in this research, the drought period lasts until the turning point of SPEI, which is the moment when the value of SPEI starts to show an increasing trend and begins its climb towards wet conditions. When SPEI starts to continuously increase, it means that a large amount of precipitation has fallen, which ends the drought period and starts the recovery process.

Moreover, since this research focuses on multi-year, long-term droughts, a minimum value should be given to the duration of the drought period. This minimum is set at 12, 18, and 24 months. In case multiple drought periods exist within the same basin that fulfill all criteria, the longest one is used.

#### 4.2.2. Pre-drought and Post-drought Period

Now that the drought period is established, the pre-drought period and the post-drought period can be defined. In this case, they are defined as the 5 consecutive years before and after the drought period, respectively. However, this definition leads to another criterion in drought definition, which is data availability. Data should be available for the entire 5 years before and after the drought. Otherwise, the basin is taken out of this study.

Furthermore, to ensure the reliability of the data, no other drought events can exist within the pre-drought period nor the post-drought period. During these periods, the value of SPEI should also generally stay above the threshold value.

### 4.2.3. Criteria Overview

In summary, the selection criteria for the drought period, pre-drought period, and the post-drought period are:

- The drought period starts when SPEI falls below the threshold level.
- The drought period lasts until the turning point of SPEI, before which it increases again.
- The duration of the drought period has to be longer or equal to the defined minimum length.
- The pre-drought period and the post-drought period are 5-years before and after the starting point and the ending point of drought. Data needs to be available for these 5 years.
- The pre-drought period and the post-drought period cannot overlap another drought event.
- In the 5-year pre-drought period, there cannot be more than 12 months for which SPEI is below the threshold.
- In the 5-year post-drought period, there cannot be more than 24 months for which SPEI is below the threshold.
- In case there are multiple drought periods within the same basin, the longest one is chosen

The variables adjusted include:

- Threshold level at SPEI being equal 0, -0.5, and -1
- Minimum drought period length at 12, 18, and 24 months
- SPEI accumulation period at 12 and 24 months

An example of these criteria applied to a basin is shown in 4.3

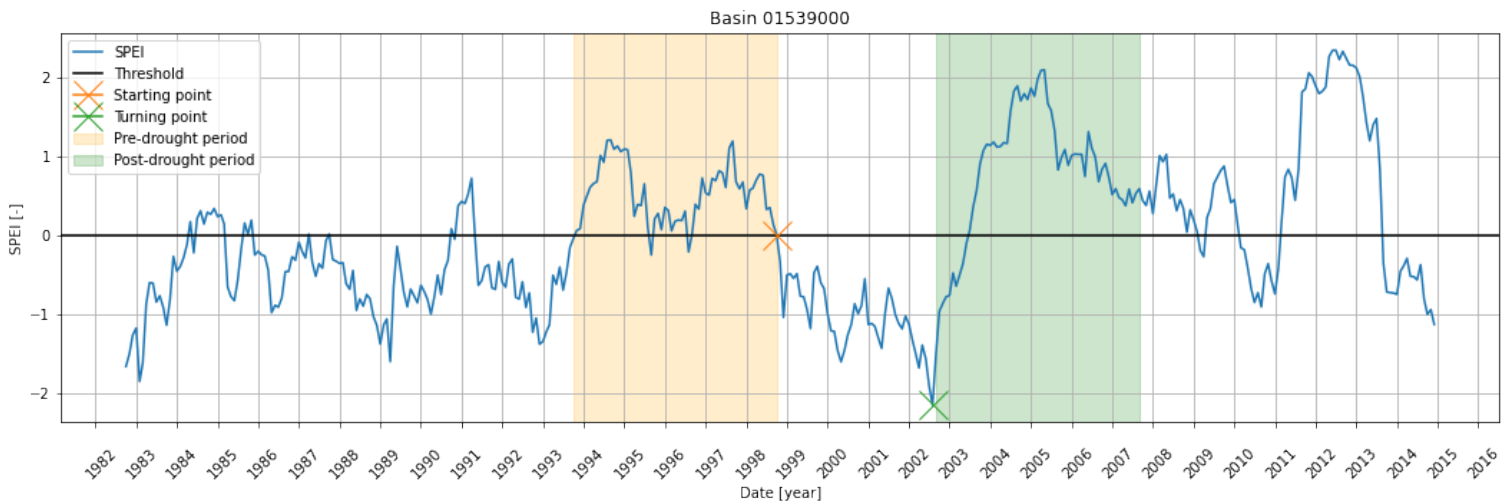


Figure 4.3: The drought periods selected for basin 01539000, using an accumulation period of 24 months, threshold level of 0 and a minimum drought period of 18 months

### 4.3. Changes in Runoff Ratio

Only basins that fulfill all criteria mentioned in the previous section are used in the rest of the analysis. First, research is done to find out whether changes in runoff ratio are detected. This is done by fitting Fu's equation to the pre-drought period and the post-drought period to obtain the free parameters  $\omega_0$  and  $\omega_1$  for every basin. Next, the Wilcoxon Rank-sum test is carried out to see if the changes in  $\omega$  are statistically significant.

To explore the relationship between drought and runoff ratio, the correlation between the drought characteristics and the change in  $\omega$  is investigated.

The hypothesis is that drought does increase flood. This means that a decrease in Fu's parameter  $\omega$  should be observed, the null hypothesis of the Rank-sum test is accepted and a strong correlation is found between the drought characteristics and the change in  $\omega$ .

#### 4.3.1. Fitting Fu's Equation

As mentioned in section 2.4.1, the relationship between the evaporative index and the aridity index can be described using Fu's equation, which is shown in equation 2.2.

In Fu's equation, the free parameter  $\omega$  can be used to indicate changes in runoff ratio before and after the drought period. A visualization of this equation is shown in figure 4.4: for a certain  $E_p/P$ , a decrease in  $\omega$  indicates a decrease in the evaporative index and a decrease in the actual evaporation. The decrease in actual evaporation may be an indicator for vegetation change, where the number of plants have reduced due to drought.

Looking at the long-term water balance in equation 3.1, at constant precipitation, a decrease in actual evaporation must mean an increase in runoff. Thus, when fitting the basins to Fu's equation, if the  $\omega$  value is smaller in the post-drought period than in the pre-drought period, it can mean that the fraction of precipitation that turns into runoff has increased.

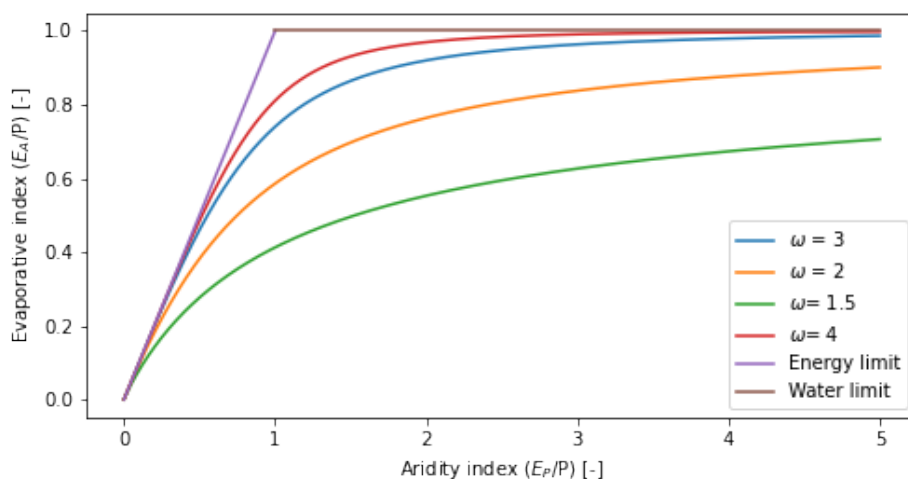


Figure 4.4: Fu's equation plotted inside the Budyko space using different values of  $\omega$

As described in section 4.2, for the selected basins, 5 years of data before and after the drought period is collected.

The data used includes the daily precipitation, runoff, and potential evaporation. This data is resampled into mean annual values. The mean actual evaporation is estimated by taking the difference between the averages of precipitation and runoff, as shown in equation 3.3 in section 3.3.

For every basin, the aridity index  $\frac{E_P}{P}$  and the evaporative index  $\frac{E_A}{P}$  are calculated for the pre-drought period and the post-drought period. Data points that fall outside the energy limit and the water limit are removed. Fu's equation is fitted to the data and the optimal value for the parameter  $\omega$  is found using the least-square method.

### 4.3.2. The Wilcoxon Rank-Sum Test

Instead of fitting Fu's equation to all basins at once, it can also be fitted to each individual basin in order to quantify the differences. Thus, using the time-series for every basin,  $\omega$  is calculated for the pre-drought period and the post-drought period. This yields 2 lists of values:

- $\omega_0$  values for every basin in the pre-drought period
- $\omega_1$  values for every basin in the post-drought period

These two lists need to be compared to see whether the differences that exist in the  $\omega$  values are statistically significant. This can be done by applying the Wilcoxon rank-sum test to the datasets. The rank-sum test is an alternative to the two-sample t-test, which is only based on the rankings of the observations. As will be further discussed in the results, the selected basins and their corresponding  $\omega$ 's do not follow a parametric distribution. Thus, the 2 sample t-test cannot be used.

To apply the rank-sum test to the  $\omega$  values, a hypothesis first needs to be made on the possible outcomes: there is a decrease in  $\omega$  in the post-drought period, or there is no change at all. This leads to two hypotheses, the null hypothesis and the alternative hypothesis. The null hypothesis predicts that no change exists and the alternative hypothesis predicts that  $\omega$  in the post-drought period is smaller than that in the pre-drought period.

$$H_0 : \omega_0 = \omega_1 \quad (4.1)$$

$$H_1 : \omega_0 > \omega_1 \quad (4.2)$$

If the null hypothesis (equation 4.1) is rejected, the alternative hypothesis (equation 4.2) is accepted.

Applying the rank-sum test to this hypothesis yields a one-sided p-value, which is an indicator for how likely the data would have occurred under the null hypothesis. It also tells us whether the null hypothesis should be rejected in favor of the alternative hypothesis. The significance level  $\alpha$  is set to 0.05, so if the p-value falls below 0.05, the null hypothesis can be rejected.

### 4.3.3. Effects of Drought Duration, Intensity and Severity

As described in section 2.2, drought duration, drought intensity, and drought severity are characteristic parameters that can influence the degree of impact drought has on other variables.

As illustrated in figure 4.5, drought duration is defined as the number of months between the start and the end of drought. Drought severity is the total area between SPEI and the threshold, bounded by the start of drought and the end of drought. Lastly, drought intensity is calculated by taking the average of the SPEI values during the drought period, which is also the quotient between drought severity and drought duration.

The drought characteristics are plotted against the change in  $\omega$  between the post-drought period and the pre-drought period, where the change in  $\omega$ ,  $\Delta\omega$ , is defined in equation 4.3. If  $\Delta\omega$  is negative, an increase in runoff is likely to have taken place. If  $\Delta\omega$  is positive, it suggests a decrease in the runoff.

$$\Delta\omega = \omega_1 - \omega_0 \quad (4.3)$$

The Pearson's correlation coefficient is calculated to find whether a linear relationship exists between  $\Delta\omega$  and the drought characteristics. The degree of correlation is characterized according to table 4.2.

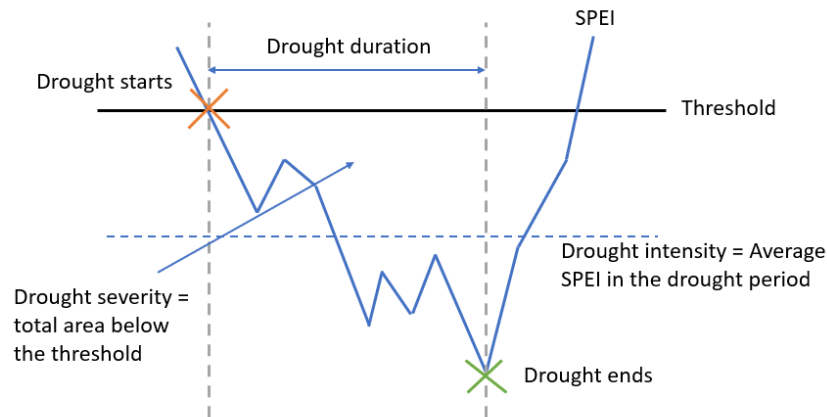


Figure 4.5: Illustration of the drought characteristics: duration, intensity and severity

	Pearson's coefficient $r$	
	Positive	Negative
Strong	1 to 0.8	-0.8 to -1
Moderate	0.8 to 0.5	-0.5 to -0.8
Weak	0.5 to 0.3	-0.3 to -0.5
No correlation	0.3 to 0	0 to -0.3

Table 4.2: Table showing the range of Pearson's correlation coefficient  $r$

#### 4.3.4. Regional Differences

To find whether regional differences exist in  $\Delta\omega$  between humid and arid regions, the basins are grouped based on their aridity index and are plotted against  $\Delta\omega$ .

### 4.4. Effects of Drought on the Partitioning of Fluxes

After having established that changes do exist in the runoff ratio (as shown in the results section), research is done to explore what causes these changes. This research focuses on vegetation: the role it plays in the hydrological cycle, and how it is related to the runoff changes. It is expected that drought causes vegetation to decrease, which decreases the evaporative fluxes and increases runoff.

First, the movements of the basins from pre-drought to post-drought are plotted inside the Budyko space, to detect changes in the evaporative fluxes. Next, the movements are separated into climate and residual effects to see if the vegetation-related residual effects are dominant factors in causing the movements.

#### 4.4.1. Movement Inside the Budyko Space

As described in chapter 2.4.2, the movements of the basins from pre-drought to post-drought can be separated into climate effects and residual effects, where climate effects represent changes in the aridity index and residual effects represent landscape-related changes.

If forest biomass increases, it should lead to an increase in the actual evaporation  $E_A$ . The greater root depth and a larger canopy area mean that transpiration is higher, which leads to higher total evaporation. Under constant precipitation, this would mean an upward movement of the basin inside the Budyko space. The opposite is true if vegetation decreases: the lack of vegetation would reduce evaporation. Thus, the basin should move downwards.

A schematic representation of the movement inside the Budyko space is shown in figures 4.6. For every basin, the 5-year average conditions in the pre-drought period are indicated by  $t_1$  and the 5-year average conditions

in the post-drought period are indicated by t2.

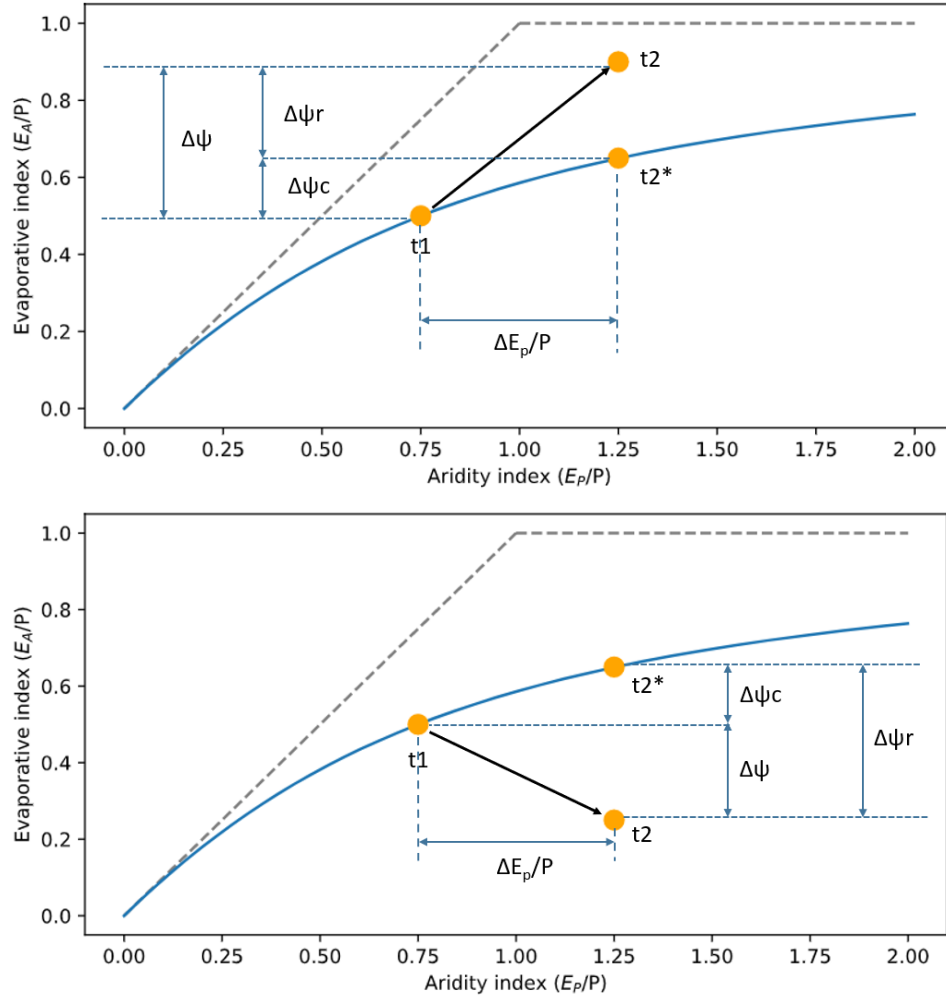


Figure 4.6: Schematic representation of the upward and downward movement of the basin inside the Budyko space

Once t1 and t2 are calculated for all the selected basins, the movements from t1 to t2 are plotted in polar coordinates to quantify these changes. This is done in terms direction and magnitude, using equations 4.4 and 4.5 as developed by Jaramillo and Destouni (2014).

$$r = \sqrt{\Delta\Psi^2 + \left(\Delta\frac{E_P}{P}\right)^2} \quad (4.4)$$

$$\theta = \begin{cases} \arctan\left(\frac{\Delta\Psi}{\Delta\frac{E_P}{P}}\right), & \text{if } \Delta\Psi > 0 \\ \arctan\left(\frac{\Delta\Psi}{\Delta\frac{E_P}{P}}\right) + 180, & \text{if } \Delta\Psi < 0 \end{cases} \quad (4.5)$$

Where:

$r$  = magnitude of movement

$\Delta\Psi$  = change in evaporative index

$\Delta E_P/P$  = change in aridity index

$\theta$  = direction of movement [°]

#### 4.4.2. Dominance of Residual Effects

Figure 4.6 also shows how the movement from t1 to t2 can be separated into climate effects and residual effects. To do so, an elliptic curve is first plotted using Fu's equation, fitted through point t1.

The change in  $E_A/P$  from t1 to t2 is represented by the total change in the evaporative index,  $\Delta\Psi$ .  $\Delta\Psi$  can be separated into the residual effects  $\Delta\Psi_r$  and the climate effects  $\Delta\Psi_c$ . The climate effects are shown by a movement along the curve, from t1 to t2\*. The residual effects are shown by a movement up or down the curve, from t2\* to t2.

To determine if vegetation change is the main cause for the movements, it is necessary to find out if the movements are more driven by climate effects or by residual effects. If residual effects are dominant, then there is a high likelihood that vegetation is the main driver for the change in the actual evaporation.

To find whether the residual effects are dominant, equation 4.6 is used.

$$\begin{cases} \left| \frac{\Delta\Psi_r}{\Delta\Psi_c} \right| > 1, & \text{if } \Delta\Psi_r \text{ is dominant} \\ \left| \frac{\Delta\Psi_r}{\Delta\Psi_c} \right| < 1, & \text{if } \Delta\Psi_c \text{ is dominant} \end{cases} \quad (4.6)$$

### 4.5. Detecting Vegetation Changes

As shown in the results in the next chapter, the residual effects are indeed dominant for some basins. Thus, to research if the residual effects are caused by vegetation and not by other landscape-related factors, the vegetation-related changes are investigated. This includes the root-zone storage deficit and the vegetation index NDVI. The correlation coefficient between these variables and  $\Delta\Psi_r$  are calculated.

#### 4.5.1. Storage Deficit

To illustrate the concept of storage deficit, a simple bucket model showing the vegetation-related fluxes can be found in figure 4.7. When it rains or snows, the precipitating first enters the interception reservoir. Due to interception, the flux  $E_i$  evaporates into the atmosphere. Once the reservoir is full and the maximum interception volume is reached. The effective precipitation  $P_e$  enters the storage reservoir, where it becomes runoff if the reservoir is full, or evaporates due to transpiration if the maximum capacity of the reservoir is not reached.

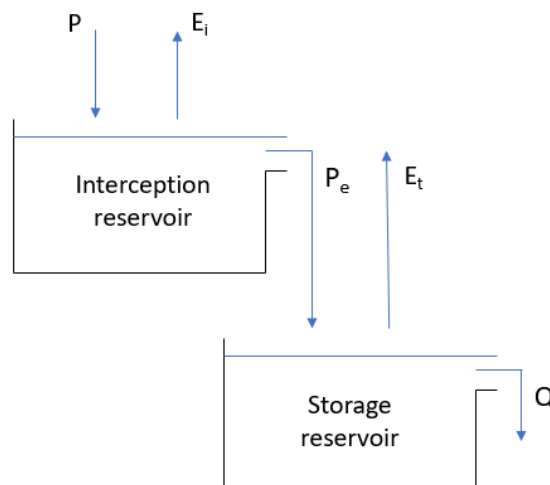


Figure 4.7: Bucket model showing the vegetation related fluxes

Assuming that the storage reservoir is infinitely large and that no interception  $E_i$  takes place, runoff  $Q$  be-

comes 0, and transpiration  $E_t$  is equal to the actual evaporation  $E_A$ . The storage deficit can be calculated using the following steps:

1. Estimate the long term average  $E_t$  using equation 4.7. Over long time periods,  $\frac{dS}{dt}$  approaches 0.

$$\overline{E_t} = \overline{P} - \overline{Q} - \frac{dS}{dt} \quad (4.7)$$

2. Distribute long term average  $E_t$  over the year by scaling it with the daily  $E_P$ , using formula 4.8.

$$E_t(t) = \frac{E_P(t)}{\overline{E_P}} \overline{E_t} \quad (4.8)$$

3. Compute the daily storage deficit as the sum of P-E using formula 4.9.

$$S_D(t) = \min(0, \sum_{i=1}^t (P(t) - E_t(t))) \quad (4.9)$$

For every basin, the storage deficit is calculated over the 5-year post-drought period and the largest deficit  $S_{R,5yr}$  is calculated. The largest deficit is the maximum amount of water that vegetation needs for optimal growth, also known as the vegetation-used water storage volume. A schematic representation of the maximum deficit over the 5 years is shown in figure 4.8.

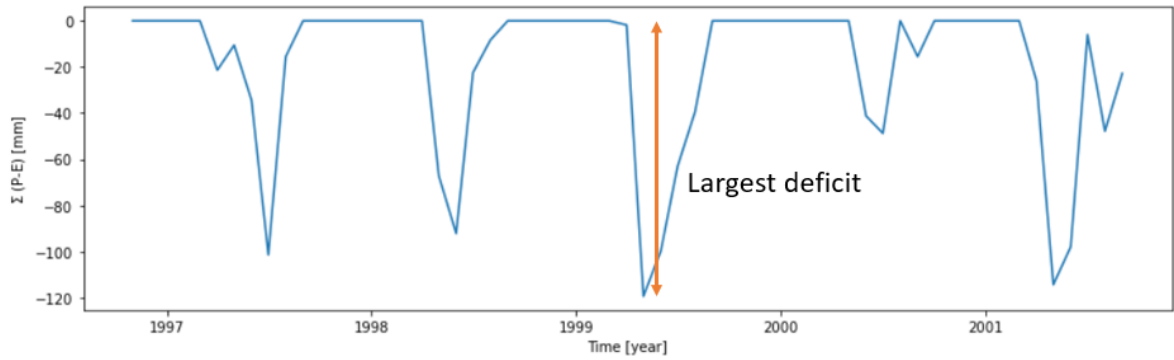


Figure 4.8: Illustration of the largest storage deficit

The largest storage deficit  $S_{R,5yr}$  represents the catchment's vegetation water demand and it is plotted against  $\Delta\Psi_r$  to see if a relationship exists between the two variables.

#### 4.5.2. NDVI

To investigate changes in the density of healthy vegetation, NDVI data is collected for the pre-drought period and the post-drought period.

For the 5-year pre-drought period, the average NDVI value of the basin is extracted for every pixel. Next, the average of the pixels is taken to yield one average NDVI value per basin. The same is done for the 5-year post-drought period and the results are compared to see if changes exist in the averages before and after drought.

For the post-drought period, the average NDVI is also calculated per year, for 1, 2, 3, 4, and 5 years after drought. For each year, the post-drought NDVI is compared to the pre-drought value to see what the changes are per year.

# 5

## Results

In this chapter, the results are presented and described. The chapter starts with the outcomes of the basin selection. The selected basins and their corresponding drought periods form the basis of this research and are used to generate the results of the rest of the analysis. Next, the results of the runoff changes are presented, followed by the results related to vegetation changes. Finally, the basin groups that show more prominent changes are revisited, and additional analyses are done.

### 5.1. Basin Selection

Applying the list of criteria established in section 4.2 to the definition of drought and the drought periods yields a portion of basins that fulfill these criteria. Depending on the free variable (threshold level, minimum drought period length, and SPEI accumulation period), the number of basins differs. Of the 659 basins, the number of basins that meet all selection criteria is shown in figure 5.1.

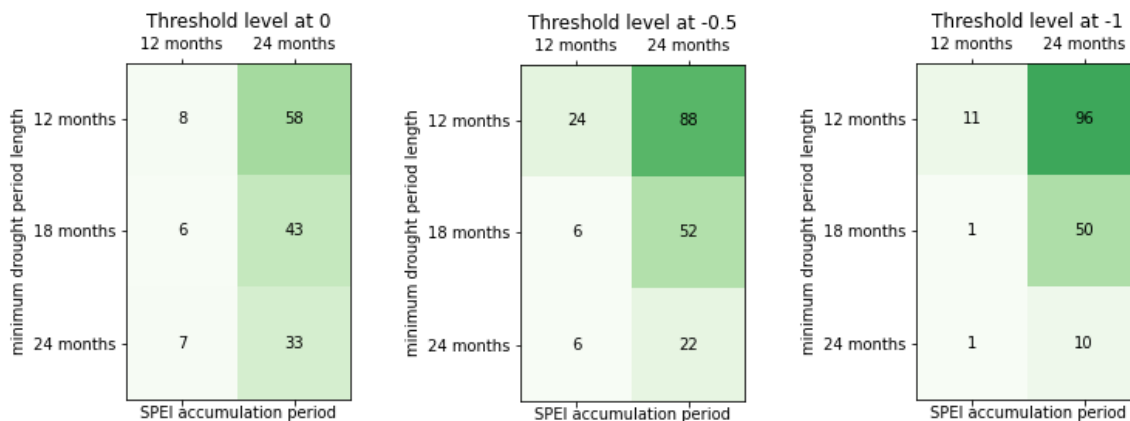


Figure 5.1: Number of basins that meet all selection criteria for different combinations of threshold level, minimum drought period length, and SPEI accumulation period

It can be seen that for a smaller accumulation period of 12 months, a small number of basins are qualified. However, for a longer accumulation period of 24 months where SPEI has fewer fluctuations, more basins are accepted. Furthermore, a shorter minimum drought period length yields more basins. This is because a shorter minimum length can include basins that also belong to a longer period, but not vice versa. Lastly, a threshold level of 0 leads to the least amount of basins in general, and no clear differences are visible between threshold -0.5 and 1.

The combination of a 12 months minimum drought period length, a threshold level at -1, and a SPEI accumulation period of 24 months yields 96 basins, the highest of all combinations. These basins are tested again

on the long-term water balance for the pre-drought period as well as the post-drought period. This leads to a final number of 83 basins and these basins are used in the rest of the analysis. A map showing the locations of these basins can be found in figure 5.2.

For the selected basins, several examples of the graphical representation of the pre-drought period, drought period, and post-drought period are shown in appendix A.

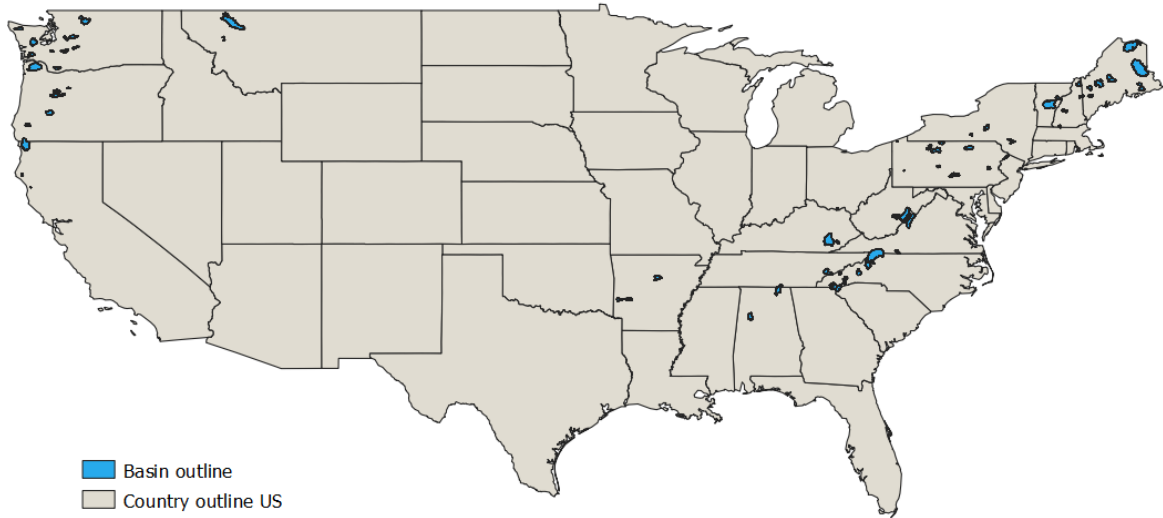


Figure 5.2: Map showing the locations of the basins selected using threshold level = 1, minimum drought period = 12 months, and SPEI accumulation period = 12 months

### 5.1.1. Aridity Indices of the Selected Basins

As shown in table 5.1, the aridity index of the selected basins ranges from 0.2 to 0.9, with the 0.6 - 0.7 being the most frequently occurring interval.

All basins have an aridity index of less than 1. This means that there is more precipitation than potential evaporation. Thus, the basins are all located in relatively humid areas. Furthermore, an aridity index of lower than 1 also indicates that the basins are more limited by energy than by water availability.

Aridity index	0.2 - 0.3	0.3 - 0.4	0.4 - 0.5	0.5 - 0.6	0.6 - 0.7	0.7 - 0.8	0.8 - 0.9
Number of basins	2	6	6	12	35	16	6

Table 5.1: Table showing the number of basins per aridity index, for the basins selected using threshold level = 1, minimum drought period = 12 months, and SPEI accumulation period = 12 months

## 5.2. Changes in Runoff Ratio

For the selected basins, the long-term  $E_A/P$  and  $E_P/P$  values are calculated for the pre-drought period and the post-drought period.

Due to the large number of basins, it would be too crowded to plot all data points in the same graph, as 2 points are calculated for each basin: 1 indicating the 5-year average of the pre-drought period, and the other indicating the 5-year average of the post-drought period. To solve this issue, all values are grouped by an interval of 0.05 based on the x-axis. This means that for the points that fall into a certain aridity index range, the average is taken and 1 point is plotted for those basins. For example, there are 2 basins in the pre-drought period that have an aridity index of between 0.2 and 0.25, the mean of these 2 points are taken and plotted inside the Budyko space. The results are shown in figure 5.3.

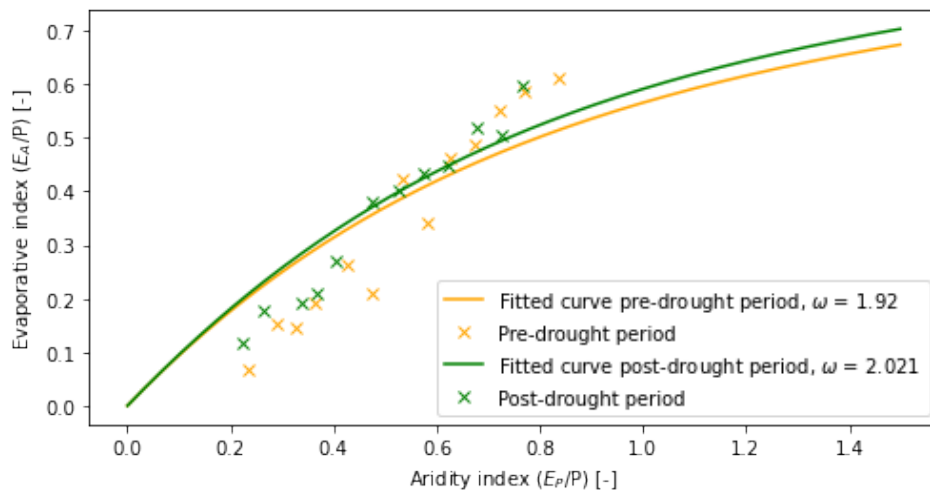


Figure 5.3: Long-term averages of the post-drought period and pre-drought period for the selected basins and their fitted  $\omega$  values

Fitting Fu's equation to the basins points yields 2 curves with their own  $\omega$  values. For the pre-drought period, the fitted  $\omega$  is 1.92 and for the post-drought period, the fitted  $\omega$  is 2.021. As explained in section 4.3, if a decrease in  $\omega$  is observed in the post-drought period as compared to the pre-drought period, the runoff ratio has increased. In this case, a slight increase in  $\omega$  is found, which signals a decrease in the runoff ratio.

### 5.2.1. Rank-Sum Test and $\Delta\omega$

On a smaller scale, the runoff ratio  $\omega$  is calculated for each basin individually by inverting Fu's equation. As described in subsection 4.3.2, the runoff ratio before drought  $\omega_0$  is calculated for the pre-drought period and the runoff ratio after drought  $\omega_1$  is calculated for the post-drought period. Histograms are plotted for these 2 lists of values and the results are shown in figures 5.4 and 5.5.

Figures 5.4 and 5.5 show that neither  $\omega_0$  nor  $\omega_1$  seem to follow a parametric distribution. Thus, the Wilcoxon rank-sum test is carried out on the null hypothesis. The result of this test yields a p-value of 0.273. Thus, under the null hypothesis, the data is likely to occur 27.3% of the time. This is larger than the chosen  $\alpha$ -value of 0.05. Therefore, looking at all the basins together, the results are not statistically significant enough to allow us to reject the null hypothesis.

Furthermore, for each basin, the difference between  $\omega_1$  and  $\omega_0$  is calculated. This is denoted by  $\Delta\omega$  and a histogram of the distribution of  $\Delta\omega$  is shown in figure 5.6.

It can be observed that the highest frequency occurs at  $\Delta\omega = 0$ , where no change in runoff ratio is detected. However, out of the 83 basins, 39 of them do show a negative change in  $\omega$ . This is 47% of the basins. In other words, 47% of the basins have shown an increase in runoff ratio.

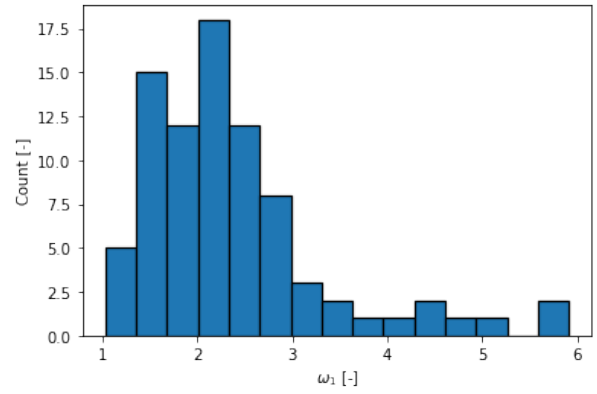
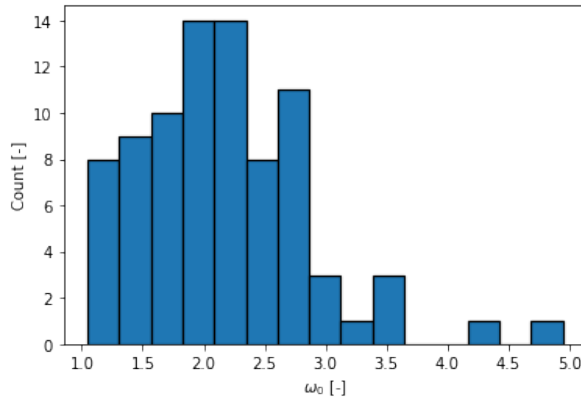


Figure 5.4: Histogram showing the distribution of the runoff ratio in the pre-drought period,  $\omega_0$

Figure 5.5: Histogram showing the distribution of the runoff ratio in the post-drought period,  $\omega_1$

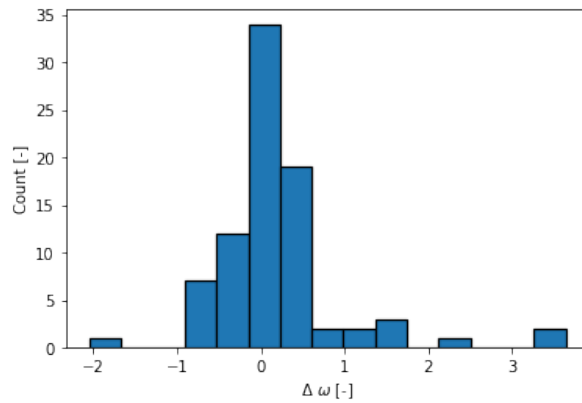


Figure 5.6: Histogram showing the distribution in the changes in runoff ratio from the pre-drought period to the post-drought period,  $\Delta\omega$

The correlation between the change in evaporative index  $\Delta E_A/P$  and the change in runoff ratio  $\Delta\omega$  is also calculated and the results are shown in figure 5.7. A moderate positive relationship is found between the two variables: a lower runoff ratio corresponds to greater evaporation. However, a strong relationship with a higher  $r$  was expected. Figure 5.7 also shows that 2 straight lines can be possibly fitted to the points instead of 1. This is investigated in chapter 6.

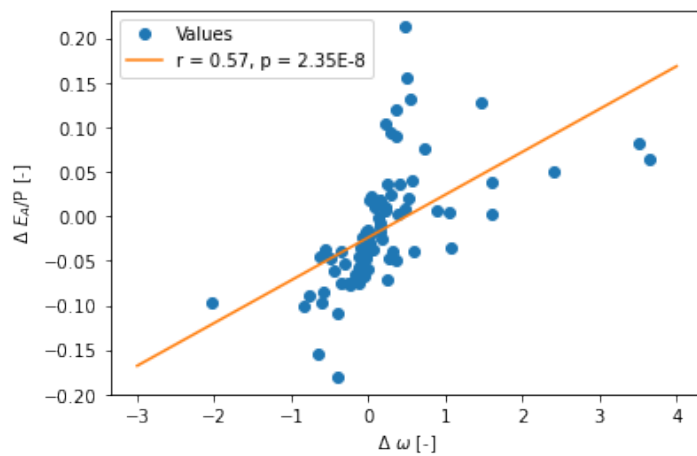


Figure 5.7: Correlation between the change in evaporative index  $\Delta E_A/P$  and the change in runoff ratio  $\Delta\omega$

### 5.2.2. Effects of Drought Duration, Intensity and Severity

As explained in section 4.3.3, the change in runoff ratio  $\Delta\omega$  is plotted against the characteristics of drought: drought duration, intensity, and severity. This is done to explore the relationship between drought and the runoff ratio  $\omega$ . The hypothesis is that the longer the drought and the more intensity and severity the drought is, the more vegetation could die, which leads to a more negative  $\Delta\omega$ .

The results show that this is not the case, as can be seen in figures 5.8, 5.9, 5.10. Pearson's correlation  $r$  is calculated between the variables, together with their corresponding p-values.

The basins selected have a drought duration that ranges from 12 to 34 months, as shown in figure 5.8. There seems to be little relationship between drought duration and the change in runoff ratio, since a correlation of  $-0.0019$  is found, together with a p-value of  $0.99$ . The correlation between the change in runoff ratio  $\Delta\omega$  and drought intensity seems to be the strongest of all three drought characteristics. However, an r-value of  $-0.1$  still indicates a very weak correlation between the two variables. Moreover, plotting  $\Delta\omega$  against drought severity in figure 5.10 again shows that there is no linear relationship between the variables.

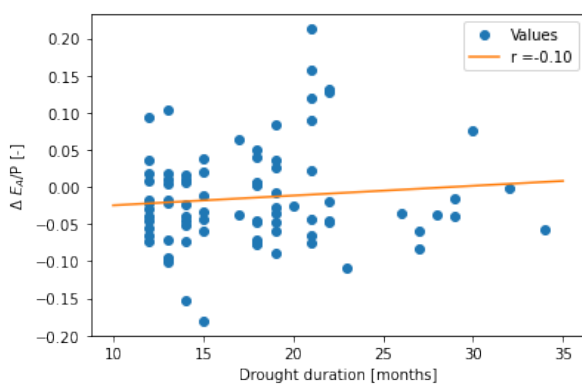


Figure 5.8: Correlation between the change in runoff ratio  $\Delta\omega$  and drought duration

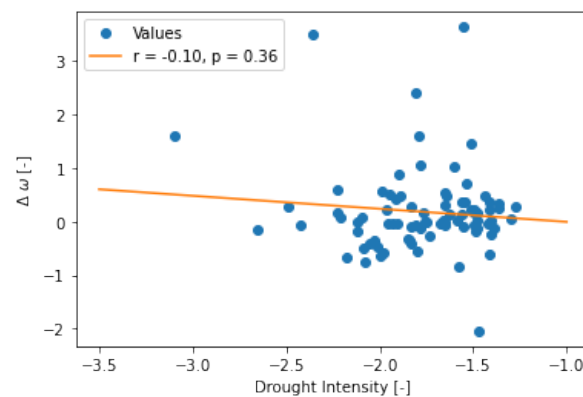


Figure 5.9: Correlation between the change in runoff ratio  $\Delta\omega$  and drought intensity

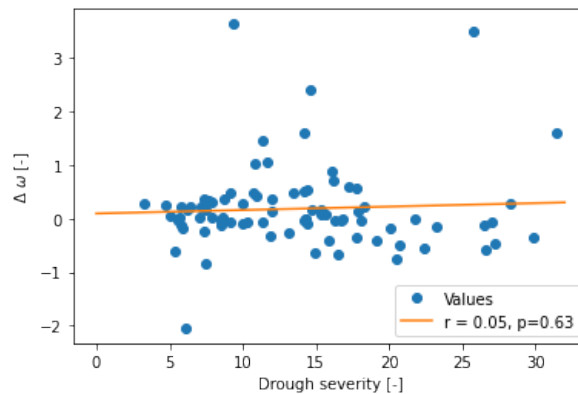


Figure 5.10: Correlation between the change in runoff ratio  $\Delta\omega$  and drought severity

### 5.2.3. Regional Differences

As illustrated in section 5.1.1, the selected basins all have relatively small aridity index, meaning that they are located in humid climate zones. For these basins, the change in runoff ratio is plotted against the aridity index and the results are shown in figure 5.11.

In general, there seems to be no significant relationship between the change in runoff ratio and the aridity index. However, looking at the plots carefully, some variations can be seen: the basins that have an aridity

index of below 0.5 mostly have a  $\Delta\omega$  of larger than 0, which indicates a decrease in runoff ratio in these basins. For the basins with an aridity index of larger than 0.5 on the other hand, both positive and negative  $\Delta\omega$  values are observed. The corresponding movements of these basins inside the Budyko space are shown in figure 5.12. Due to the large number of basins that have an aridity index of larger than 0.5, only some representative basins are plotted in the figure. As displayed, basins with an aridity index of smaller than 0.5 mostly show an upward movement, indicating a decrease in runoff ratio. Basins with an aridity index of larger than 0.5 show both upward and downward movements.

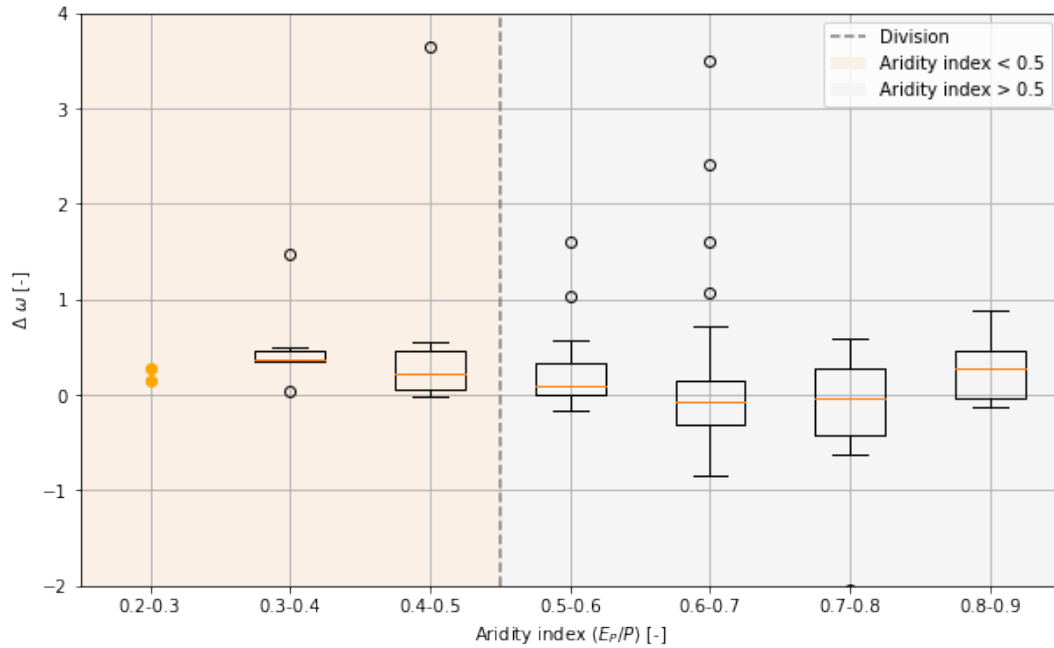


Figure 5.11: Box plots showing the changes in runoff ratio  $\Delta\omega$  for every aridity index

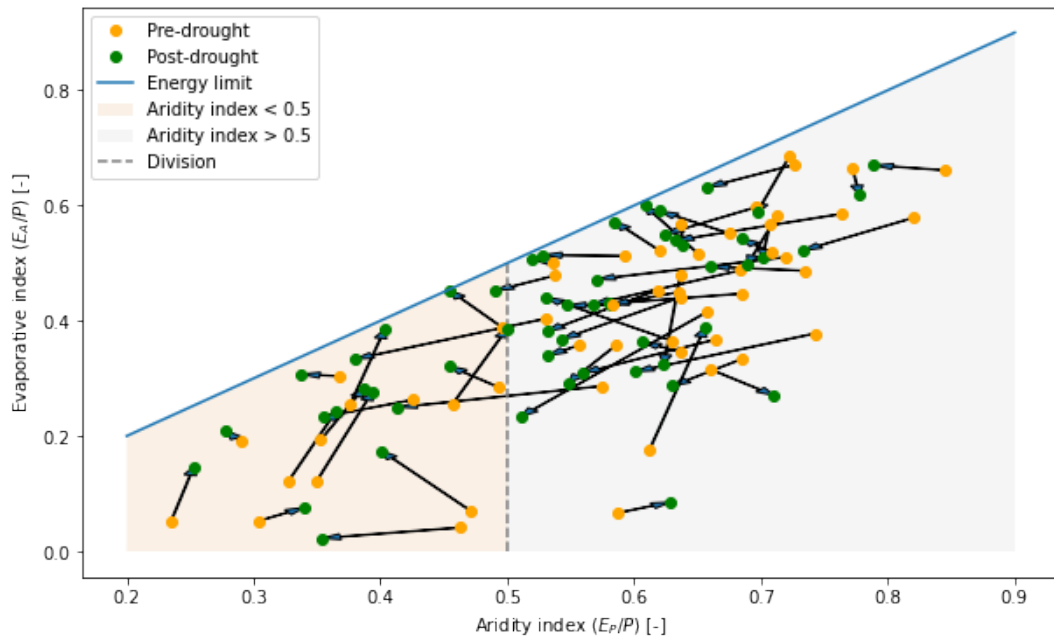


Figure 5.12: Examples of the movements of the basins inside the Budyko space for different aridity indices

### 5.3. Effects of Drought on the Partitioning of Fluxes

The results from the previous section show that in general, there is no significant change in the runoff ratio before and after the drought and that no correlation is found between the drought characteristics and the runoff ratio.

However, looking at the individual basins on a smaller scale, some basins do display an increase in runoff ratio, whilst for other basins, the opposite is observed. Thus, the results of this section aim to explain why these differences exist. This is done by investigating how the fluxes change due to drought, and if the residual effects are causing this change.

#### 5.3.1. Drought Effects on Basin Movement

As shown in section 5.2.1, when comparing the post-drought period to the pre-drought period, the selected basins display an increase in runoff ratio or a decrease in runoff ratio, signaled by a negative  $\Delta\omega$  and a positive  $\Delta\omega$ , respectively. Thus, when investigating the movement of the basins, the basins are separated into 2 groups: basins with  $\Delta\omega < 0$  and basins with  $\Delta\omega > 0$ . This is done to better identify the potential relationships between runoff ratio and vegetation.

For the basins that display an increase in runoff ratio ( $\Delta\omega < 0$ ), the movement of these basins are plotted in figures 5.13 and 5.14. As shown in the figures, most basins show a movement between  $180^\circ$  and  $270^\circ$ . This means that there is a decrease in the aridity index as well as the evaporative index. The basins have become more humid and the actual evaporation has decreased. However, the magnitudes of the movements are relatively small, meaning that there is not a very significant decrease in the aridity index nor the evaporative index.

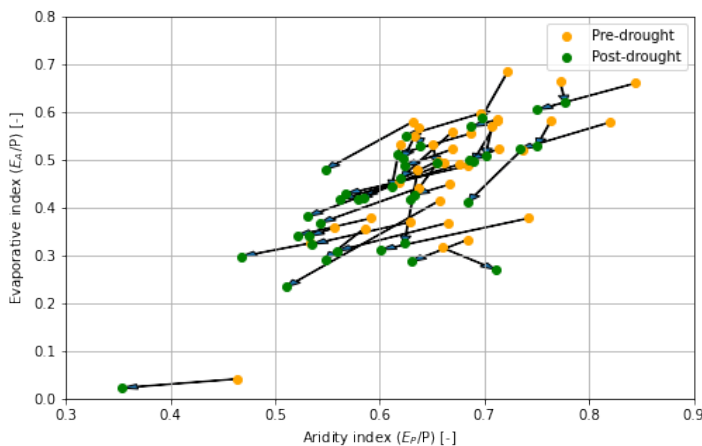


Figure 5.13: Movement of the basins inside the Budyko space: basins with an increase in runoff ratio  $\Delta\omega < 0$

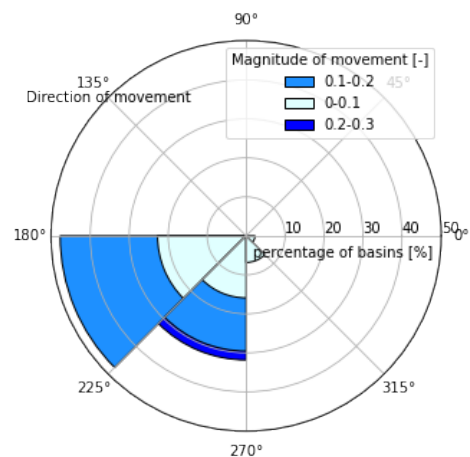


Figure 5.14: Radial plot of the magnitude and the direction of movement of the basins inside the Budyko space: basins with an increase in runoff ratio  $\Delta\omega < 0$

For the basins that display a decrease in runoff ratio ( $\Delta\omega > 0$ ), the movements are plotted in figures 5.15 and 5.16. The figures show that the movements of the basins are more widely spread as compared to the basins with  $\Delta\omega < 0$ . The direction of the movements ranges from  $0^\circ$  to  $225^\circ$ , with a majority between  $135^\circ$  and  $225^\circ$ . Thus, most basins have become more humid with a lower aridity index, accompanied by higher evaporation. Similar to the basins with  $\Delta\omega < 0$ , the magnitudes of the movements are again not big.

For more detailed graphs of the movements of the individual basins before and after drought, several basins are selected as examples, and their movements inside the Budyko space as well as their corresponding  $\omega$  values are plotted. This is shown in appendix B.

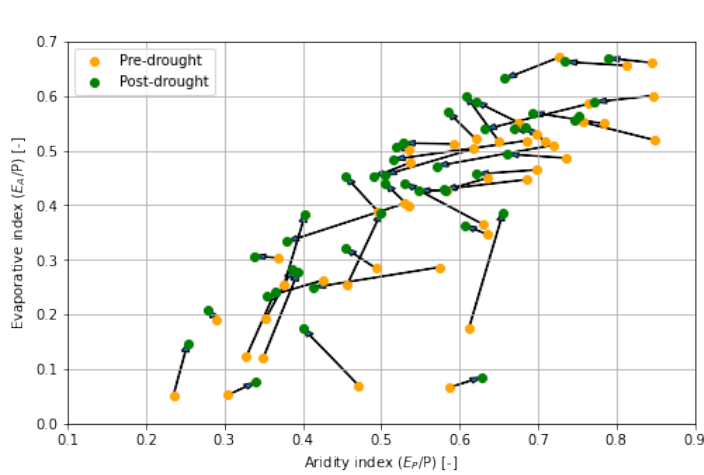


Figure 5.15: Movement of the basins inside the Budyko space: basins with a decrease in runoff ratio  $\Delta\omega > 0$

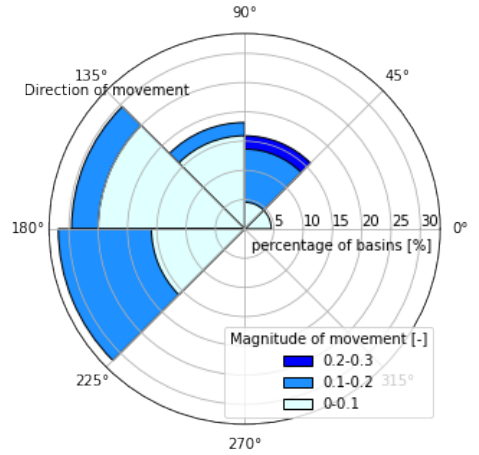


Figure 5.16: Radial plot of the magnitude and the direction of movement of the basins inside the Budyko space: basins with a decrease in runoff ratio  $\Delta\omega > 0$

### 5.3.2. Separating Climate and Residual Effects

Although the magnitudes of the basin movements are small, some visible patterns are found. This subsection aims to explore the factors that drive the movements from the pre-drought period to the post-drought period: are the movements mainly driven by residual effects or climate effects?

As described in section 4.4.2, the movement of the basin from the pre-drought period to the post-drought period inside the Budyko space can be separated into climate effects and residual effects, where climate effects are represented by movements along the curve of Fu's equation, and the residual effects are represented by a movement up or down the curve. Residual effects are caused by landscape-related factors, which can indicate vegetation changes.

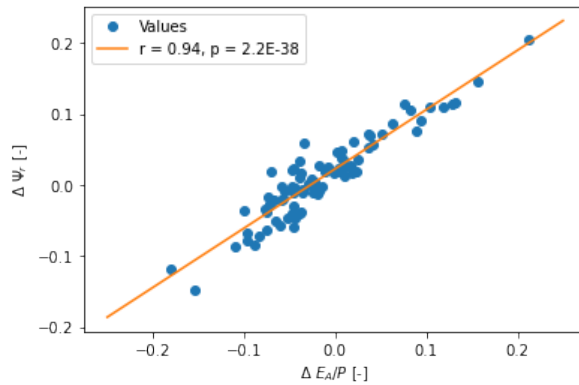


Figure 5.17: Correlation between the residual effects  $\Delta\Psi_r$  and the change in evaporative index  $\Delta E_A/P$

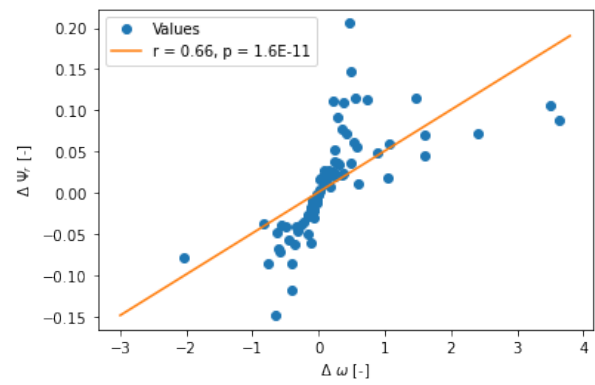


Figure 5.18: Correlation between the residual effects  $\Delta\Psi_r$  and the change in runoff ratio  $\Delta\omega$

The residual effects  $\Delta\Psi_r$  is found to be positively correlated to the evaporative index  $\Delta E_A/P$  and moderately correlated to the change in runoff ratio  $\Delta\omega$ , as shown in figure 5.17 and 5.18: the larger the residual, the larger the change in evaporation and the lower the runoff. Due to the fact that a positive  $\Delta E_A/P$  does not necessarily mean a positive  $\Delta\omega$  (as shown in figure 5.7), only a moderate correlation is found between  $\Delta\omega$  and  $\Delta\Psi_r$ .

For basins with an increase in runoff ratio ( $\Delta\omega < 0$ ) and decrease in runoff ratio ( $\Delta\omega > 0$ ), the residual effects  $\Delta\Psi_r$  are calculated and histograms of their distributions are shown in figures 5.19 and 5.20, respectively. As expected, all basins that experience an increase in runoff have negative residual effects, indicated by a down-

ward movement of  $F_u$ 's curve. The opposite is true for the basins with a decrease in runoff ratio: the upward movement of the curve has resulted in positive residual effects. Furthermore, for all basins, the magnitudes of the residual effects are relatively small. The distributions of the residual effects for both graphs are skewed towards 0. This is supported by the plots of the movements in figures in the previous subsection: the movement of basins is of the same magnitude as the residual effects.

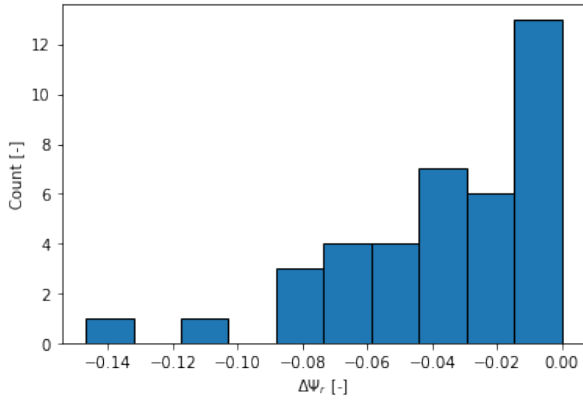


Figure 5.19: Histogram showing the distribution of the residual effects  $\Delta\Psi_r$ , for basins with an increase in runoff ratio  $\Delta\omega < 0$

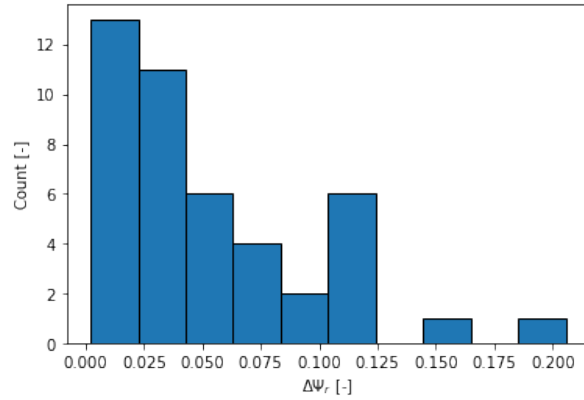


Figure 5.20: Histogram showing the distribution of the residual effects  $\Delta\Psi_r$ , for basins with a decrease in runoff ratio  $\Delta\omega > 0$

The yearly changes in residual effects are also investigated and the results are shown in appendices C. No clear pattern is visible in how the residual effects change from year to year.

To explore the regional differences, the residual effects are plotted against the aridity index in figure 5.21. Looking at the distribution of  $\Delta\Psi_r$ , differences are observed. It can be seen that  $\Delta\Psi_r$  is mostly positive for basins with an aridity index of less than 0.5. For basins with a higher aridity index of larger than 0.5 on the other hand, the mean  $\Delta\Psi_r$  fluctuates around 0.

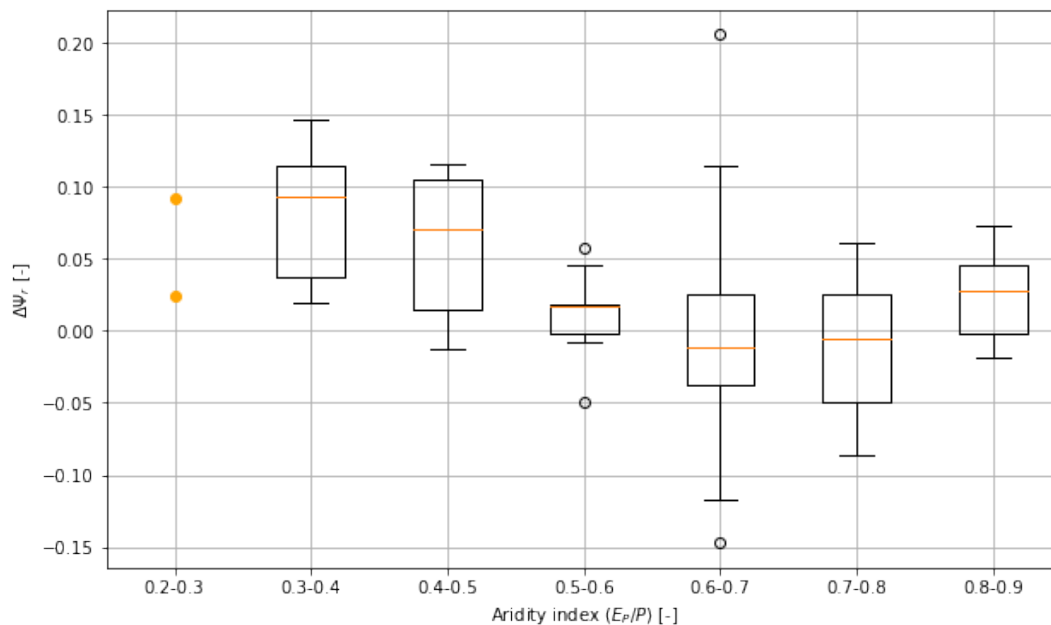


Figure 5.21: Box plots showing the residual effects  $\Delta\Psi_r$  for every aridity index

### 5.3.3. Dominance of Residual Effects

To find whether the movements of the basins are mostly driven by residual effects or climate effects, the absolute ratio  $|\frac{\Delta\Psi_r}{\Delta\Psi_c}|$  is calculated for every basin. A  $|\frac{\Delta\Psi_r}{\Delta\Psi_c}|$  of larger than 1 indicates that the residual effects are dominant. It is found that:

- For basins with an increase in runoff ratio,  $\Delta\omega < 0$ , the residual effects are dominant for 40% of the basins.
- For basins with a decrease in runoff ratio,  $\Delta\omega > 0$ , the residual effects are dominant for 68% of the basins.

Furthermore,  $|\frac{\Delta\Psi_r}{\Delta\Psi_c}|$  is also plotted against the aridity index, shown in figure 5.22. Here, a similar trend is observed as from figure 5.21: basins with an aridity index of less than 0.5 show more dominant residual effects, meaning that they are potentially more linked to vegetation changes.

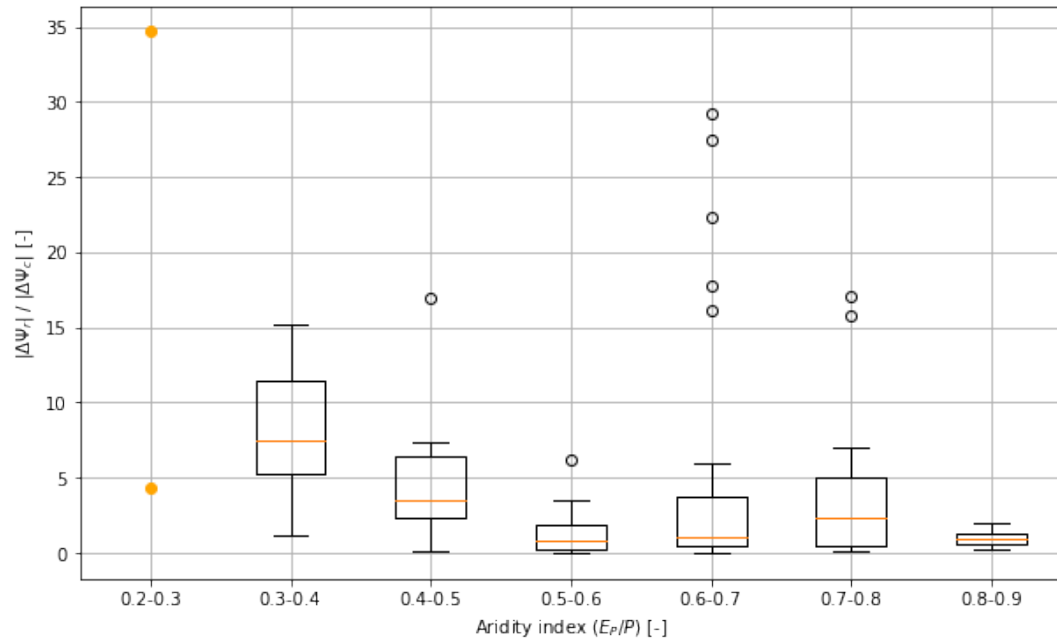


Figure 5.22: Box plots showing the absolute ratio between the residual effects and the climate effects  $|\frac{\Delta\Psi_r}{\Delta\Psi_c}|$  for every aridity index

## 5.4. Vegetation Changes

To detect changes in vegetation, the storage deficit in the root zone and changes in the vegetation index NDVI are investigated. The results are as follows.

### 5.4.1. Storage Deficit

As described in section 4.5.1, the storage deficit describes the amount of water vegetation needs for transpiration. The larger the deficit, the less the water availability. It is expected that due to drought, the deficit in the post-drought period would be high, which decreases plant productivity and causes some plants to die. The decrease in vegetation would lead to a smaller residual effect and therefore, an increase in runoff ratio.

The distribution of the 5-year maximum deficit  $S_{R,5yr}$  is shown in figure 5.23. The graph is skewed to the left. Thus, for most basins, the maximum storage deficit is quite small.

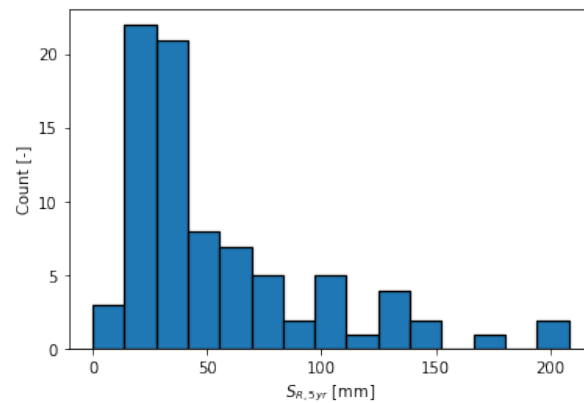


Figure 5.23: Histogram showing the distribution of the maximum storage deficit  $S_{R,5yr}$

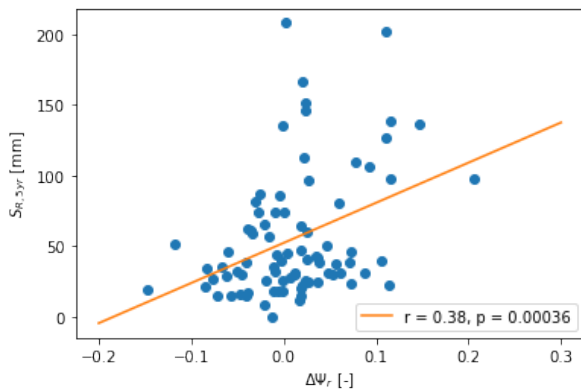


Figure 5.24: Correlation between the maximum storage deficit  $S_{R,5yr}$  and residual effects  $\Delta\Psi_r$

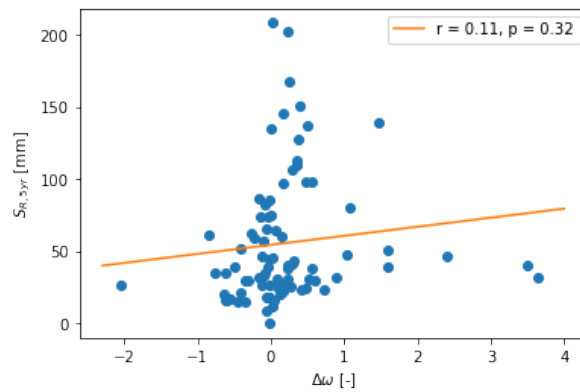


Figure 5.25: Correlation between the maximum storage deficit  $S_{R,5yr}$  and the change in runoff ratio  $\Delta\omega$

Plotting the maximum storage deficit in the 5-year pre-drought period against the residual effects and change in runoff ratio in figures 5.24 and 5.25 show that a weak positive correlation exists between  $S_{R,5yr}$  and  $\Delta\Psi_r$ : the larger the deficit, the bigger the residual effects. This is the opposite of what is expected. Furthermore, due to the fact that the relationship between  $\Delta\Psi_r$  and  $\Delta\omega$  is not perfectly linear, no correlation is detected between  $S_{R,5yr}$  and  $\Delta\omega$ .

Looking at the deficit per aridity index in figure 5.26, the basins that are located in very humid areas do show a larger deficit relative to the basins with a larger aridity index.

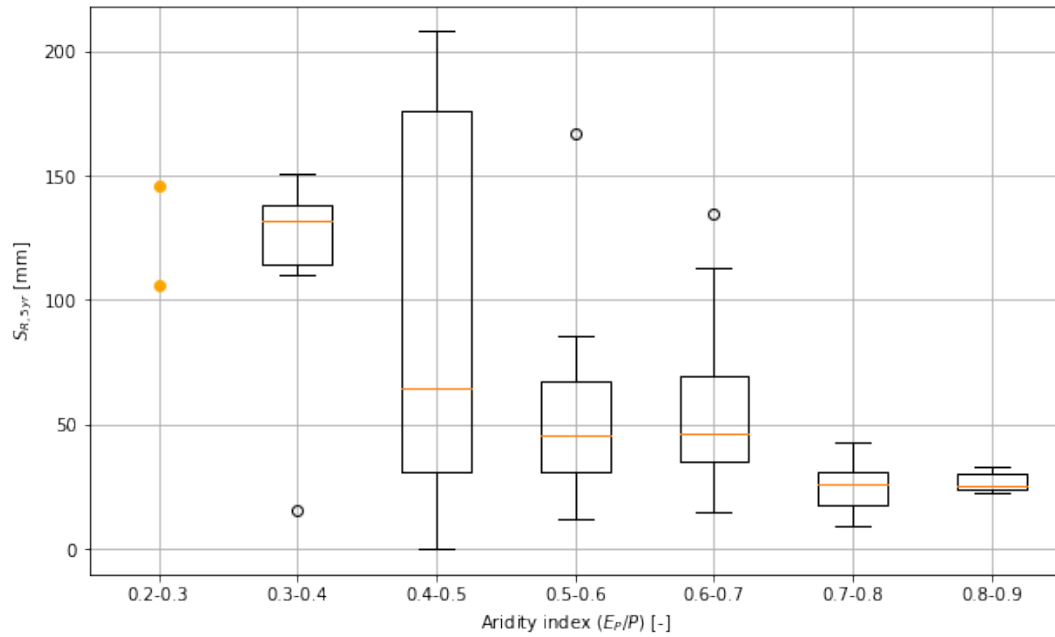


Figure 5.26: Box plots showing the maximum storage deficit  $S_{R,5yr}$  for every aridity index

#### 5.4.2. NDVI

For the 5-year pre-drought period and the 5-year post-drought period, the average NDVI values for the selected basins are calculated and a box-plot of their distributions is shown in figure 5.27. It can be seen that most basins have a relatively small NDVI value, meaning that the vegetation density is quite low. Furthermore, on average, little difference are found between the NDVI values in the post-drought period and the pre-drought period. This is verified by figure 5.28, where the count is the highest around  $\Delta\text{NDVI} = 0$ .

However, figure 5.28 shows that 63% of the basins have a  $\Delta\text{NDVI}$  of larger than 0, meaning that vegetation has increased after drought.

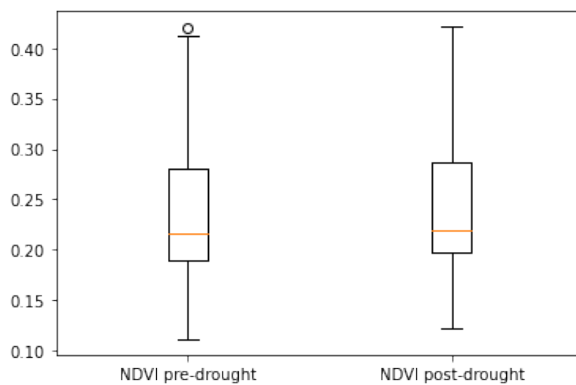


Figure 5.27: Boxplot of NDVI in the before and after drought

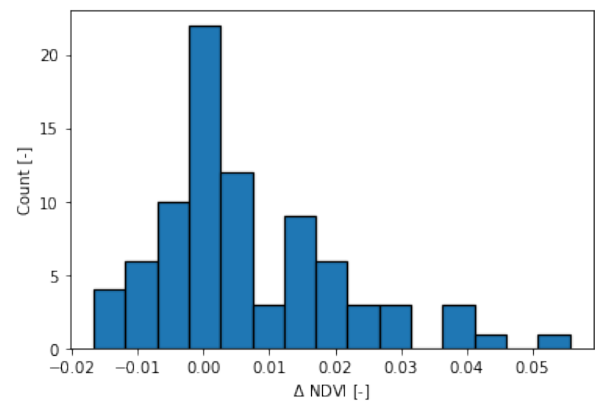


Figure 5.28: Histogram showing the distribution of the change in NDVI from the pre-drought period to the post-drought period

In figures 5.29 and 5.30,  $\Delta\text{NDVI}$  is plotted against the residual effects  $\Delta\Psi_r$  and the change in runoff ratio  $\Delta\omega$  and their correlation coefficients are calculated. No correlation is found between  $\Delta\text{NDVI}$  and  $\Delta\Psi_r$ , nor between  $\Delta\text{NDVI}$  and  $\Delta\omega$ .

For every year in the post-drought period, the yearly average NDVI is calculated for every basin and the re-

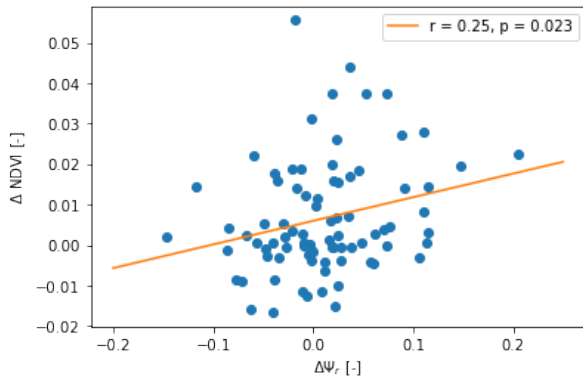


Figure 5.29: Correlation between ΔNDVI and the residual effects ΔΨ<sub>r</sub>

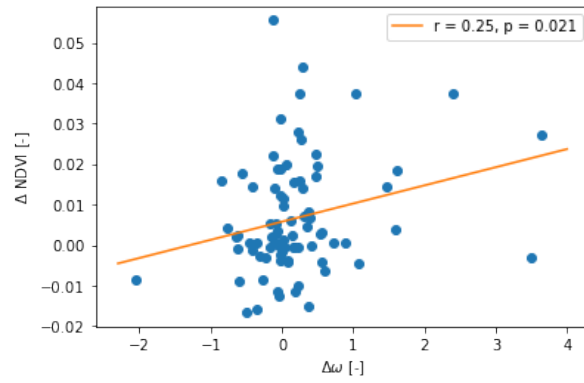


Figure 5.30: Correlation between ΔNDVI and the change in runoff ratio Δω

sults are shown in appendix D. No clear pattern is found in the yearly changes.

Looking at the regional differences per aridity index in figure 5.31, the change in NDVI is positive for almost all basins with an aridity index of less than 0.5. For the other basins with a higher aridity index, both positive and negative changes are observed.

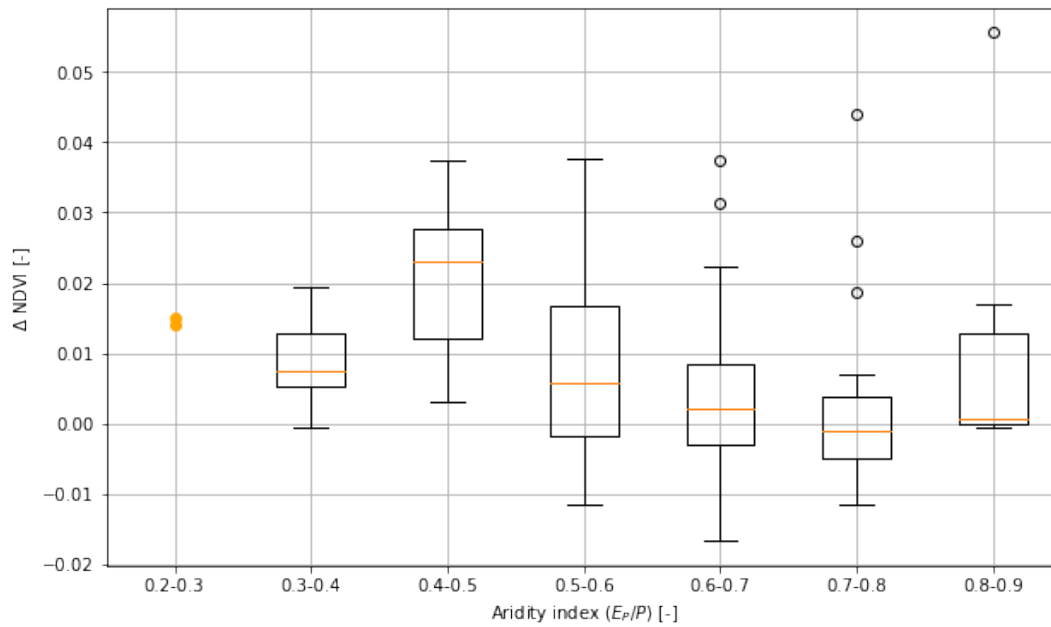


Figure 5.31: Box plots showing the change in vegetation index NDVI for every aridity index

### 5.4.3. Correlation Between the Maximum Storage Deficit and NDVI

The correlation between the maximum storage deficit  $S_{R,5yr}$  and the changes in vegetation density  $\Delta NDVI$  are plotted, and the results are shown in figure 5.32. No correlation is found between the two variables.

Furthermore, figure 5.32 shows that basins with a high storage deficit do not seem to follow the trending. According to figure 5.26, these are mostly basins with a smaller aridity index.

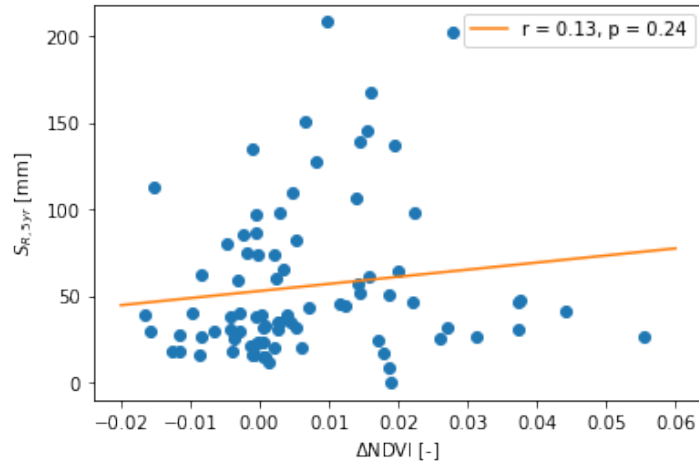


Figure 5.32: Correlation between the maximum storage deficit  $S_{R,5yr}$  and the change in NDVI

## 5.5. Overview

To provide a clear overview of the correlations between the different variables, a correlation matrix is created and it is shown in figure 5.33. A strong correlation is found between the change in evaporative index and residual effect and a moderate correlation is found between the residual effects and the change in runoff ratio. However, weak or no correlations are found between the vegetation-related factors and the other variables.

$\Delta E_A / P$	1				
$\Delta \psi_r$	0.94	1			
$\Delta \omega$	0.57	0.66	1		
$S_{R,5yr}$	-	0.38	0.11	1	
$\Delta NDVI$	-	0.25	0.25	0.13	1
	$\Delta E_A / P$	$\Delta \psi_r$	$\Delta \omega$	$S_{R,5yr}$	$\Delta NDVI$

Figure 5.33: Matrix showing Pearson's correlation coefficient between all variables

### 5.6. Basins Revisited

In the previous sections of this chapter, three distinct observations are made in the results:

1. For the basins with a decrease in runoff ratio,  $\Delta\omega > 0$ , the the movement from the pre-drought period to the post-drought period is mainly driven by residual effects ( $|\frac{\Delta\Psi_r}{\Delta\Psi_c}| > 1$ ).
2. Some differences exist between basins with aridity index  $< 0.5$  and aridity index  $> 0.5$ . The basins with a lower aridity index show higher values of residual effects  $\Delta\Psi_r$  as well as the ratio between residual effects and climate effects  $|\frac{\Delta\Psi_r}{\Delta\Psi_c}|$ .
3. Basins with aridity index  $< 0.5$  have larger maximum storage deficit  $S_{R,5yr}$  and larger changes in  $\Delta NDVI$ .

In this section, these basins are revisited to see what can potentially cause these differences.

#### 5.6.1. Basins with Dominant Residual Effects

To explore why differences exist regarding the dominance of residual effects, the basins with more dominant residuals are tested again on the drought characteristics. The hypothesis is that for this group of basins, a more significant relationship may exist between the change in runoff ratio and the drought length, intensity, or severity.

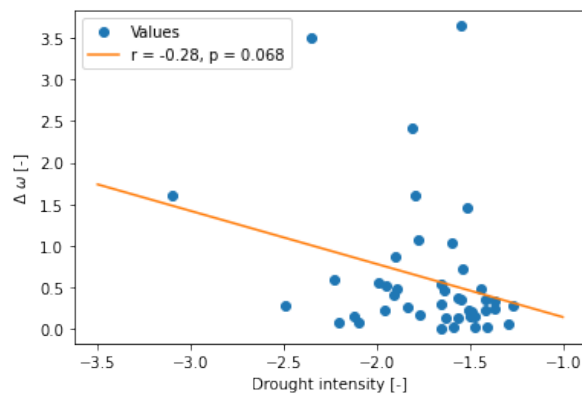
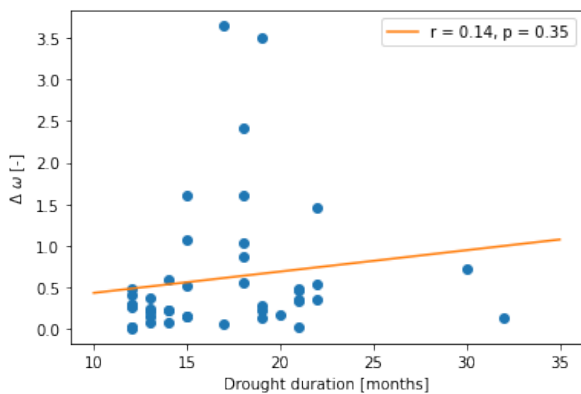


Figure 5.34: Correlation between the change in runoff ratio  $\Delta\omega$  and drought duration, for basins that experience a decrease in runoff ratio

Figure 5.35: Correlation between the change in runoff ratio  $\Delta\omega$  and drought intensity, for basins that experience a decrease in runoff ratio

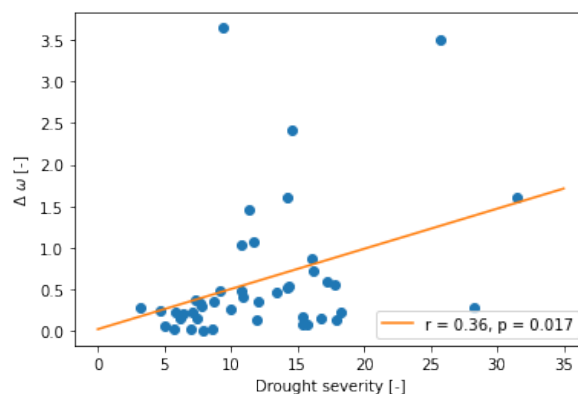


Figure 5.36: Correlation between the runoff ratio  $\Delta\omega$  and drought severity, for basins that experience a decrease in runoff ratio

Thus, for these basins where 68% of the basins experience dominating residual effects, the change in runoff ratio is again plotted against the drought characteristics in figures 5.34, 5.35 and 5.36. Comparing these graphs to the ones in section 5.2.2, somewhat stronger correlations are found. However, the correlations

are still too weak to be significant. A stronger, albeit still weak correlation is found between  $\Delta\omega$  and drought severity, as shown in figure 5.36. As the severity of drought increases,  $\Delta\omega$  increases as well, indicating that drought leads to a lower runoff ratio.

### 5.6.2. Residual Effects in Different Regions

The basins that show larger residuals effects are divided into two groups based on their aridity indices. The first group consists of basins in a more humid area, that have an aridity index of less than 0.5. The second group consists of basins with an aridity index of larger than 0.5. Plots of the movement of these basins inside the Budyko space are shown in figures 5.37, 5.38, 5.39, and 5.40.

The figures shows that the majority of the basins have a magnitude of movement of 0.1-0.2, together with a direction of movement of  $45^\circ - 90^\circ$ . This means that these basins have become less humid and the evaporation is higher. The basins with an aridity index  $> 0.5$  on the other hand, display mostly a downwards movement to the left, where the basins become more humid with lower evaporation.

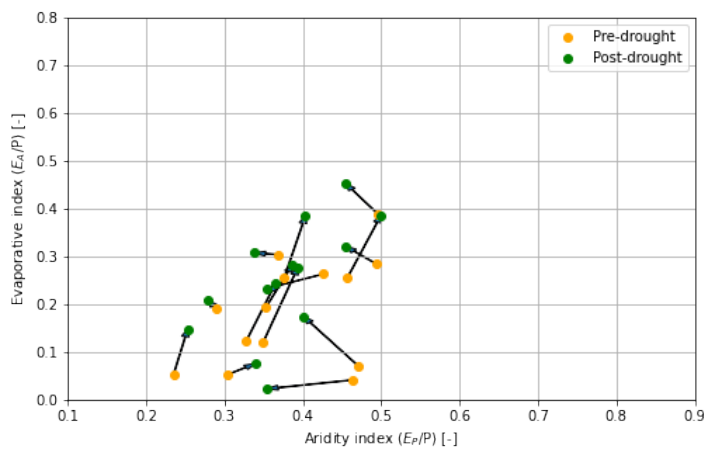


Figure 5.37: Movement of the basins inside the Budyko space: basins with aridity index  $< 0.5$

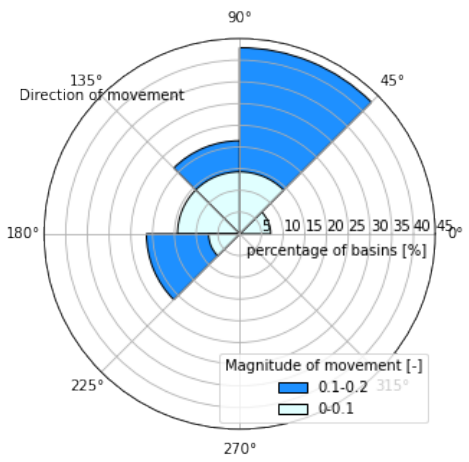


Figure 5.38: Radial plot of the magnitude and the direction of movement of the basins inside the Budyko space: basins with aridity index  $< 0.5$

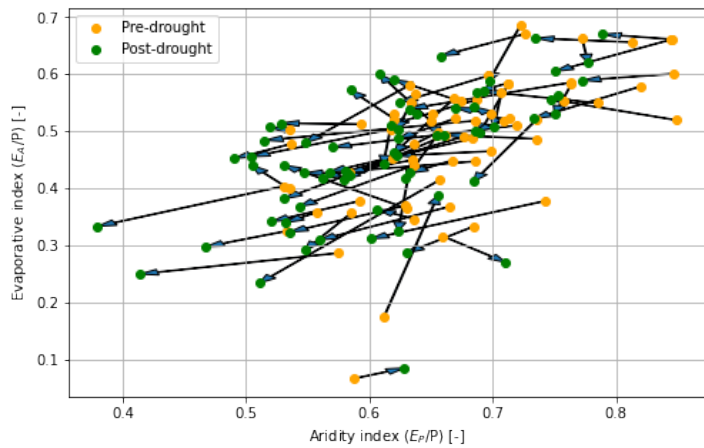


Figure 5.39: Movement of the basins inside the Budyko space: basins with aridity index  $> 0.5$

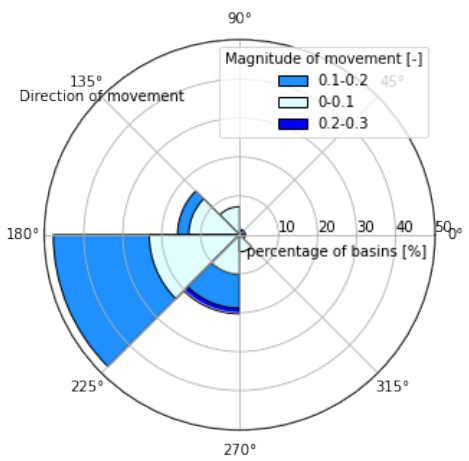


Figure 5.40: Radial plot of the magnitude and the direction of movement of the basins inside the Budyko space: basins with aridity index  $> 0.5$

### 5.6.3. Regional Differences in $S_{R,5yr}$ and NDVI

Basins with a smaller aridity index experience a greater storage deficit as well as greater changes in vegetation density. Thus, the basins are separated into two groups: basins with aridity index  $< 0.5$  and basins with aridity index  $> 0.5$ . The correlation coefficients are calculated between the different variables to explore the regional differences.

For both groups, the correlation coefficient between the maximum deficit  $S_{R,5yr}$ , the residual effects  $\Delta\Psi_r$  and the change in runoff ratio  $\Delta\omega$  are shown in tables 5.2 and 5.3. Little correlation is found between the variables.

	$\Delta\Psi_r$	
	Aridity index $<0.5$	Aridity index $>0.5$
$S_{R,5yr}$	0.25	0.20

Table 5.2: Correlation coefficient  $r$  between  $S_{R,5yr}$  and  $\Delta\Psi_r$

	$\Delta\omega$	
	Aridity index $<0.5$	Aridity index $>0.5$
$S_{R,5yr}$	-0.23	0.11

Table 5.3: Correlation coefficient  $r$  between  $S_{R,5yr}$  and  $\Delta\omega$

The correlation coefficients between  $\Delta\text{NDVI}$ , the residual effects  $\Delta\Psi_r$  and the change in runoff ratio  $\Delta\omega$  are shown in tables 5.4 and 5.5. A weak positive correlation is shown between  $\Delta\text{NDVI}$  and  $\Delta\Psi_r$  for basins with a lower aridity index.

	$\Delta\Psi_r$	
	Aridity index $<0.5$	Aridity index $>0.5$
$\Delta\text{NDVI}$	0.14	0.16

Table 5.4: Correlation coefficient  $r$  between  $\Delta\text{NDVI}$  and  $\Delta\Psi_r$

	$\Delta\omega$	
	Aridity index $<0.5$	Aridity index $>0.5$
$\Delta\text{NDVI}$	0.30	0.19

Table 5.5: Correlation coefficient  $r$  between  $\Delta\text{NDVI}$  and  $\Delta\omega$

Finally, the correlation coefficient between the maximum deficit  $S_{R,5yr}$  and  $\Delta\text{NDVI}$  are shown in table 5.6. No correlation is found between the variables.

	$\Delta\text{NDVI}$	
	Aridity index $<0.5$	Aridity index $>0.5$
$S_{R,5yr}$	-0.13	0.03

Table 5.6: Correlation coefficient  $r$  between  $S_{R,5yr}$  and  $\Delta\text{NDVI}$



# 6

## Discussion

### 6.1. Basin Selection

To select the basins used in this research, the drought index SPEI is used, together with the following combination of variables:

- Threshold level = -1
- SPEI accumulation period = 24 months
- Minimum drought period length = 12 months

When looking at the results, it should be kept in mind that the results correspond to this specific combination of variables. Another combination may lead to very different results and can be investigated further in future research.

Interestingly, the results show that sometimes, a lower threshold level yields more basins than a higher threshold level. The reason for this is that the basins selected need to meet a list of criteria, as listed in subsection 4.2.3. Thus, a higher threshold level doesn't necessarily lead to more basins. This is illustrated in figures 6.1 and 6.2.

To ensure data availability, the basin is rejected if less than 5 years of data is available in the pre-drought period and the post-drought period. For basin 2011460 shown in figure 6.1 for example, if a threshold level of 0 is chosen, there wouldn't be enough data for the pre-drought period. Thus, this basin is only accepted for threshold levels = -0.5 and -1.

Another scenario for which a lower threshold is accepted but not a higher one is shown in figure 6.2. It is stated in the criteria that SPEI cannot be below the threshold level for more than 24 months in the post-drought period, to make sure that the selected drought does not overlap another drought event. Thus, this basin is rejected when the threshold is 0 or -0.5.

It is clear that the criteria established for the basin selection process do not work perfectly. Further investigation can be carried out to find a better way to define the drought periods and to better select the basins.

When detecting runoff changes, the results show that in general, the basins display very minimal changes in the runoff ratio and vegetation, the effects of drought on the partitioning of the hydrological fluxes are minimal as well. The reason for this could be that the drought events of the selected basins are not long, intense, or severe enough to cause any significant changes. It is possible that more significant changes would be observed if a longer minimum drought period and a lower threshold level were used.

Furthermore, most basins selected have an aridity index between 0.5 to 0.8. When looking at all the basins together, it should be kept in mind that the changes in the parameters are mainly caused by basins with a higher aridity index.

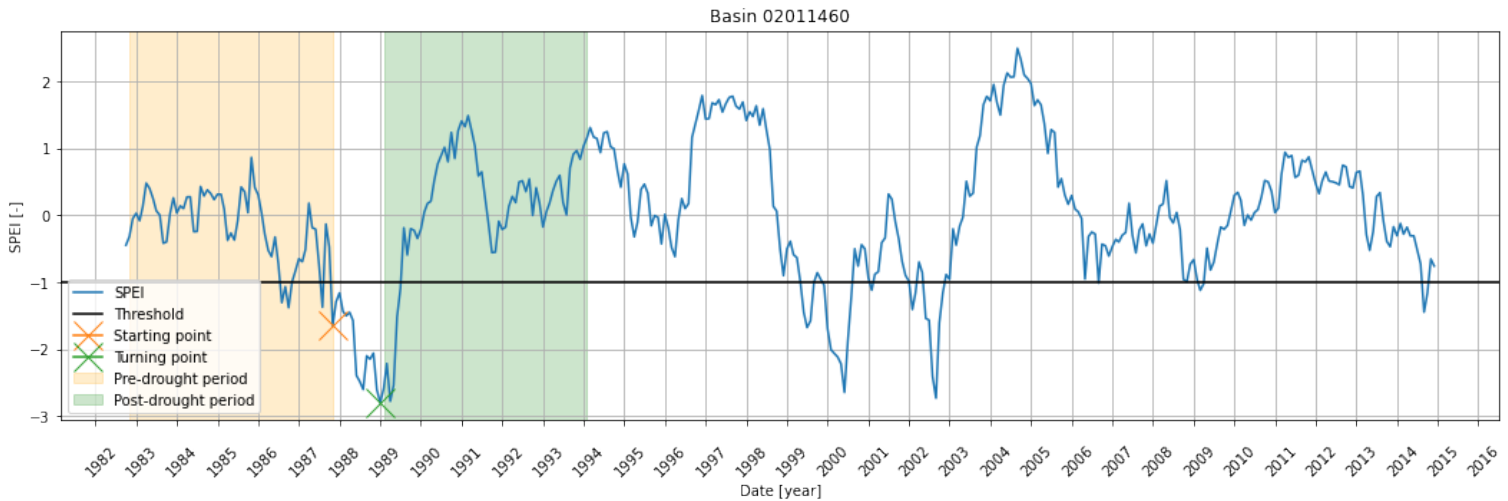


Figure 6.1: Selected drought periods for basin 2011460



Figure 6.2: Selected drought periods for basin 3010655

Another factor that may influence the results is the use of calendar years in selecting the drought periods instead of hydrological years. Using hydrological years, the hydrological conditions in the basins are better reflected. At the beginning of the hydrological year on 1 October, the basin is at its driest. Gradually, it becomes wetter and wetter until the end of the hydrological year on 30 September. Thus, the post-drought period defined in this research can, for example, end in the middle of the hydrological year, where the natural cycle from dry to wet is not completed. This can lead to an underestimation or an overestimation of precipitation and evaporation.

### 6.1.1. Drought Index

The drought index used, SPEI, does not show the best performance. In this research, a large accumulation period of 24 months is used, which means that relatively small changes in precipitation and evaporation are not detected. This accumulation period might also be too long for SPEI to capture the water conditions during the vegetation growth season, which is typically several months. However, if a shorter accumulation period is used, the sample size of this research would be too small to yield any scientifically significant results. Thus, this compromise is made.

Moreover, the basins selected using this method all belong to humid areas. This could be caused by the fact

that SPEI measures the basin's change in precipitation and potential evaporation relative to its normal conditions. Thus, 'drought' does not happen in arid areas where precipitation and potential evaporation are already low normally.

A possible solution to this problem is to include a more elaborate comparative study on the performance of different drought indices. Other meteorological drought indices such as Percent of Normal Precipitation and Deciles could be compared together with SPEI, SPI, and SRI.

The drought defined in this study is meteorological drought. Other types of non-meteorological droughts such as agricultural or hydrological droughts may show different results. If the drought defined is an agricultural drought, soil moisture could be used as a drought indicator, which may lead to better results.

Unfortunately, the CAMELS dataset does not include soil moisture data. This means that another case study area needs to be used, or that other basins from other datasets in the United States should be used. Another solution to this problem is to use the Palmer Drought Severity Index, which is a soil moisture indicator that uses precipitation, temperature, and potential evaporation as inputs.

## 6.2. Change in Runoff Ratio

It is hypothesized that drought leads to an increase in the runoff ratio and that the longer, more intense, and more severe the drought, the higher the runoff ratio becomes. However, this is not reflected in the results. In fact, very few changes in the runoff ratio before and after drought is detected and no correlation is found between the change in runoff ratio  $\Delta\omega$  and drought characteristics. Interestingly, slightly more than half of the basins show a slight decrease in runoff, which is the opposite of what is expected.

To investigate this, the 3-months average value of the aridity index,  $E_A/P$ , are plotted for the entire time-series for all basins. A typical example of the outcome is shown in figure 6.3.

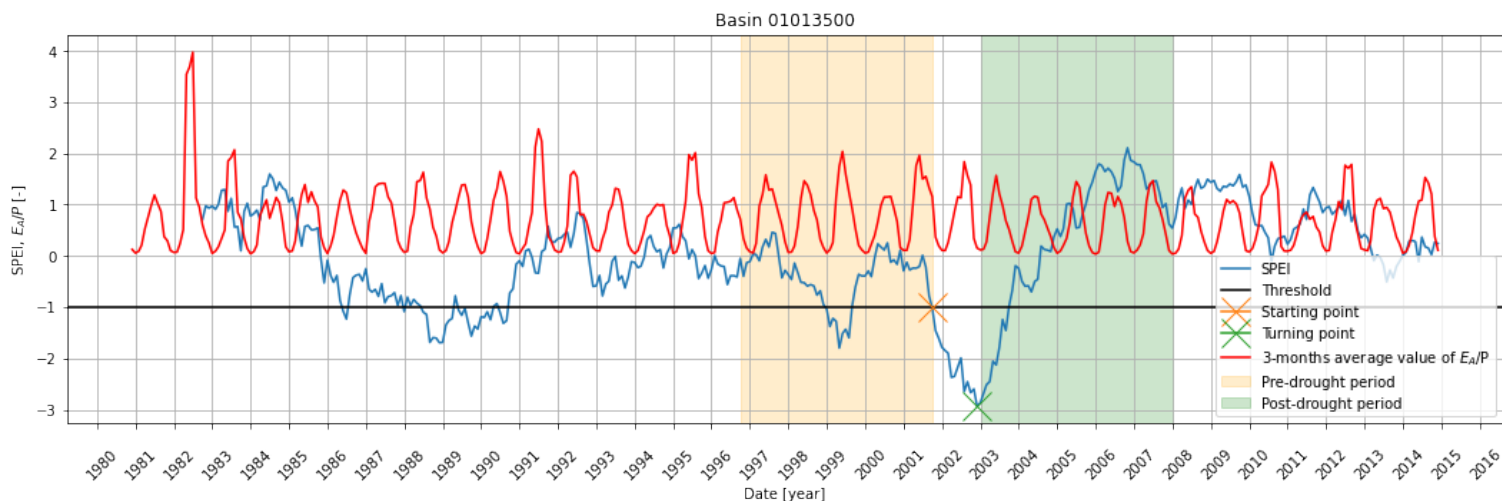


Figure 6.3: The change in SPEI and the 3-months average value of  $E_A/P$  over the years, for basin 1013500

As shown in the figure, yearly changes in the aridity index do exist. It is higher in the summer due to higher evaporation and it is lower in the winter. However, looking at the change in  $E_A/P$  over time, there seems to be no clear relationship between evaporation and SPEI. There are also no significant changes in  $E_A/P$  before, during, or after drought, which is also shown in the results in chapter 5.3.1, where the basins display minimal vertical movements inside the Budyko space. Thus, in general, the drought defined in this research does not significantly influence the basin's evaporation, nor the rainfall-runoff relationship.

This result is not in line with the findings of Peterson et al. (2021), where they investigated the effects of the

millennium drought in Australia. They have found that most basins persist to be in a low runoff state years after the drought has ended. In other words, they have found a close relationship between drought and the runoff ratio, whereas in this research, no significant relationship is found. The reason for this could be that the millennium drought in Australia lasted much longer, from around 1997 to 2010. This difference in drought duration might lead to different basin responses. Different plant species are also found in Australia compared to the US, which can also contribute to different results. Furthermore, in the study by Peterson et al. (2021), streamflow and precipitation are directly measured using gauges, whereas in this research, the runoff ratio is estimated using the long-term water balance and Fu's equation. This difference in methodology may also explain the differences in the results between these two studies.

It is also possible that the method used in this research does not successfully detect drought. Looking at figure 6.3, the problem does not seem to lie on the threshold level, nor the starting/ending point of drought. Thus, it is more likely that the drought indicator used, SPEI, does not successfully detect changes in the hydrological fluxes. Another possibility is that drought is detected, but the vegetation is so resistant to drought that it doesn't lead to changes in evaporation or runoff. This is elaborated further in the next section.

Furthermore, plotting the change in runoff ratio against the change in aridity index in figure 5.7 has shown that two possible trendlines can be fitted to the basins. To investigate this problem, the basins are clustered into 2 groups: basins with an aridity index of smaller than 0.5 and basins with an aridity index of larger than 0.5. The correlation coefficient is calculated again for these clusters, and it is shown in figure 6.4.

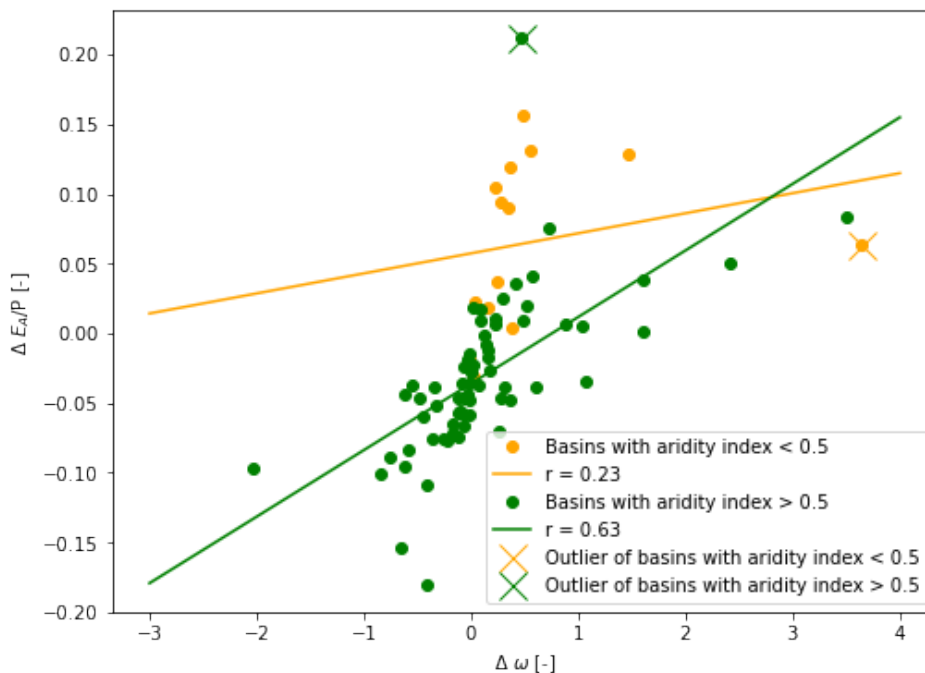


Figure 6.4: The correlation between  $\Delta\omega$  and  $\Delta E_A/P$ , clustered by aridity index

Without clusters, the correlation coefficient between the two variables is 0.57. This clustering leads to a higher coefficient for basins with a higher aridity index, but a lower coefficient for the basins in more humid regions. It can be seen from figure 6.4 that the results are largely influenced by 2 outliers, indicated by the orange and the green crosses. These two basins have an aridity index near 0.5 and 0.6. This might mean that basins with an aridity index of around 0.5 and 0.6 are more likely to behave unpredictably. However, more research is needed to verify this.

As shown in figure 6.5, removing these outliers does yield a higher correlation coefficient between the change in runoff ratio and change in aridity index for both clusters.

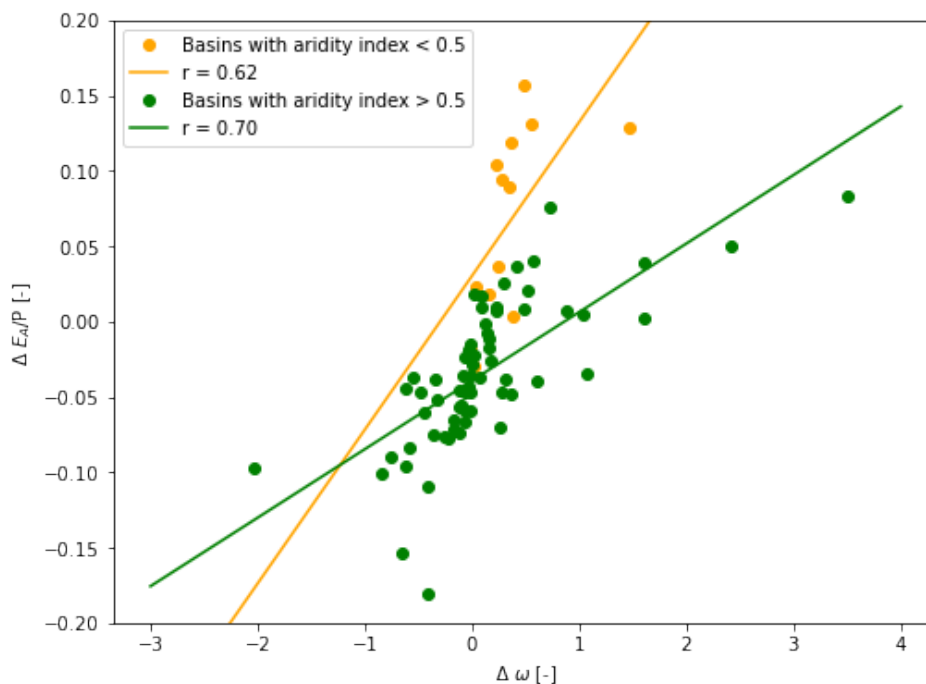


Figure 6.5: The correlation between  $\Delta\omega$  and  $\Delta E_A/P$ , clustered by aridity index and with outliers removed

Moreover, the basins can also be clustered based on other attributes, such as vegetation type, the elevation of the basin, and the slope of the basin. With these clusters, a stronger or weaker correlation may be found between the variables, which can provide us better insights into the basins' behavior. As an experiment, another cluster is made based on the change in the vegetation index, NDVI. The results are shown in Appendix E. On average, a stronger correlation is also found between the change in runoff ratio and the change in evaporative index when grouping the basins by  $\Delta\text{NDVI}$ , as compared to no clustering at all.

### 6.3. Changes Inside the Budyko Space

Plotting the movement of the basins in chapter 5.3.1 shows that the magnitude of the change is in general very small, which is explained by the small  $\Delta\omega$  values. For basins with an increase in runoff ratio,  $\Delta\omega < 0$ ,  $E_A/P$  slightly decreases, and for basins with a decrease in runoff ratio,  $\Delta\omega > 0$ , there is on average a slight increase in  $E_A/P$ . Thus, for most basins, an increase in runoff ratio corresponds to a decrease in evaporation, and vice versa. However, more than 30% of the basins with a decrease in runoff ratio show a small decrease in the aridity index, which is not what is expected.

This can be explained by looking at figure 6.6. Basin 105700 is one of the basins that have a positive  $\Delta\omega$  (decrease in runoff ratio), as well as a decrease in evaporation. The reason for this is that basin is quite humid, where evaporation is limited by the energy input rather than water availability. Thus, when there is little energy for evaporation, it is possible that a further increase in the basin's humidity leads to lower evaporation as well as a higher runoff. This is also the reason why  $\Delta\omega$  and  $\Delta E_A/P$  are only moderately correlated, whereas  $\Delta\Psi_r$  and  $\Delta E_A/P$  are strongly correlated.

The results also show that drought has made most basins more humid, indicated by the decrease in aridity index. This is caused by the climate effects. After the drought, the precipitation increases, which decreases the aridity index under the assumption that the potential evaporation stays the same. Furthermore, the selected basins are located in humid climates where evaporation is energy limited. It is also possible that the net radiation is low in the post-drought period, which leads to a smaller  $E_p$  and therefore, a lower aridity index.

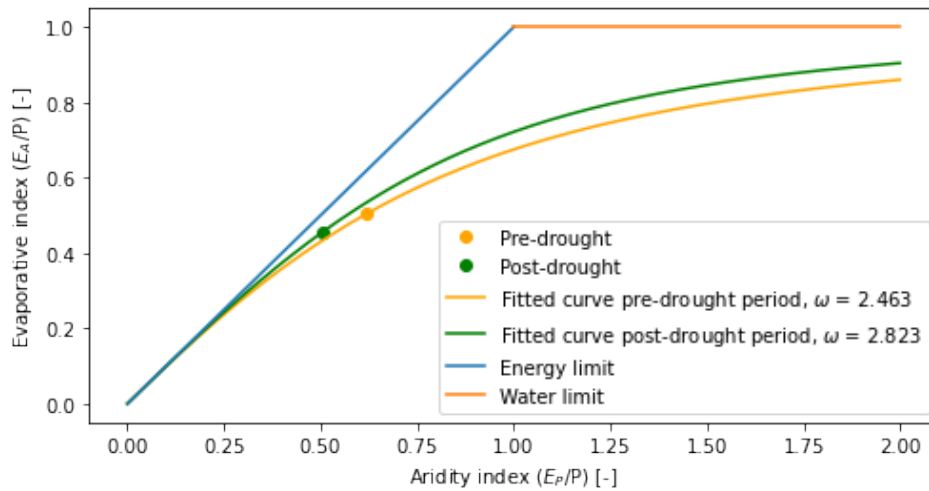


Figure 6.6: Movement of basin 1057000 from the pre-drought period to the post-drought period

### 6.3.1. Residual Effects

For the entire post-drought period,  $\Delta\Psi_r$  is negative for  $\Delta\omega < 0$  and positive for  $\Delta\omega > 0$ , which is the expected results. However, for each year after drought,  $\Delta\Psi_r$  fluctuates from positive to negative values. No clear pattern is found on how  $\Delta\Psi_r$  changes, since movements of the basins from year to year seem to be very random. The reason for this could be that the yearly post-drought  $E_A$  values are estimated using the difference between  $P$  and  $E$ , which can be a good estimate if long-term data is used. However, in this case, one year may not be long enough to allow us to neglect the change in storage, which makes the results unreliable.

The residual effects are more dominant for basins with a decrease in runoff ( $\Delta\omega > 0$ ). For these basins, a weak correlation is found between the drought severity and  $\Delta\omega$ : the more severe the drought, the lower the runoff ratio. As discussed in chapter 2, this could be caused by a shift in vegetation towards more drought-resistant species, or that the water use efficiency of the vegetation has increased due to the lack of water, alleviating the effects of drought.

Residual effects are landscape-related effects, which can be vegetation changes. However, there are also other factors that can cause changes in  $\Delta\Psi_r$ . For example, agriculture, irrigation, and hydro-power plants can increase the basin's evaporation (Jaramillo and Destouni, 2014), although this is unlikely because the basins in the CAMELS dataset are minimally influenced by humans. Thus, other factors that cause landscape-related flux changes are more likely to be the cause. This can include for example groundwater changes, forest fires, deforestation, afforestation, and changes in the type of vegetation that grows in the basin.

The results show that a weak correlation exists between  $\Delta\Psi_r$  and the vegetation-related factors  $S_{R,5yr}$ , but there is no correlation between  $\Delta\Psi_r$  and  $\Delta\text{NDVI}$ . This means that to some extent, the residual effects are caused by changes in vegetation. However, other landscape-related factors are likely to have contributed more to  $\Delta\Psi_r$ .

## 6.4. Vegetation Changes

As shown in figures 5.25 and 5.32 in the results section, no correlation is found between the maximum storage deficit and the change in runoff ratio, nor between the maximum storage deficit and the change in NDVI. However, looking at the way the basins scatter in these plots, it seems as though the basins can be clustered into different groups, which may show a better correlation between the variables.

Thus, for these two plots, the basins are clustered based on the aridity index and the results are shown in Appendix F. Unfortunately, no correlation is found again. As previously mentioned, clustering the basins using other attributes may lead to different results. More research is needed to do so.

### 6.4.1. Storage Deficit

The results show that a weak correlation exists between the maximum storage deficit and  $\Delta\Psi_r$ . Furthermore, no correlation is found between  $S_{R,5yr}$  and  $\Delta\omega$ . This may be caused by the following reasons:

- The magnitude of  $S_{R,5yr}$  is relatively small for most basins, which may not have significant effects on vegetation.
- The method of calculating  $S_{R,5yr}$  assumes that there is no evaporation due to interception. Other non-vegetation-related fluxes such as evaporation from the soil surface are not taken into account. Thus, a large proportion of evaporative fluxes may be neglected in this case.
- The storage reservoir is assumed to be infinitely large, which means there is no runoff, and that vegetation only takes water from the unsaturated zone, not from groundwater. This is unrealistic in real life.
- Gao et al. (2014) have found that the root system of vegetation can access enough water to bridge droughts that have a return period of 10-20 years. The selected droughts that took place may have a shorter return period, and therefore, may not be severe enough to affect vegetation.

### 6.4.2. NDVI

During drought, some plant species can increase their water use efficiency (a measure for the amount of biomass produced per unit of water used by a plant). According to Zhao et al. (2020a), the water use efficiency of different plants under drought conditions can be ranked from high to low. The ranking is as follows:

1. Forests
2. Shrublands
3. Croplands
4. Grasslands

The results show that a large portion of the basins experiences a slight increase in NDVI after drought, which may be caused by the increase in the plant's water use efficiency. Therefore, they can maintain healthy growth despite the water deficit caused by drought.

In figure 6.7, an elevation map of the United States is presented. It can be seen that most of the selected basins are located at higher altitudes, with an elevation of around 1000 meters. At this altitude, the most common vegetation that grows is conifer forests. Thus, it is very likely that these trees are resistant to drought. This could also be the reason that little changes in runoff ratio are detected, and that a large  $S_{R,5yr}$  does not lead to a decrease in NDVI. However, more research is needed on how exactly the vegetation in the selected basins responds to drought.

## 6.5. Regional Differences

Basins located in humid areas with an aridity index of less than 0.5 show the opposite results as expected. In these humid basins, a decrease in runoff ratio and an increase in evaporation is observed after drought. Furthermore, although the storage deficit is high, vegetation seems to have increased.

The results do not support the research done by Saft et al. (2015), where they have found that long term droughts are more likely to affect the rainfall-runoff relationship in drier, less forested regions. The results also show maximum storage deficit is higher for basins with a lower aridity index, which is not expected.

Furthermore, basins with an aridity index  $< 0.5$  display a very weak correlation between  $\Delta\text{NDVI}$  and  $\Delta\omega$ . However, there is no correlation between  $\Delta\text{NDVI}$  and  $\Delta\Psi_r$ , nor between  $\Delta\text{NDVI}$  and  $S_{R,5yr}$ . Thus, the decrease in runoff ratio may be related to vegetation changes to some extent, but the connection is weak. There may be

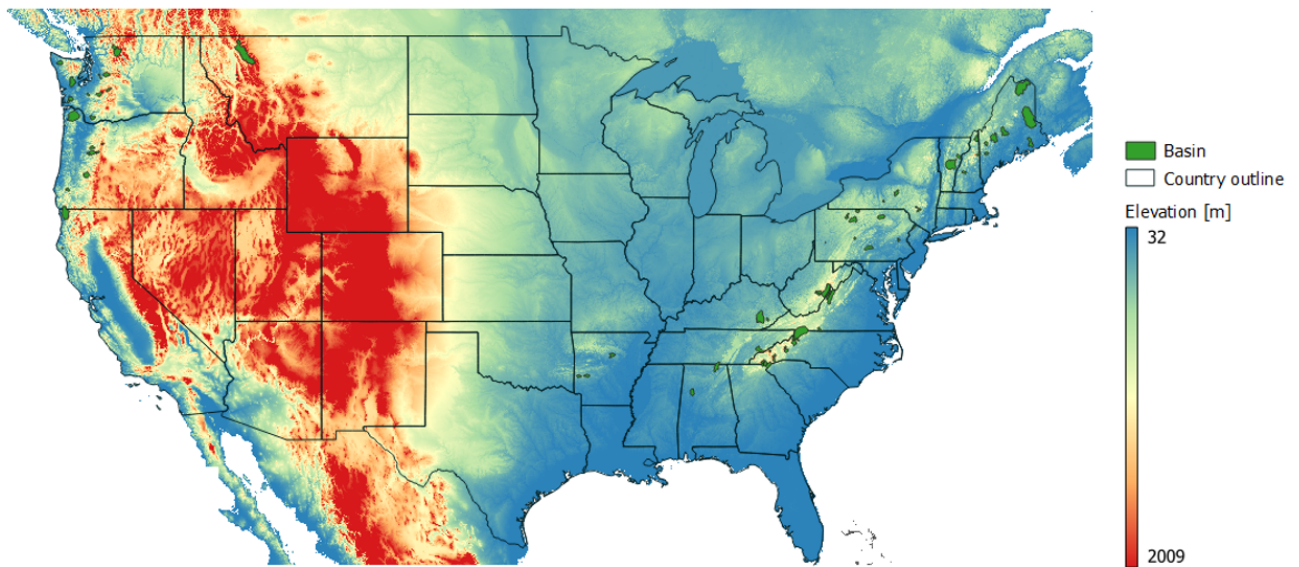


Figure 6.7: Elevation map showing the altitudes of the selected basins

other non-vegetation-related factors that contribute to the runoff changes. More research is needed in this case to find out what those factors are.

Moreover, it can be argued how scientifically significant the results are for basins with an aridity index of less than 0.5. In total, 14 basins belong to this group. Due to the lack of data, the results from these basins could in theory be outliers and are not representative of reality. This may also be the reason that the results differ from research done by Saft et al. (2015), and that the maximum storage deficit is higher for the more humid basins.

# 7

## Conclusion

The goal of this research is to investigate the link between multi-year droughts and post-drought floods. To do so, the United States is used as a case study area and hydrological data, as well as remote sensing data, is collected and analysed. In this research, the main research question is established together with 4 sub-questions. The research questions are:

Is there a relationship between multi-year droughts and the floods that occur in the post-drought period in the United States?

- Do long-term droughts lead to an increase in the runoff ratio in the post-drought period as compared to the pre-drought period?
- Is vegetation the main driver for the change in the precipitation partitioning in the post-drought period?
- Can a correlation be found between vegetation changes and runoff ratio?
- What are the regional differences in the results?

The hypothesis is that drought decreases vegetation and increases floods. However, results found in this research do not support this hypothesis. This is illustrated by answering the research questions in the following paragraphs.

1. Do long-term droughts lead to an increase in the runoff ratio in the post-drought period as compared to the pre-drought period?

Fitting the selected basins to Fu's equation, little changes are observed in the runoff ratio before and after drought. Applying the rank-sum test to the  $\omega$  values has shown that we cannot reject the null hypothesis (there is no change in runoff ratio) in favor of the alternative hypothesis (there is an increase in runoff ratio). Furthermore, drought duration, intensity, and severity do not seem to have influences on the runoff ratio.

2. Is vegetation the main driver for the change in the precipitation partitioning in the post-drought period?

Drought does have influences on the way precipitation is partitioned into evaporation and runoff in the post-drought period. Under constant precipitation, most basins that show a decrease in runoff have also shown an increase in evaporation and positive residual effects, which can be driven by vegetation changes. The opposite is true for basins that experience an increase in runoff. However, the vegetation-related residual effects are only dominant in basins with a decrease in runoff ratio.

### 3. Can a correlation be found between vegetation changes and runoff ratio?

Vegetation changes are indicated by the maximum storage deficit and the vegetation index NDVI. Pearson's correlation coefficient shows a weak correlation between the maximum storage deficit and the residual effects, but no relationship between the storage deficit and NDVI. Furthermore, no correlation is found between storage deficit and runoff ratio, nor between NDVI and runoff ratio.

### 4. What are the regional differences in the results?

After the drought, basins with an aridity index of smaller than 0.5 show a decrease in runoff ratio and more dominant residual effects. The basins also display an increase in vegetation density. However, only a weak correlation of 0.3 is found between  $\Delta\text{NDVI}$  and  $\Delta\omega$  and no correlation is found between  $\Delta\omega$  and  $S_{R,5yr}$ . Thus, for basins with an aridity index  $< 0.5$ , a decrease in runoff is detected, but the role vegetation plays in causing this decrease is very small. Furthermore, these results are based on a small number of basins, which means that the results are not very reliable.

For basins with an aridity index of larger than 0.5, no significant changes are detected.

Based on the answered to the sub-research questions, it can be concluded that using the methodology described in this research, no significant relationship is found between multi-year droughts and the floods that occur in the post-drought period in the United States.

# Bibliography

- Anderegg, W. R. L., Schwalm, C., Biondi, F., Camarero, J. J., Koch, G., Litvak, M., Ogle, K., Shaw, J. D., Shevliakova, E., and Williams, A. P. (2015). Pervasive drought legacies in forest ecosystems and their implications for carbon cycle models. *Science*, 349(6247):528–532.
- Bosch, J. M. and Hewlett, J. D. (1982). A review of catchment experiments to determine the effect of vegetation changes on water yield and evapotranspiration. *Journal of hydrology*, 55(1-4):3–23.
- Bruijnzeel, L. A. (1989). forestation and dry season flow in the tropics: A closer look. *Journal of Tropical Forest Science*, pages 229–243.
- Budyko, M. I., Miller, D. H., and Miller, D. H. (1974). *Climate and life*, volume 508. Academic press New York.
- Dai, A. (2013). Increasing drought under global warming in observations and models. *Nature climate change*, 3(1):52–58.
- Davenport, F. V., Burke, M., and Diffenbaugh, N. S. (2021). Contribution of historical precipitation change to US flood damages. *Proceedings of the National Academy of Sciences*, 118(4).
- DeChant, C. M. and Moradkhani, H. (2015). Analyzing the sensitivity of drought recovery forecasts to land surface initial conditions. *Journal of Hydrology*, 526:89–100.
- Esfahanian, E., Nejadhashemi, A. P., Abouali, M., Daneshvar, F., Alireza, A. R., Herman, M. R., and Tang, Y. (2016). Defining drought in the context of stream health. *Ecological Engineering*, 94:668–681.
- Fu, B. P. (1981). On the calculation of the evaporation from land surface. *Sci. Atmos. Sin*, 5(1):23–31.
- Gao, H., Hrachowitz, M., Schymanski, S. J., Fenicia, F., Sriwongsitanon, N., and Savenije, H. H. G. (2014). Climate controls how ecosystems size the root zone storage capacity at catchment scale. *Geophysical Research Letters*, 41(22):7916–7923.
- Hayes, M., Svoboda, M., Wall, N., and Widhalm, M. (2011). The Lincoln declaration on drought indices: universal meteorological drought index recommended. *Bulletin of the American Meteorological Society*, 92(4):485–488.
- IF, A. J., YUSTE, J. C., and OGAYA, R. (2010). Introducing the climate change effects on Mediterranean forest ecosystems: observation, experimentation, simulation and management. *Forêt méditerranéenne*.
- Jaramillo, F., Cory, N., Arheimer, B., Laudon, H., Velde, Y. v. d., Hasper, T. B., Teutschbein, C., and Uddling, J. (2018). Dominant effect of increasing forest biomass on evapotranspiration: interpretations of movement in Budyko space. *Hydrology and Earth System Sciences*, 22(1):567–580.
- Jaramillo, F. and Destouni, G. (2014). Developing water change spectra and distinguishing change drivers worldwide. *Geophysical Research Letters*, 41(23):8377–8386.
- Kundzewicz, Z. W., Mata, L. J., Arnell, N. W., Döll, P., Jimenez, B., Miller, K., Oki, T., Şen, Z., and Shiklomanov, I. (2008). The implications of projected climate change for freshwater resources and their management. *Hydrological sciences journal*, 53(1):3–10.
- Liu, L., Gudmundsson, L., Hauser, M., Qin, D., Li, S., and Seneviratne, S. I. (2019). Revisiting assessments of ecosystem drought recovery. *Environmental Research Letters*, 14(11):114028.
- Lyon, B., Bell, M. A., Tippet, M. K., Kumar, A., Hoerling, M. P., Quan, X.-W., and Wang, H. (2012). Baseline probabilities for the seasonal prediction of meteorological drought. *Journal of Applied Meteorology and Climatology*, 51(7):1222–1237.

- Mallakpour, I. and Villarini, G. (2015). The changing nature of flooding across the central United States. *Nature Climate Change*, 5(3):250–254.
- McKee, T. B., Doesken, N. J., and Kleist, J. (1993). The relationship of drought frequency and duration to time scales. In *Proceedings of the 8th Conference on Applied Climatology*, volume 17, pages 179–183. Boston.
- Mishra, A. K. and Singh, V. P. (2010). A review of drought concepts. *Journal of hydrology*, 391(1-2):202–216.
- Morid, S., Smakhtin, V., and Moghaddasi, M. (2006). Comparison of seven meteorological indices for drought monitoring in Iran. *International Journal of Climatology: A Journal of the Royal Meteorological Society*, 26(7):971–985.
- Mueller, R. C., Scudder, C. M., Porter, M. E., Talbot Trotter III, R., Gehring, C. A., and Whitham, T. G. (2005). Differential tree mortality in response to severe drought: evidence for long-term vegetation shifts. *Journal of Ecology*, 93(6):1085–1093.
- Newman, A. J., Clark, M. P., Sampson, K., Wood, A., Hay, L. E., Bock, A., Viger, R. J., Blodgett, D., Brekke, L., and Arnold, J. R. (2015). Development of a large-sample watershed-scale hydrometeorological data set for the contiguous USA: data set characteristics and assessment of regional variability in hydrologic model performance. *Hydrology and Earth System Sciences*, 19(1):209–223.
- Peterson, T. J., Saft, M., Peel, M. C., and John, A. (2021). Watersheds may not recover from drought. *Science*, 372(6543):745–749.
- Pike, J. G. (1964). The estimation of annual run-off from meteorological data in a tropical climate. *Journal of Hydrology*, 2(2):116–123.
- Saft, M., Western, A. W., Zhang, L., Peel, M. C., and Potter, N. J. (2015). The influence of multiyear drought on the annual rainfall-runoff relationship: An Australian perspective. *Water Resources Research*, 51(4):2444–2463.
- Schwalm, C. R., Anderegg, W. R. L., Michalak, A. M., Fisher, J. B., Biondi, F., Koch, G., Litvak, M., Ogle, K., Shaw, J. D., and Wolf, A. (2017). Global patterns of drought recovery. *Nature*, 548(7666):202–205.
- Sheffield, J. and Wood, E. F. (2012). *Drought: past problems and future scenarios*. Routledge.
- Shukla, S. and Wood, A. W. (2008). Use of a standardized runoff index for characterizing hydrologic drought. *Geophysical research letters*, 35(2).
- Strzepek, K., Yohe, G., Neumann, J., and Boehlert, B. (2010). Characterizing changes in drought risk for the United States from climate change. *Environmental Research Letters*, 5(4):044012.
- Vertessy, R. A. (1999). The impacts of forestry on streamflows: a review.
- Vicente-Serrano, S. M., Gouveia, C., Camarero, J. J., Beguería, S., Trigo, R., López-Moreno, J. I., Azorín-Molina, C., Pasho, E., Lorenzo-Lacruz, J., and Revuelto, J. (2013). Response of vegetation to drought time-scales across global land biomes. *Proceedings of the National Academy of Sciences*, 110(1):52–57.
- Vose, J. M., Miniati, C. F., Luce, C. H., Asbjornsen, H., Caldwell, P. V., Campbell, J. L., Grant, G. E., Isaak, D. J., Loheide II, S. P., and Sun, G. (2016). Ecohydrological implications of drought for forests in the United States. *Forest Ecology and Management*, 380:335–345.
- Zhang, L., Dawes, W. R., and Walker, G. R. (2001). Response of mean annual evapotranspiration to vegetation changes at catchment scale. *Water resources research*, 37(3):701–708.
- Zhang, L., Hickel, K., Dawes, W. R., Chiew, F. H. S., Western, A. W., and Briggs, P. R. (2004). A rational function approach for estimating mean annual evapotranspiration. *Water resources research*, 40(2).
- Zhang, L., Xiao, J., Zhou, Y., Zheng, Y., Li, J., and Xiao, H. (2016). Drought events and their effects on vegetation productivity in China. *Ecosphere*, 7(12):e01591.
- Zhao, J., Xu, T., Xiao, J., Liu, S., Mao, K., Song, L., Yao, Y., He, X., and Feng, H. (2020a). Responses of water use efficiency to drought in southwest China. *Remote Sensing*, 12(1):199.
- Zhao, Y., Weng, Z., Chen, H., and Yang, J. (2020b). Analysis of the Evolution of Drought, Flood, and Drought-Flood Abrupt Alternation Events under Climate Change Using the Daily SWAP Index. *Water*, 12(7):1969.

# A

## Examples of the Drought Periods of the Selected Basins



Figure A.1: The drought periods selected for basin 1047000

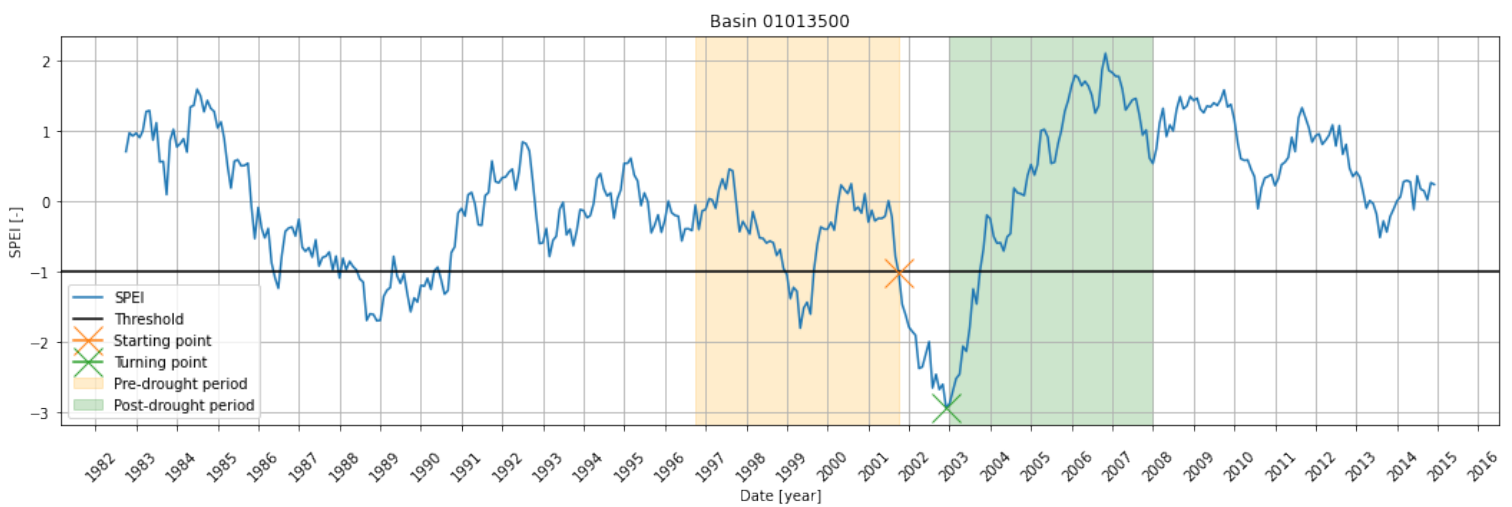


Figure A.2: The drought periods selected for basin 1013500



Figure A.3: The drought periods selected for basin 1139800

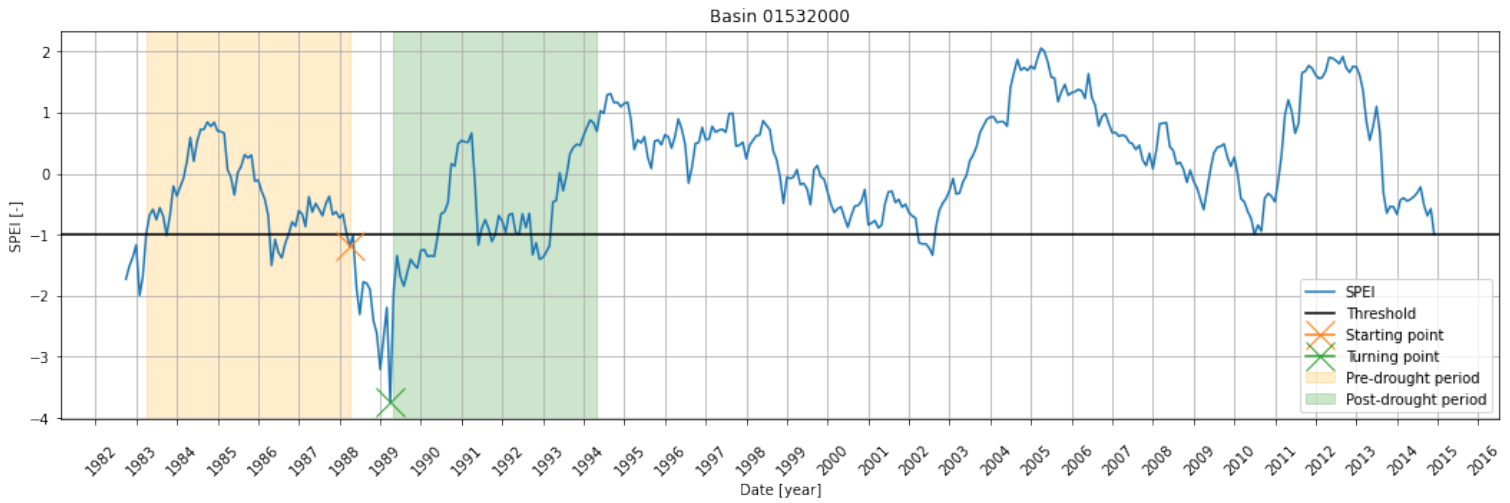


Figure A.4: The drought periods selected for basin 1532000



Figure A.5: The drought periods selected for basin 3049800

# B

## Examples of the Basins' Movements from Pre- to Post-drought Period

### B.1. Basins that experience an increase in runoff ratio: $\Delta\omega < 0$

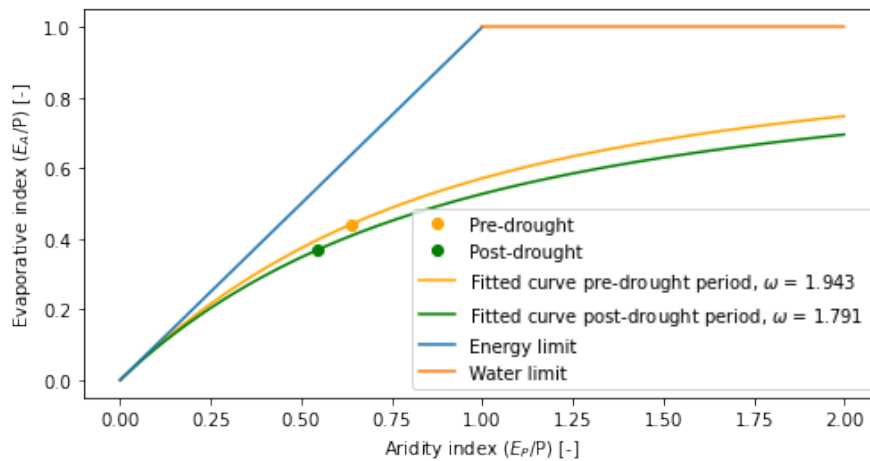


Figure B.1: Movement of basin 1022500

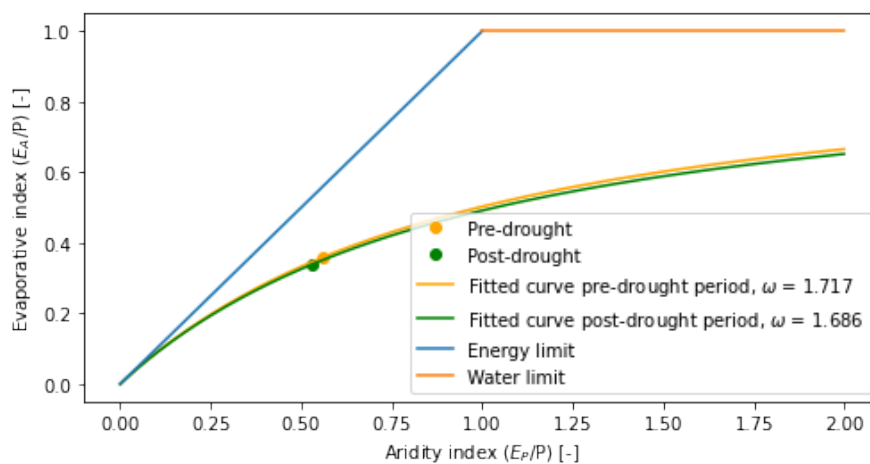


Figure B.2: Movement of basin 1434025

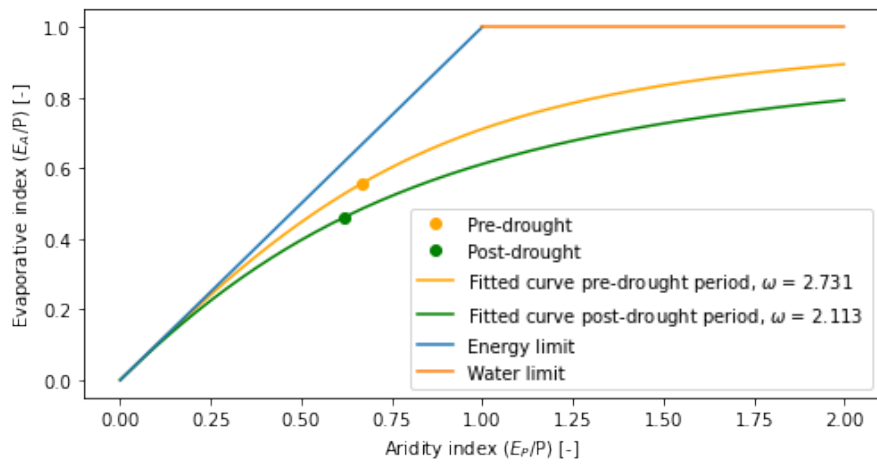


Figure B.3: Movement of basin 1510000

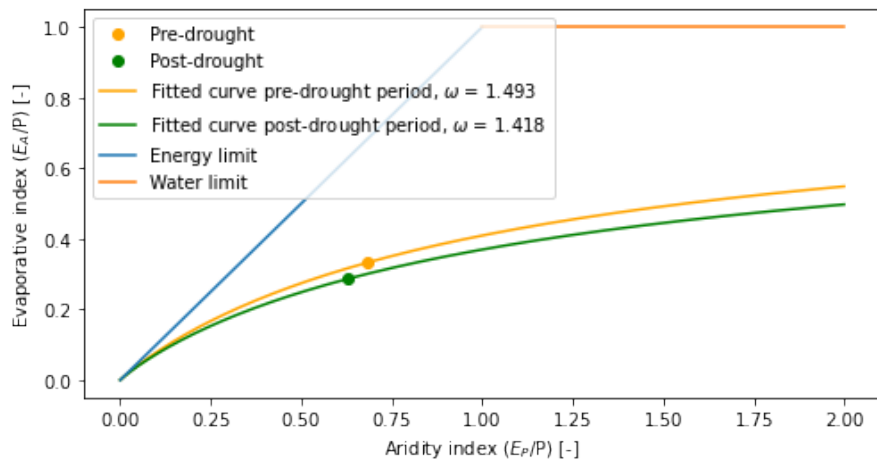


Figure B.4: Movement of basin 12358500

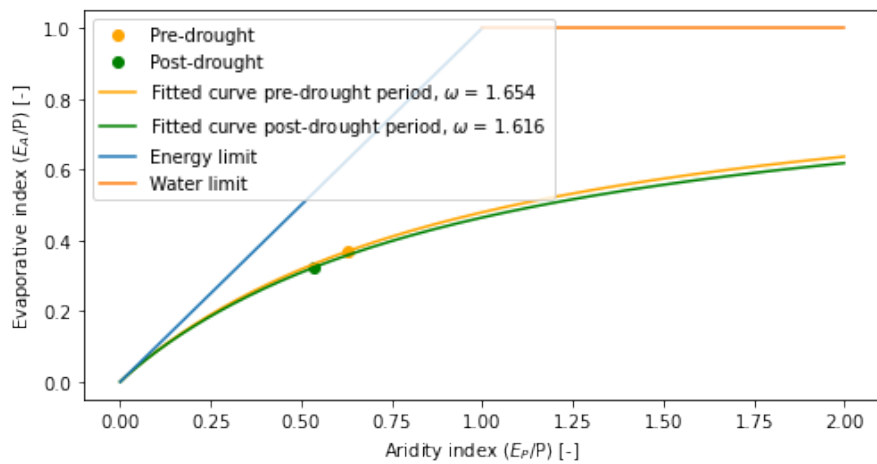


Figure B.5: Movement of basin 1055000

### B.2. Basins that experience a decrease in runoff ratio: $\Delta\omega > 0$

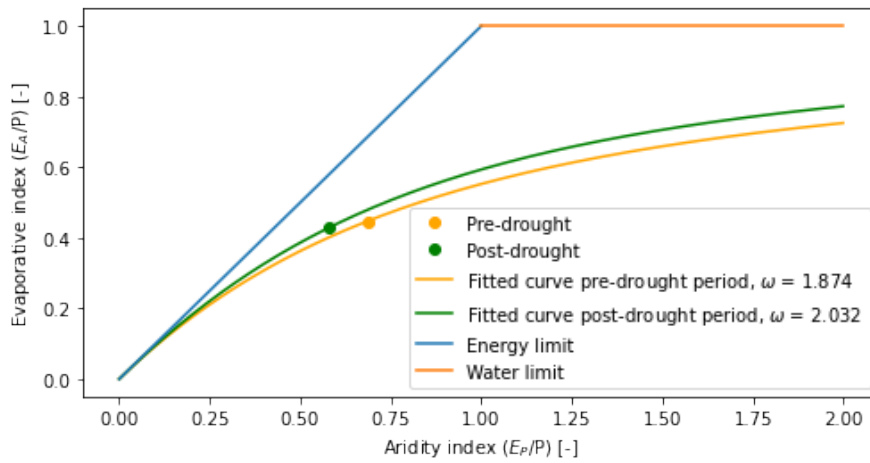


Figure B.6: Movement of basin 1030500

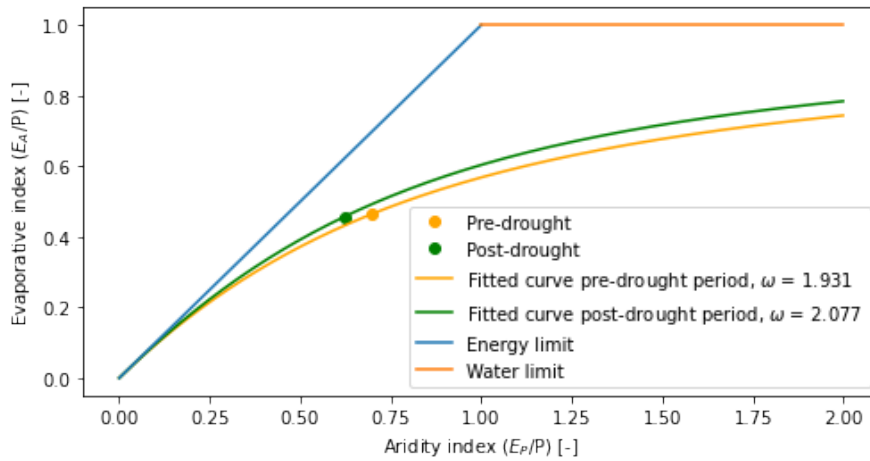


Figure B.7: Movement of basin 1139000

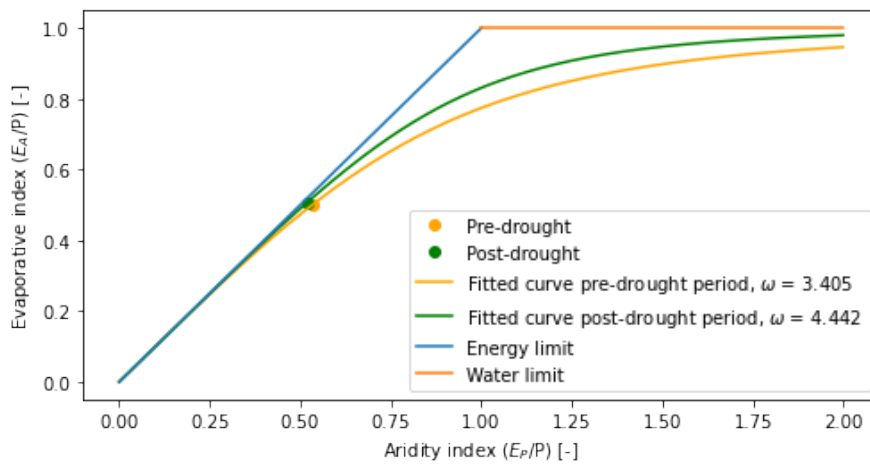


Figure B.8: Movement of basin 3500000

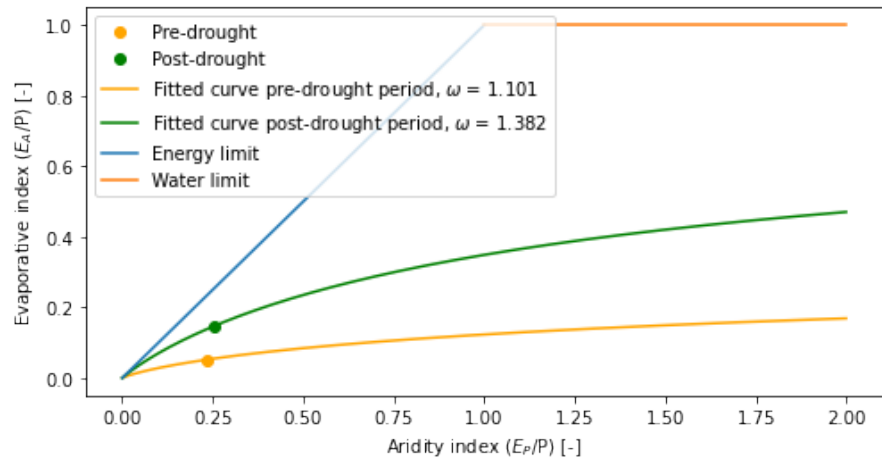


Figure B.9: Movement of basin 12010000

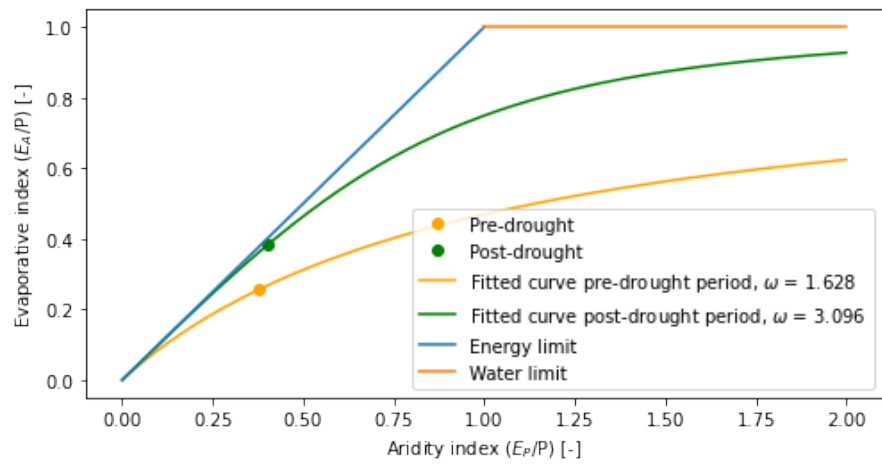


Figure B.10: Movement of basin 14187000

# C

## The Basins' Yearly Changes in Residual Effects Post-drought

### C.1. Basins that experience an increase in runoff ratio: $\Delta\omega < 0$

For every year in the post-drought period, the residual effects are plotted for the basins. As shown in figures C.1  $\Delta\Psi_r$  fluctuates from year to year, containing both positive values and negative values.

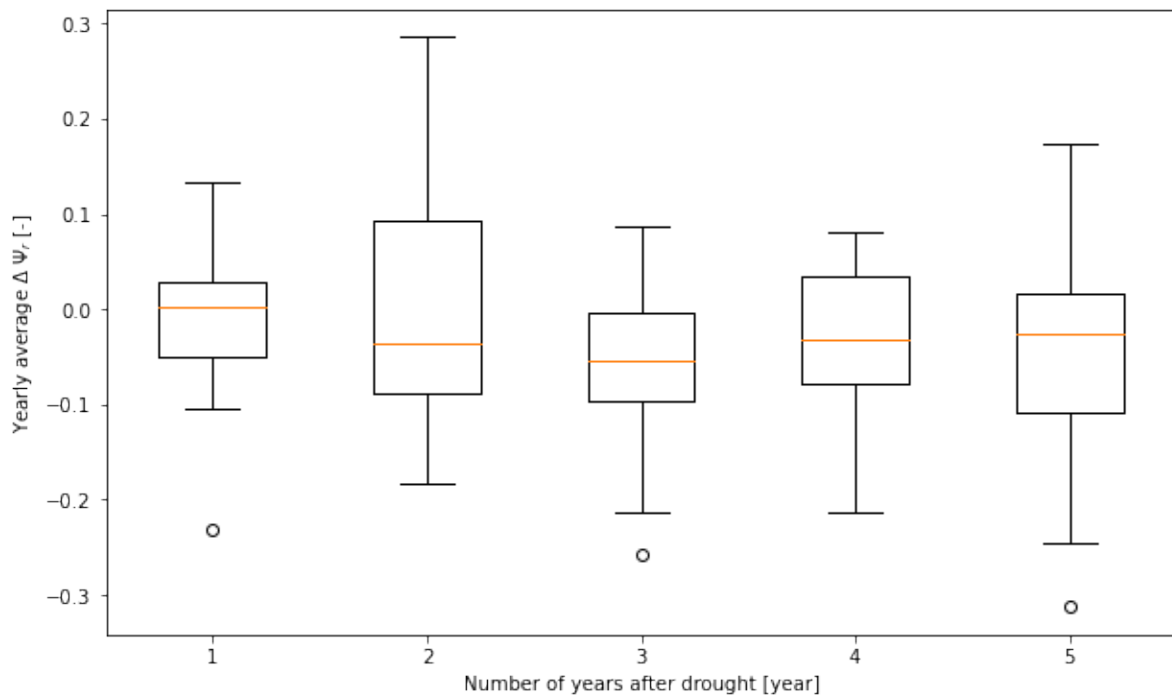


Figure C.1: Change in average  $\Delta\Psi_r$  for every year in the post-drought period: basins with  $\Delta\omega < 0$

To investigate these changes, the yearly movement of the individual basins inside the Budyko space are plotted, as shown in the figures in the next page. The residual effects is the vertical distance between the point and the curve. No clear pattern is found in the results.

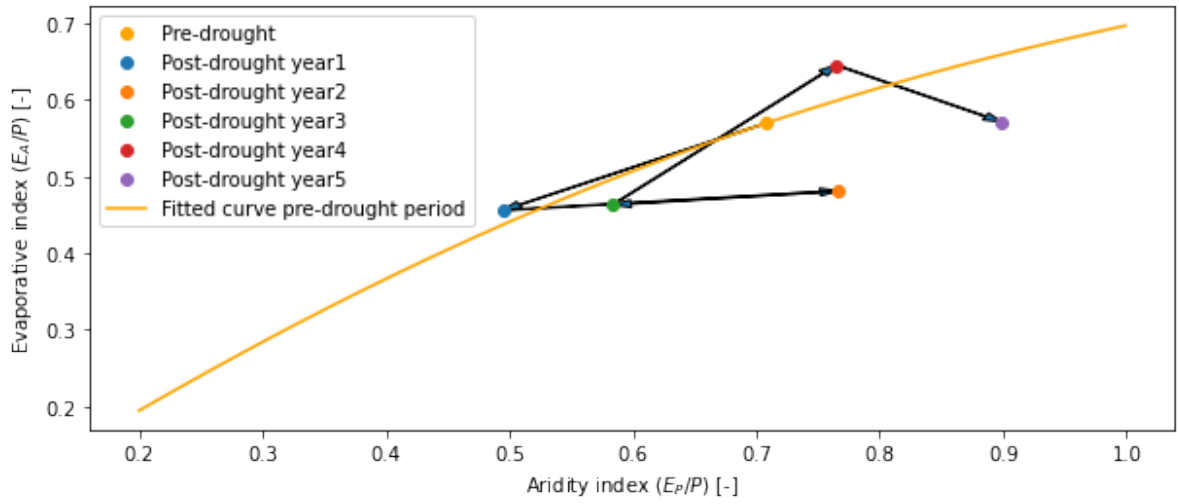


Figure C.2: Yearly movement of basin 211180

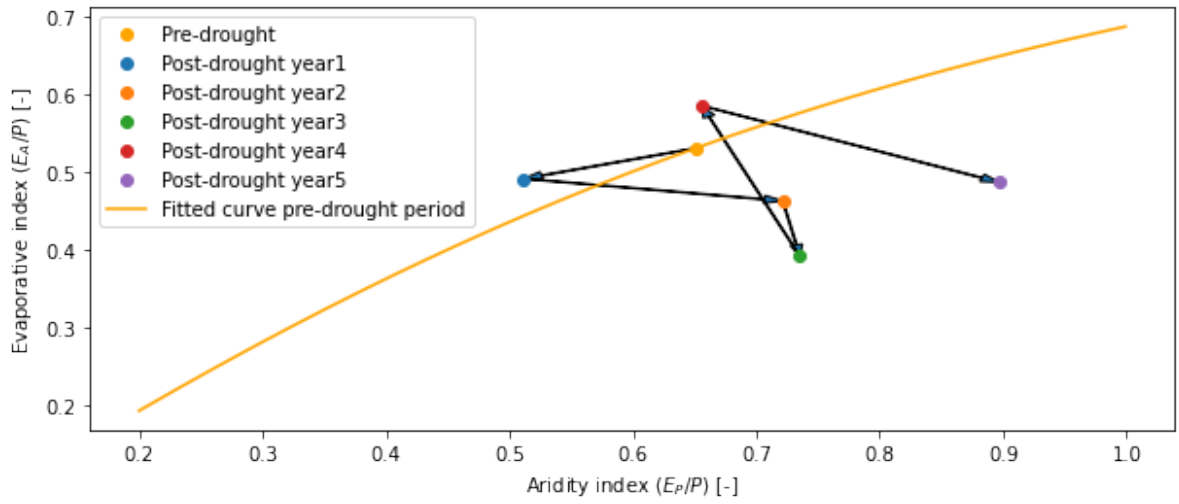


Figure C.3: Yearly movement of basin 3161000

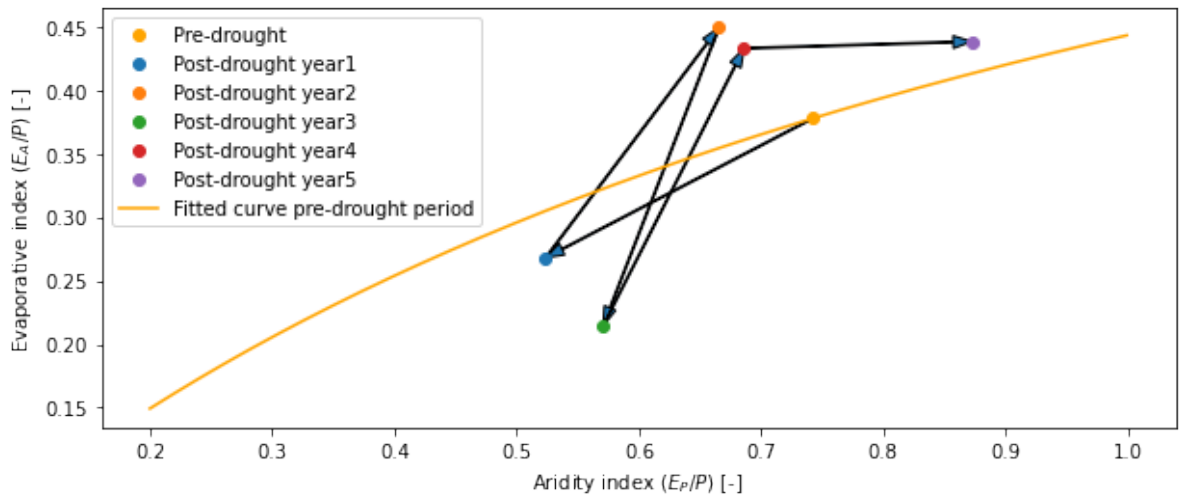


Figure C.4: Yearly movement of basin 3464400

### C.2. Basins that experience a decrease in runoff ratio: $\Delta\omega > 0$

The same is done for basins that experience a decrease in runoff ratio. No clear pattern is found for these basins either.

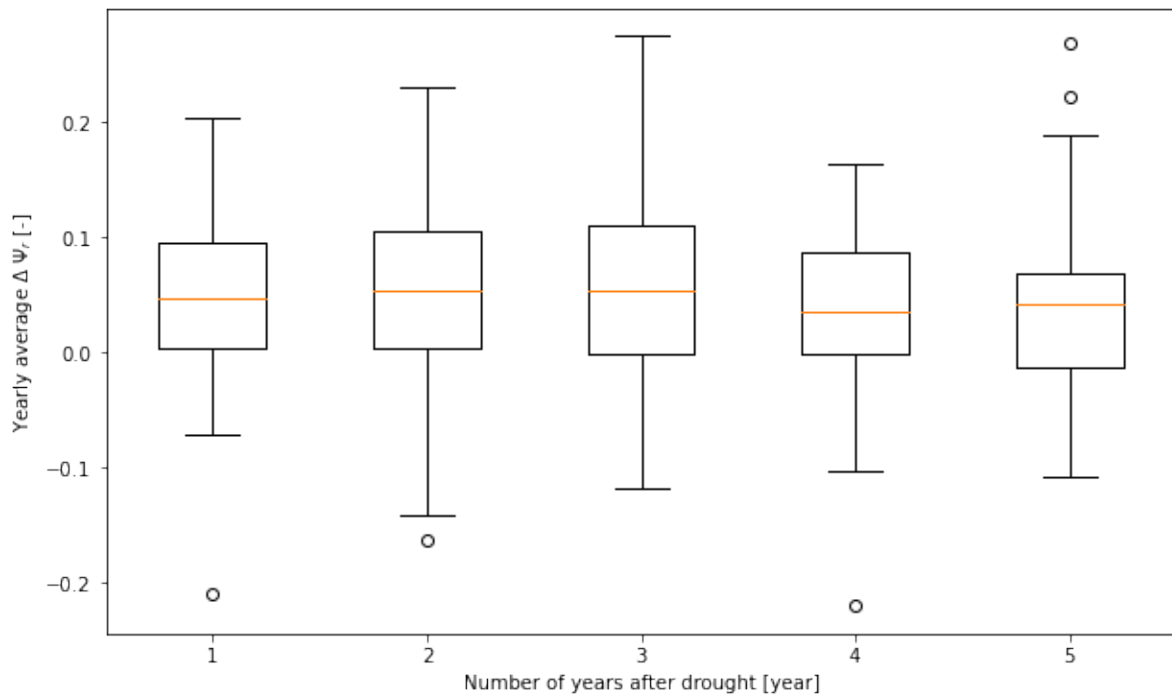


Figure C.5: Change in average  $\Delta\Psi_r$  for every year in the post-drought period: basins with  $\Delta\omega > 0$

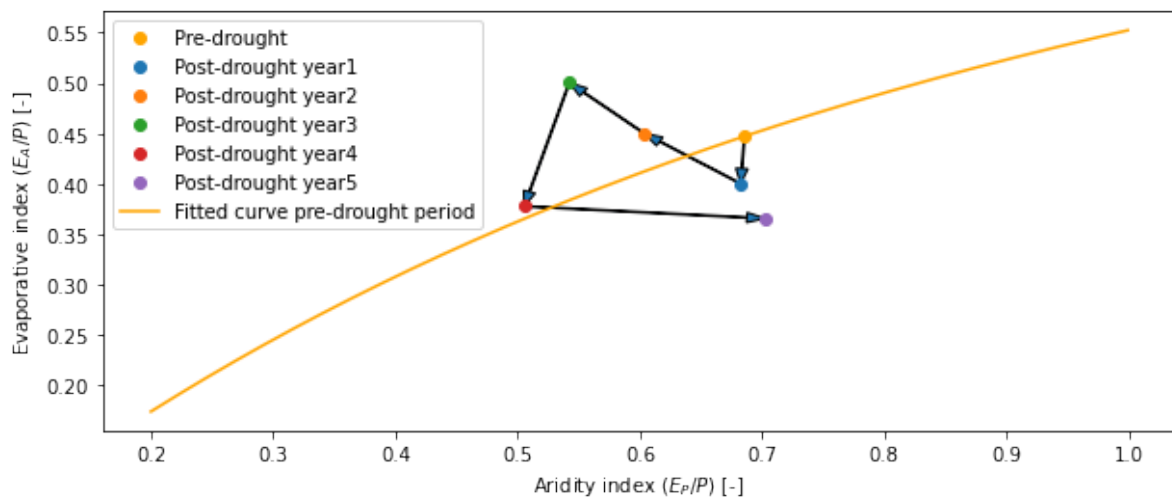


Figure C.6: Yearly movement of basin 1030500

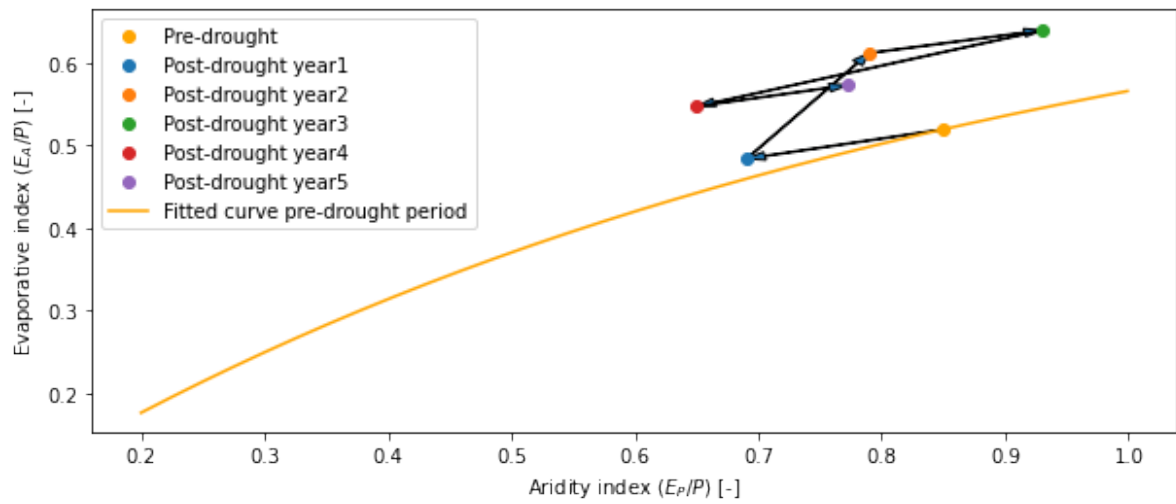


Figure C.7: Yearly movement of basin 2015700

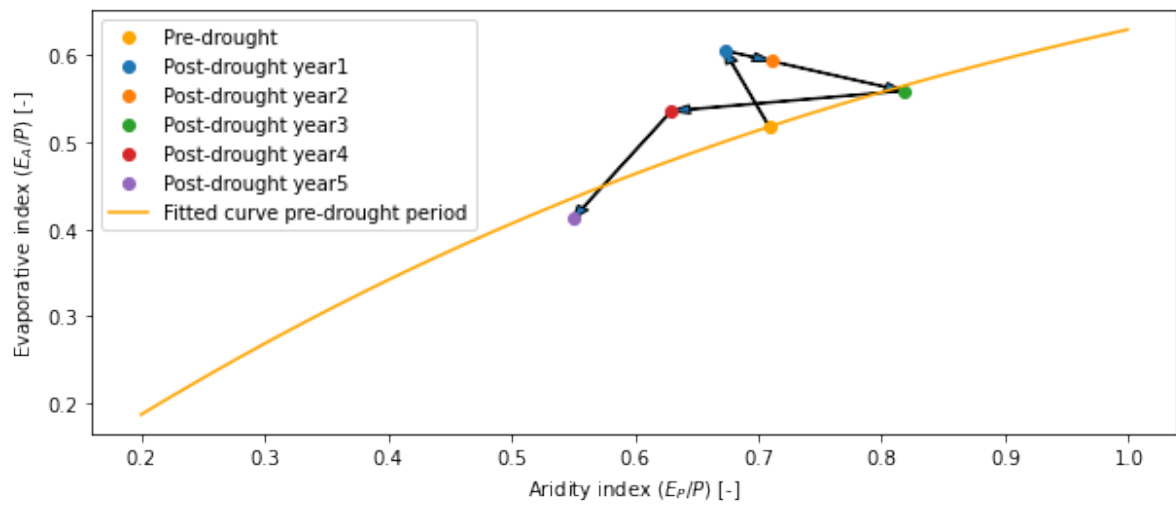


Figure C.8: Yearly movement of basin 4213075

# D

## Yearly Changes in NDVI Post Drought

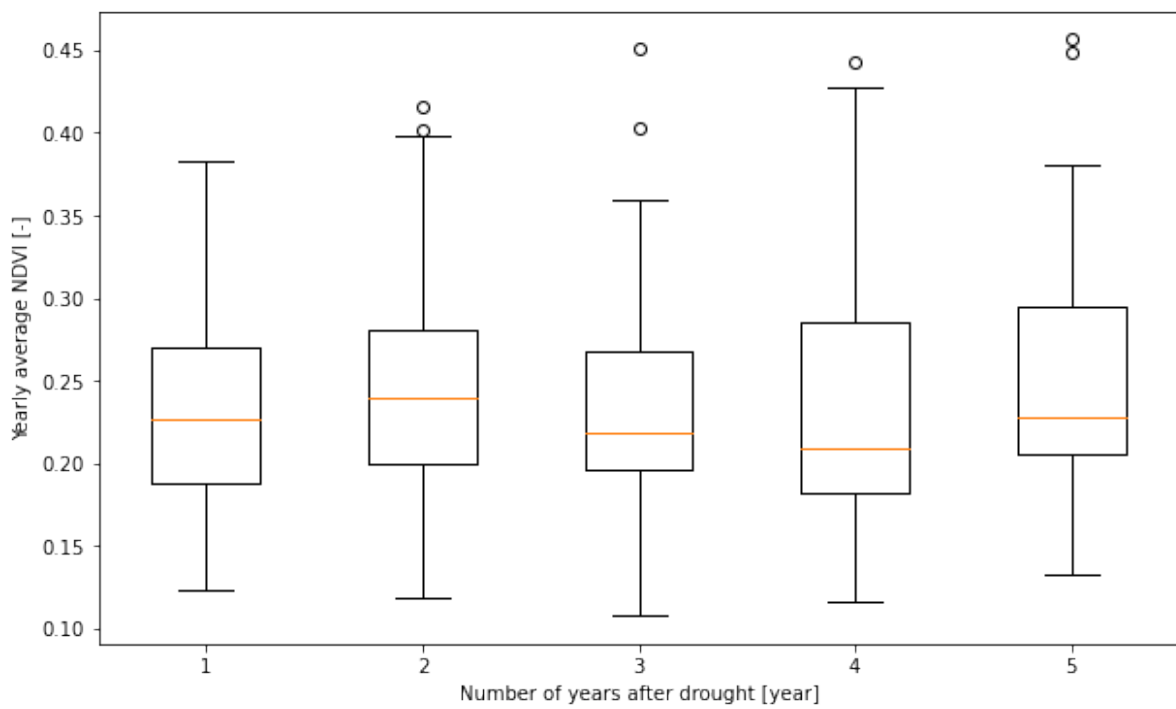


Figure D.1: Average NDVI for every year in the post-drought period



# E

## Results of Clustering the Basins Using Changes in NDVI

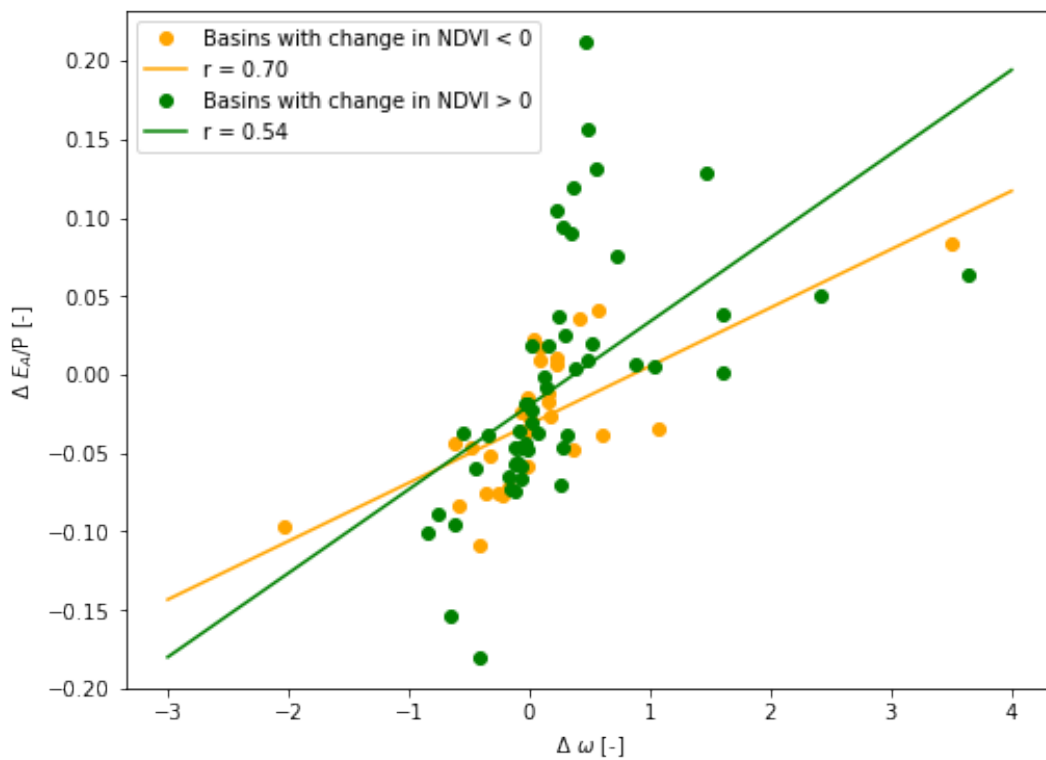


Figure E.1: The correlation between  $\Delta \omega$  and  $\Delta E_A/P$ , clustered using  $\Delta \text{NDVI}$



# F

## Results of Clustering the Vegetation-related Variables Using Aridity Index

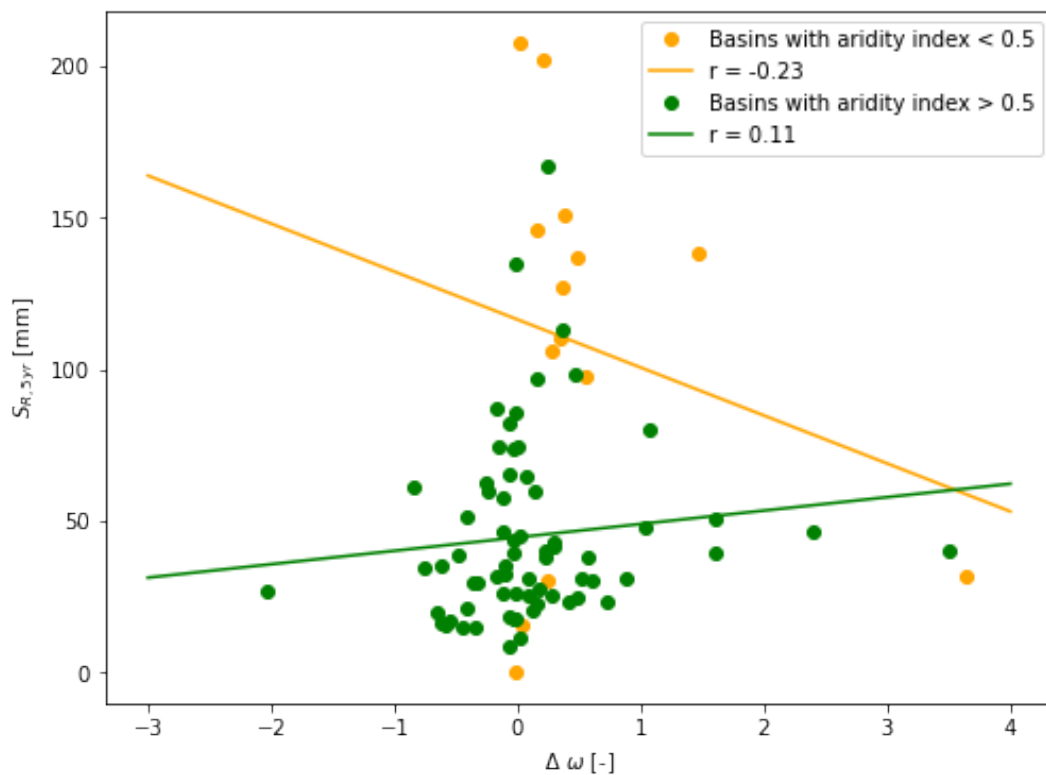


Figure F1: The correlation between  $S_{R,5yr}$  and  $\Delta \omega$ , clustered using the aridity index

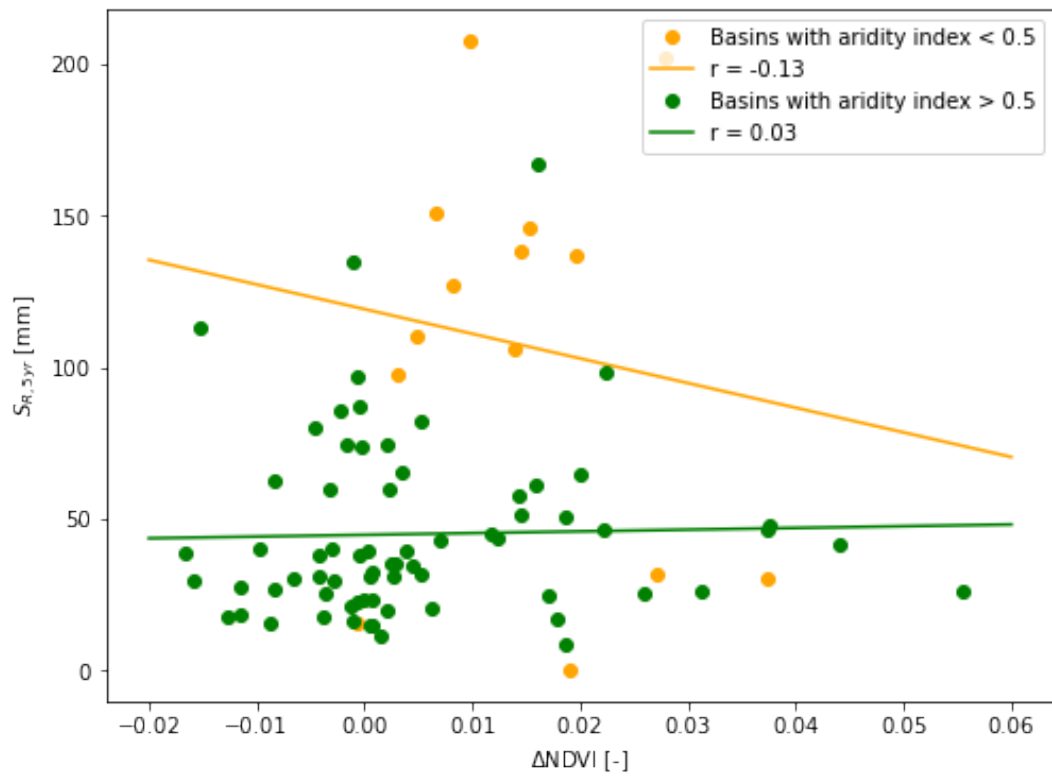


Figure F2: The correlation between  $S_{R,5yr}$  and  $\Delta NDVI$ , clustered using the aridity index